

# Oncology and Translational Medicine

Volume 7 • Number 2 • April 2021

## Expression and role of PTV1 lncRNA in glioma cells progression

Yue Li, Yuling Bai, Yan Qi, Chang Cai, Ying Liao, Xiuzhu Liu, Pengchen He 51

## Differentially expressed genes analysis and target genes prediction of miR-22 in breast cancer

Tao Fan, Chaoqi Wang (Co-first author), Kun Zhang, Hong Yang, Juan Zhang, Wanyan Wu, Yingjie Song 59

## Study on the antitumor effects of autologous and allogeneic CIK cells in patients with breast cancer

Xia Chen, Zhijian Dai, Xiangji Lu, Meng Ren, Zhenshan Guo, Yanwei Gao 65

## KIF15 expression characteristics: Relevance toneo-adjuvant chemotherapy efficacy in breast cancer

Mengting Dong, Chunyang Li, Patiguli-Jiapaer, Xiaofei Li, Xiaohong Xue, Ke Jiang, Jiayu Sheng 69

## Application of endoscopic nasobiliary cutting in the treatment of hilar cholangiocarcinoma

Shujuan Jiang, Zhongyin Zhou 76

Oncology and Translational Medicine

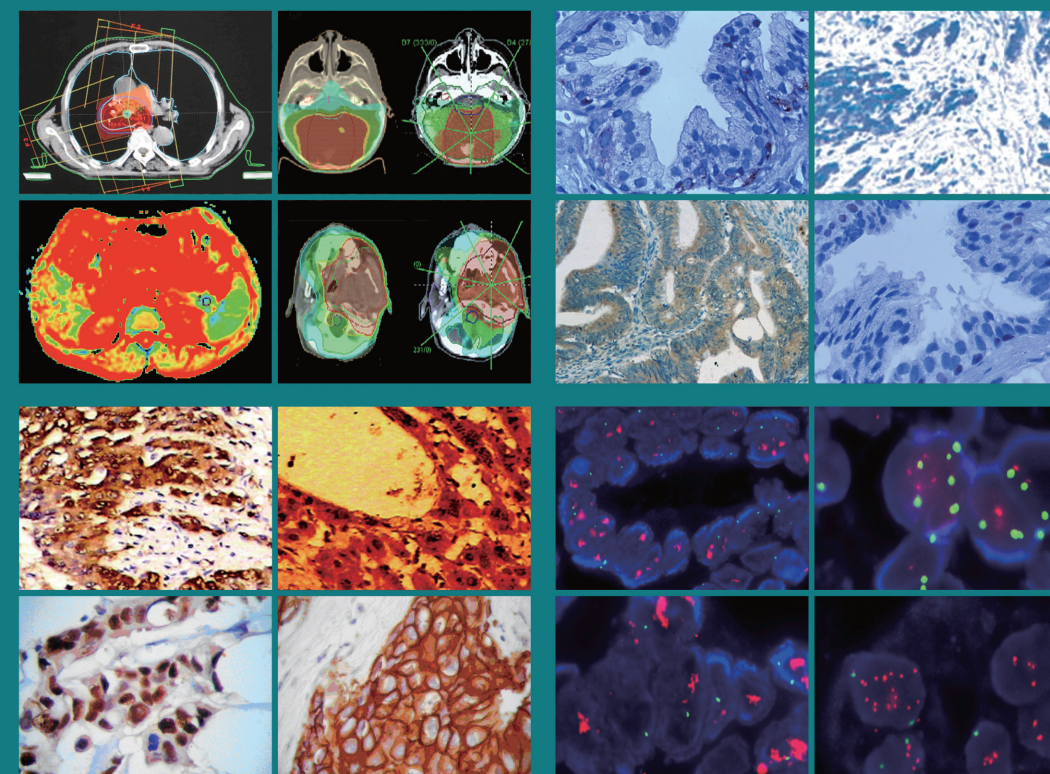
Volume 7 • Number 2 • April 2021

pp 51-98

ISSN 2095-9621  
CN 42-1865/R

# Oncology and Translational Medicine

## 肿瘤学与转化医学（英文）



**Online First**  
Immediately Online

[otm.tjh.com.cn](http://otm.tjh.com.cn)

Faster  
publication!

邮发代号: 38-121

ISSN 2095-9621



GENERAL INFORMATION  
» [otm.tjh.com.cn](http://otm.tjh.com.cn)

Volume 7  
Number 2  
April 2021





## Honorary Editors-in-Chief

W.-W. Höpker (Germany)  
Mengchao Wu (China)  
Yan Sun (China)

## Editors-in-Chief

Anmin Chen (China)  
Shiying Yu (China)

## Associate Editors

Yilong Wu (China)  
Shukui Qin (China)  
Xiaoping Chen (China)  
Ding Ma (China)  
Hanxiang An (China)  
Yuan Chen (China)

## Editorial Board

A. R. Hanauske (Germany)  
Adolf Grünert (Germany)  
Andrei Iagaru (USA)  
Arnulf H. Hölscher (Germany)  
Baoming Yu (China)  
Bing Wang (USA)  
Binghe Xu (China)  
Bruce A. Chabner (USA)  
Caicun Zhou (China)  
Ch. Herfarth (Germany)  
Changshu Ke (China)  
Charles S. Cleeland (USA)  
Chi-Kong Li (China)  
Chris Albanese (USA)  
Christof von Kalle (Germany)  
D Kerr (United Kingdom)  
Daoyu Hu (China)  
Dean Tian (China)  
Di Chen (USA)  
Dian Wang (USA)  
Dieter Hoelzer (Germany)  
Dolores J. Schendel (Germany)  
Dongfeng Tan (USA)  
Dongmin Wang (China)  
Ednin Hamzah (Malaysia)  
Ewerbeck Volker (Germany)  
Feng Li (China)  
Frank Elsner (Germany)  
Gang Wu (China)  
Gary A. Levy (Canada)  
Gen Sheng Wu (USA)  
Gerhard Ehninger (Germany)  
Guang Peng (USA)  
Guangying Zhu (China)  
Gunther Bastert (Germany)  
Guoan Chen (USA)

Guojun Li (USA)  
Guoliang Jiang (China)  
Guoping Wang (China)  
H. J. Biersack (Germany)  
Helmut K. Seitz (Germany)  
Hongbing Ma (China)  
Hongtao Yu (USA)  
Hongyang Wang (China)  
Hua Lu (USA)  
Huaqing Wang (China)  
Hubert E. Blum (Germany)  
J. R. Siewert (Germany)  
Ji Wang (USA)  
Jiafu Ji (China)  
Jianfeng Zhou (China)  
Jianjie Ma (USA)  
Jianping Gong (China)  
Jihong Wang (USA)  
Jilin Yi (China)  
Jin Li (China)  
Jingyi Zhang (Canada)  
Jingzhi Ma (China)  
Jinyi Lang (China)  
Joachim W. Dudenhausen (Germany)  
Joe Y. Chang (USA)  
Jörg-Walter Bartsch (Germany)  
Jörg F. Debatin (Germany)  
JP Armand (France)  
Jun Ma (China)  
Karl-Walter Jauch (Germany)  
Katherine A Siminovitch (Canada)  
Kongming Wu (China)  
Lei Li (USA)  
Lei Zheng (USA)  
Li Zhang (China)  
Lichun Lu (USA)  
Lili Tang (China)  
Lin Shen (China)  
Lin Zhang (China)  
Lingying Wu (China)  
Luhua Wang (China)  
Marco Antonio Velasco-Velázquez (Mexico)  
Markus W. Büchler (Germany)  
Martin J. Murphy, Jr (USA)  
Mathew Casimiro (USA)  
Matthias W. Beckmann (Germany)  
Meilin Liao (China)  
Michael Buchfelder (Germany)  
Norbert Arnold (Germany)  
Peter Neumeister (Austria)  
Qing Zhong (USA)  
Qinghua Zhou (China)

Qingyi Wei (USA)  
Qun Hu (China)  
Reg Gorczynski (Canada)  
Renyi Qin (China)  
Richard Fielding (China)  
Rongcheng Luo (China)  
Shenjiang Li (China)  
Shenqiu Li (China)  
Shimosaka (Japan)  
Shixuan Wang (China)  
Shun Lu (China)  
Sridhar Mani (USA)  
Ting Lei (China)  
Ulrich Sure (Germany)  
Ulrich T. Hopt (Germany)  
Ursula E. Seidler (Germany)  
Uwe Kraeuter (Germany)  
W. Hohenberger (Germany)  
Wei Hu (USA)  
Wei Liu (China)  
Wei Wang (China)  
Weijian Feng (China)  
Weiping Zou (USA)  
Wenzhen Zhu (China)  
Xianglin Yuan (China)  
Xiaodong Xie (China)  
Xiaohua Zhu (China)  
Xiaohui Niu (China)  
Xiaolong Fu (China)  
Xiaoyuan Zhang (USA)  
Xiaoyuan (Shawn) Chen (USA)  
Xichun Hu (China)  
Ximing Xu (China)  
Xin Shelley Wang (USA)  
Xishan Hao (China)  
Xiuyi Zhi (China)  
Ying Cheng (China)  
Ying Yuan (China)  
Yixin Zeng (China)  
Yongjian Xu (China)  
You Lu (China)  
Youbin Deng (China)  
Yuankai Shi (China)  
Yuguang He (USA)  
Yuke Tian (China)  
Yunfeng Zhou (China)  
Yunyi Liu (China)  
Yuquan Wei (China)  
Zaide Wu (China)  
Zefei Jiang (China)  
Zhangqun Ye (China)  
Zhishui Chen (China)  
Zhongxing Liao (USA)

# Oncology and Translational Medicine

April 2021 Volume 7 Number 2

## Contents

Expression and role of PTV1 lncRNA in glioma cells progression

*Yue Li, Yuling Bai, Yan Qi, Chang Cai, Ying Liao, Xiuzhu Liu, Pengchen He* 51

Differentially expressed genes analysis and target genes prediction of miR-22 in breast cancer

*Tao Fan, Chaoqi Wang (Co-first author), Kun Zhang, Hong Yang, Juan Zhang, Wanyan Wu, Yingjie Song* 59

Study on the antitumor effects of autologous and allogeneic CIK cells in patients with breast cancer

*Xia Chen, Zhijian Dai, Xiangji Lu, Meng Ren, Zhenshan Guo, Yanwei Gao* 65

KIF15 expression characteristics: Relevance to neo-adjuvant chemotherapy efficacy in breast cancer

*Mengting Dong, Chunyang Li, Patiguli-Jiapaer, Xiaofei Li, Xiaohong Xue, Ke Jiang, Jiayu Sheng* 69

Application of endoscopic nasobiliary cutting in the treatment of hilar cholangiocarcinoma

*Shujuan Jiang, Zhongyin Zhou* 76

Analyses of the clinical characteristics of 49 cases of malignancy with multiple bone lesions as the first manifestation

*Yu Huang, Ping Peng, Peng Zhang, Lei Zhou, Yingying Wu* 83

Analysis of the adverse reactions of atezolizumab: A real-world study based on FAERS database

*Hao Liu, Yujing Zhang, Jingyi Li, Rong Yan* 88

A case report of iodine-125 seed placement during operation for the treatment of advanced gallbladder carcinoma with septic shock

*Zhuo Zhong, Fei Gao, Zhuo Lv, Zhihui Zhong, De Long* 95

## Aims & Scope

**Oncology and Translational Medicine** is an international professional academic periodical. The Journal is designed to report progress in research and the latest findings in domestic and international oncology and translational medicine, to facilitate international academic exchanges, and to promote research in oncology and translational medicine as well as levels of service in clinical practice. The entire journal is published in English for a domestic and international readership.

## Copyright

Submission of a manuscript implies: that the work described has not been published before (except in form of an abstract or as part of a published lecture, review or thesis); that it is not under consideration for publication elsewhere; that its publication has been approved by all co-authors, if any, as well as – tacitly or explicitly – by the responsible authorities at the institution where the work was carried out.

The author warrants that his/her contribution is original and that he/she has full power to make this grant. The author signs for and accepts responsibility for releasing this material on behalf of any and all co-authors. Transfer of copyright to Huazhong University of Science and Technology becomes effective if and when the article is accepted for publication. After submission of the Copyright Transfer Statement signed by the corresponding author, changes of authorship or in the order of the authors listed will not be accepted by Huazhong University of Science and Technology. The copyright covers

the exclusive right and license (for U.S. government employees: to the extent transferable) to reproduce, publish, distribute and archive the article in all forms and media of expression now known or developed in the future, including reprints, translations, photographic reproductions, microform, electronic form (offline, online) or any other reproductions of similar nature.

## Supervised by

Ministry of Education of the People's Republic of China.

## Administered by

Tongji Medical College, Huazhong University of Science and Technology.

## Submission information

Manuscripts should be submitted to:  
<http://otm.tjh.com.cn>  
[dmedizin@sina.com](mailto:dmedizin@sina.com)

## Subscription information

ISSN edition: 2095-9621  
CN: 42-1865/R

### ■ Subscription rates

Subscription may begin at any time. Remittances made by check, draft or express money order should be made payable to this journal. The price for 2021 is as follows: US \$ 30 per issue; RMB ¥ 28.00 per issue.

## Database

**Oncology and Translational Medicine** is abstracted and indexed in EMBASE, Index Copernicus, Chinese Science and Technology Paper Citation Database (CSTPCD), Chinese Core Journals Database, Chinese Journal Full-text Database (CJFD), Wanfang

Data; Weipu Data; Chinese Academic Journal Comprehensive Evaluation Database.

## Business correspondence

All matters relating to orders, subscriptions, back issues, offprints, advertisement booking and general enquiries should be addressed to the editorial office.

## Mailing address

Editorial office of  
*Oncology and Translational Medicine*  
Tongji Hospital  
Tongji Medical College  
Huazhong University of Science and Technology  
Jie Fang Da Dao 1095  
430030 Wuhan, China  
Tel.: +86-27-69378388  
Email: [dmedizin@sina.com](mailto:dmedizin@sina.com)

## Printer

Changjiang Spatial Information  
Technology Engineering Co., Ltd.  
(Wuhan) Hangce Information  
Cartography Printing Filial, Wuhan,  
China  
Printed in People's Republic of China

## Editors-in-Chief

Anmin Chen  
Shiyong Yu

## Managing director

Jun Xia

## Executive editors

Jing Chen  
Yening Wang  
Jun Xia  
Qiang Wu

# Expression and role of PTV1 lncRNA in glioma cells progression\*

Yue Li, Yuling Bai, Yan Qi, Chang Cai, Ying Liao, Xiuzhu Liu, Pengchen He (✉)

Department of Neurosurgery, Mianyang Central Hospital, Mianyang 621000, China

## Abstract

**Objective** The aim of this study was to investigate the expression of PTV1 lncRNA in gliomas and the mechanism of its interaction with miR-203a.

**Methods** U87 and U251 cells were cultured stably and transfected with sh-PTV1 or ov-PTV1, respectively. The proliferative activity of U87 and U251 cells was detected and the transplanted tumor model nude mice were divided into U87 and U251 groups. U87-sh and u251-ov cells were injected into the armpit, then miR-203a mic and miR-203a inhibitors were administered to detect the changes in the expression of tumor-related proteins.

**Results** The relative expression of PTV1 in gliomas was significantly higher than that in normal brain tissues, while in GBM it was significantly higher than that in low-grade gliomas. Knockdown of PTV1 significantly inhibited the proliferation of U87 cells, resulting in fewer cell clones; overexpression of rPTV1 significantly promoted the proliferation of U251 cells, resulting in more cell colonies. The dual Luciferase Reporter assay showed that SP2 was a potential target of miR-203a. When U87 cells were treated with a miR-203a mimic, the expression of SP2 decreased; and when U251 cells were treated with a miR-203a inhibitor, the expression of SP2 increased significantly. SP2 was overexpressed in u87-sh cells and the proliferation, migration, and invasion of u87-sh cells were significantly enhanced. U251-ov cells showed the opposite trend. Compared with the control group mice, the tumor volume in u87-sh group mice was significantly smaller and the positive rate of SP2 in tumor tissue was significantly lower. After administration of the miR-203a inhibitor, the tumor volume increased gradually and the positive rate of SP2 increased significantly, while u251-ov mice showed the opposite trend.

**Conclusion** lncRNA PTV1 can be used as a molecule to interfere with miR-203a expression in order to downregulate SP2 and to promote the proliferation and invasion of glioma cells. lncRNA PTV1 may be a new biomarker and therapeutic target for glioma.

**Key words:** glioma; miRNA-203a; long-chain noncoding RNA; transcription factor PTV1 lncRNA

Received: 12 May 2020

Revised: 9 July 2020

Accepted: 25 July 2020

Glioma is the most common brain cancer, accounting for more than 60% of the primary brain tumors in adults. The molecular mechanisms underlying its occurrence and development are still unclear<sup>[1]</sup>. Long noncoding RNAs (lncRNAs) are a class of RNAs (> 200 nucleotides long) that are not translated into protein. They are widely involved in biological processes such as post-transcriptional regulation and chromatin modification<sup>[2]</sup>. A variety of lncRNAs have been proved to play important roles in different types of cancer cells, including colorectal cancer<sup>[3]</sup>, bladder cancer<sup>[4]</sup>, and esophageal cancer<sup>[5]</sup>. MicroRNAs (miRNAs) are also recognized as noncoding RNAs that play important roles in tumor biology. lncrna

can interact with miRNA as a competitive endogenous RNA and participate in the regulation of target gene expression. Through competition, lncRNAs sequester numerous miRNAs in the cell, reducing their ability to interfere with the target gene mRNA, thus affecting downstream gene expression at the post-transcriptional level. Such lncRNAs and mRNAs are referred to as mutually competitive endogenous RNAs (ceRNA)<sup>[6-7]</sup>. PTV1 is an lncRNA, highly expressed in thyroid and renal cancers but has not yet been reported in gliomas. In a previous study, our bioinformatic analysis with TargetScan and other software revealed that PTV1 may have a targeted effect on miR-203a and may affect the

✉ Correspondence to: Pengchen He. Email: yueyue52887@sina.com

\* Supported by a grant from the general program of NSFC (No. 81472965)

© 2021 Huazhong University of Science and Technology

expression of the downstream transcription factor SP2. In this study, we verified this conjecture through cell experiments and in vivo experiments in mice, in order to provide more efficient biological targets for the prevention and treatment of glioma.

## Materials and methods

### Clinical specimens and cell culture

From January 2018 to June 2019, 62 patients with glioma and 24 patients with subarachnoid hemorrhage or brain injury who were admitted to neurosurgery of Mianyang Central Hospital (China) were selected as research subjects. Glioma samples and normal brain tissue samples were collected from patients and quickly stored in liquid nitrogen. All glioma patients were diagnosed for the first time and had never received radiotherapy nor chemotherapy before. The human brain glial cell line Heb was purchased from Lonza (Switzerland). Glioma cell lines U87, A172, and In229 were all purchased from American type culture collection, while the glioma cell line SHG-44 U251 was purchased from the Institute of Biochemistry and Cell Biology, Chinese Academy of Sciences (China). All glioma and Heb cell lines were cultured in Modified Eagle's Medium containing 10% fetal bovine serum and were incubated at 37°C in an atmosphere containing 5% CO<sub>2</sub>.

### Plasmid construction and cell transfection

Short hairpin RNAs (shRNAs) for lncRNA PTV1 and SP2 and overexpression plasmids containing PTV1 lncRNA (OV) and SP2 were designed and synthesized by Jikai Gene Chemical Technology Co., Ltd. (China). hsa-miR-203a mimics (mimic) and inhibitors (inhibitor) were designed and synthesized by Lucky Gene Chemical Technology Co., Ltd. (China) full-length sequence of PTV1 lncRNA was amplified and cloned into pcDNA3.1 vector (GeneChem, China), and full-length cDNAs of miR-203a and SP2 were transcribed and cloned into pcDNA3.1. According to the manufacturer's protocol, oligonucleotides and constructs were transfected into the cell lines using Lipofectamine 3000 (Abcam, UK).

### RT-PCR and western blot

Total RNA was extracted from clinical samples and cell lines. The expression of PTV1 lncRNA, miR-203a, and SP2 was detected by real-time quantitative polymerase chain reaction (qRT-PCR) and normalized against that of GAPDH and U6. The primer sequence for lncRNA is as follows: lnc PTV1: forward primer 5'-CGACCAGACCACACTGAA-3', reverse primer 5'-ACACCTCCAAAGCAGCCCTCAA-3'. Western blotting was performed as follows: clinical tissues and cells were collected, cell samples were lysed using RIPA

buffer, and total protein was extracted, then protein concentration was determined with BCA protein analysis kit (Abcam, UK), which included the following steps: sample buffer mixing, boiling (denaturation), electrophoresis, membrane transfer, and sealing. Membranes containing the protein bands were probed overnight with SP2 antibody (1:1000) at 4°C. After washing, the membrane was probed with SP2 antibody and secondary antibody were purchased from Beyotime Biotechnology, and developed using the ECL reagent; GAPDH (1:10000) protein as the internal reference.

### Luciferase reporter assay

The full-length sequence and fragment of lncRNA PTV1 containing the indicated miRNA binding sequence were cloned into the pmir reporter vector. The 3'-untranslated region fragment of SP2 containing a specific miRNA binding sequence was also cloned into the pmir reporter vector. The corresponding miRNAs and reporter plasmids were transfected into the glioma cell line, while the mutant plasmid was used as control. After 48 h, the cells were collected and the luciferase activity was measured using the dual Luciferase Report Analysis System.

### CCK-8 and cell colony formation assay

Cell count kit-8 (CCK-8) and colony forming assay (CFA) were used to detect the proliferation of glioma cells. CCK-8 detection was performed by inoculating a 96 well plate with  $1 \times 10^4$  cells per well, then measuring the absorbance at 450 nm with a micro flat-panel reader. To evaluate colony formation, glioma cells were inoculated in 6-well plates at a density of  $1 \times 10^4$  cells/well and cultured in DMEM containing 10% fetal bovine serum for 14 days. The cells were then fixed with methanol and stained with 0.5% crystal violet for 10 min.

### Analysis of cell migration and invasiveness

The chamber was placed in a 24 well plate; the lower chamber contained 1:8 diluted Matrigel (60  $\mu$ L per well) and incubated in the incubator for about 5 h. In each experimental group, 4 wells were set up, and cell suspension was added into Transwell chamber, each well was about 100  $\mu$ L. Then 600  $\mu$ L DMEM containing fetal bovine serum was added to the lower chamber, and the set up was then incubated for 24 h. The medium was discarded, and cells adhering on the upper layer of the membrane were removed with a cotton swab, stained with crystal violet; after counting, 5 visual fields were randomly selected and observed under high-power microscope (Abcam, UK).

## Immunohistochemistry

Tumor tissue in mice were fixed with formaldehyde, embedded in paraffin, and sectioned. Tissue sections were dewaxed, hydrated, and incubated with H<sub>2</sub>O<sub>2</sub> deionized water. The antigen was exposed to 80°C, washed with PBS, and incubated overnight with 100 μL SP2 monoclonal antibody (1:100) at 4°C in a refrigerator. Sections were rinsed with PBS 3 times for 2 min. Then, the sections were incubated with a secondary antibody (added dropwise) at 37°C for 20–30 min, then sections were rinsed again with PBS (3 times, 2 min). The sections were stained with DAB, then dehydrated, transparent with xylene and sealed with neutral gum. The appearance of brown particles was taken as the standard of SP2. The appearance of brown particles was used as an indicator of SP2 expression.

## Mouse model construction

A total of 36 SPF-grade BALB/c nude mice were purchased from the experimental animal center of the Academy of Military Medical Sciences (China). Single-cell suspension of U87 cells stably transformed with shRNA-PTV1 and U251 cells overexpressing PTV1 was prepared using trypsin, then centrifuged, resuspended, and counted under a microscope. Thirty-six mice were randomly divided into two groups, U87 group and U251 group. The mice in U87 group were randomly divided into the following groups: (1) U87 group, injected with u87-nc glioma cells; (2) u87-sh group, injected with u87-sh glioma cells; and (3) U87 inhibitor group, injected with u87-sh glioma cells and treated with miR-203a inhibitor. U251 group mice were randomly divided into the following groups: (1) U251 group, injected with u251-nc glioma cells; (2) u251-ov group, injected with u251-ov glioma cells; and (3) U251 mimic group, injected simultaneously with miR-203a mimic and u251-sh glioma cells. After injection, all mice were observed every other day, timely provided with drinking water and feed, and checked for temperature and humidity. At the end of the experiment, the nude mice were euthanized and their subcutaneous tumor tissues were collected for observation, imaging, and measurement of tumor size. The breeding and treatment of nude mice were performed in strict accordance with the regulations of the Ethics Committee for experimental animals. The length (L) and weight (W) of the implanted tumors were measured using a vernier caliper at the designated time point and the volume of the tumor was calculated.

## Results

### Expression of PTV1 lncRNA in glioma

RT-PCR revealed that the relative expression of PTV1 in the normal brain tissue and glioma tissue was  $(1.2 \pm 0.2)$

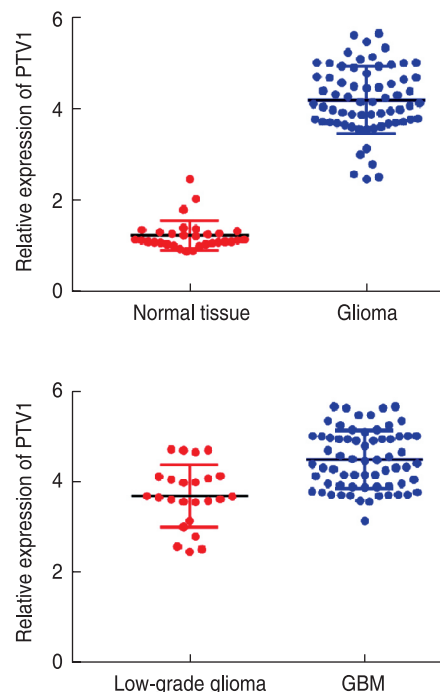
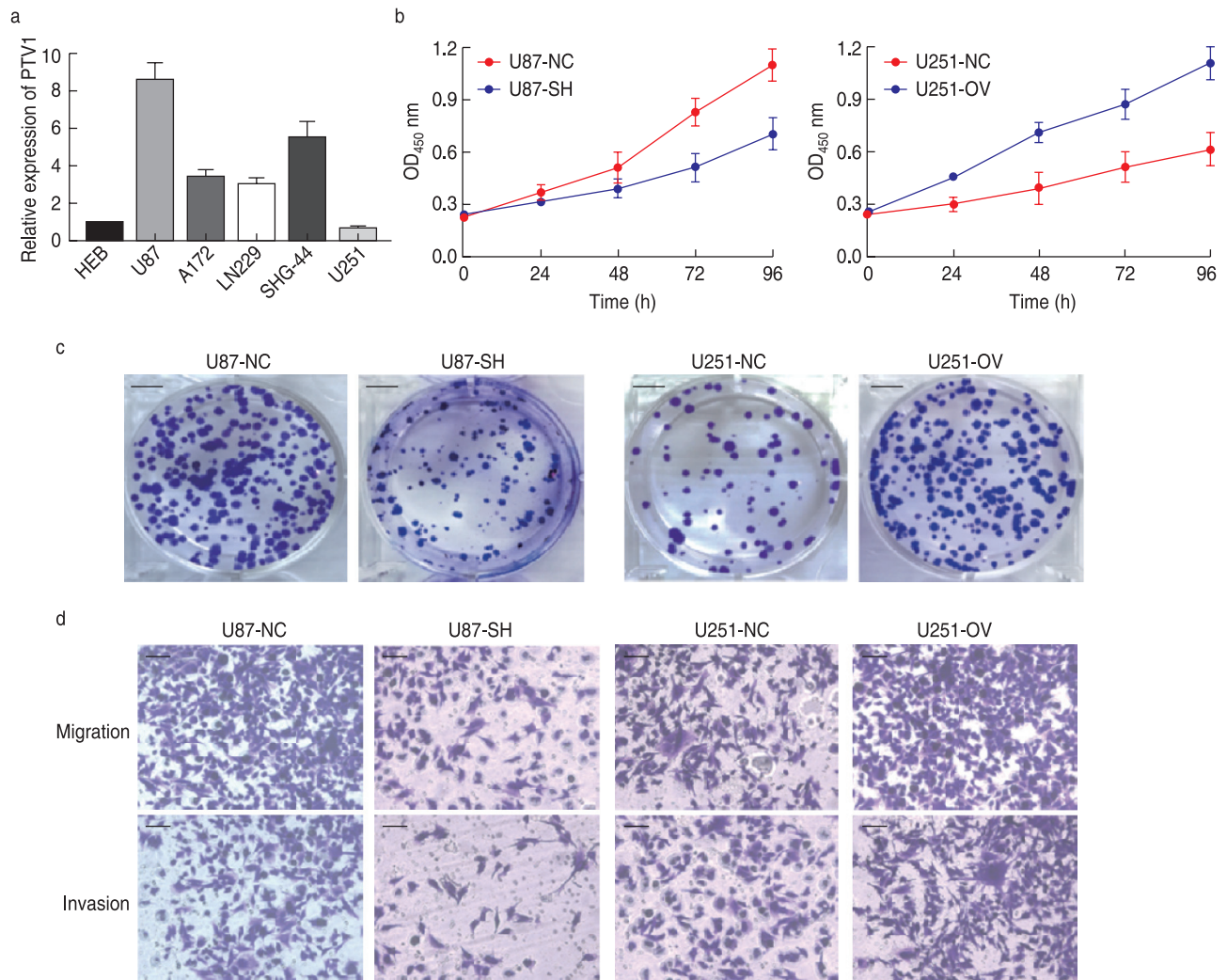


Fig. 1 Expression of lncRNA PTV1 in glioma

and  $(4.3 \pm 0.8)$ , respectively. The expression of PTV1 in glioma tissue was significantly higher ( $P < 0.05$ ). Based on the results of pathological examination, 62 patients were divided into 24 cases of low-grade glioma and 38 cases of glioblastoma multiforme (GBM). The relative expression of PTV1 was  $(3.6 \pm 0.5)$  and  $(4.7 \pm 0.9)$ , respectively. The expression of PTV1 in GBM was significantly higher than that in low-grade glioma (Fig. 1).

### lncRNA PTV1 promotes the proliferation, migration, and invasion of glioma cells

RT-PCR revealed that PTV1 was generally highly expressed in glioma cell lines U87, A172, ln229, and SHG-44; in particular, U87 had the highest expression of PTV1 and U251 had the lowest expression, compared with that in the normal human brain glioma cell line Heb (Figure 2a). Therefore, we transfected U87 cells (u87-sh) with shRNA against lncRNA PTV1, and U251 cells (u251-ov) with functional PTV1-cdna lncRNA. CCK-8 assay and cell cloning experiments revealed that knockdown of rPTV1 significantly inhibited the proliferation of U87 cells, as evidenced by fewer cell clones; OV significantly promoted the proliferation of U251 cells, which produced more colonies (Fig. 2b and 2c). Transwell migration and invasion analysis showed that the migration and invasion ability of U87 cells decreased significantly after rPTV1 lncRNA knockdown, while OV significantly promoted the migration and invasion ability of U251 cells (Fig. 2d). This indicated that PTV1 could significantly promote the



**Fig. 2** IncRNA PTV1 promotes proliferation, migration, and invasion of glioma cells. (a) Relative levels of PTV1 in different cell lines; (b) IncRNA PTV1 promotes the proliferation ability of U87 and U251; (c) Proliferation experiment of U87 and U251 cell lines; (d) Migration and invasion experiment of U87 and U251 cell lines

proliferation, migration, and invasion of glioma cells.

### PTV1 IncRNA can target miR-203a

Compared with u87-sh cells, the expression of miR-203a in u87-nc cells was significantly higher, while that in u251-ov cells was significantly lower. The potential binding site between miR-203a and IncRNA PTV1 was determined by the bioinformatic software starBase (Fig. 3).

### miR-203a directly targets SP2 in glioma cells

TargetScan revealed that SP2 may be a potential miR-203a target gene (Fig. 4a). Furthermore, upon co-transfection with miR-203a, we found that the dual luciferase reporter activity of sp1-wt in glioma cells was lower than that of SP1-Mut. The negative control group had no such effect on luciferase activity (Fig. 4b). Western

blotting revealed that the expression of SP2 decreased when U87 cells were treated with miR-203a mimic, and increased significantly when U251 cells were treated with the miR-203a inhibitor (Fig. 4c). This indicated that miR-203a could directly target SP2 in glioma cells.

### Positive regulation of SP2 expression by IncRNA PTV1 promotes the growth of glioma cells

We overexpressed SP2 in u87-sh cells and downregulated SP2 expression in u251-ov cells. The results showed that the proliferation, migration, and invasion of u87-sh cells were significantly enhanced. The corresponding activity of u251-ov cells was significantly inhibited. This suggests that PTV1 IncRNA can promote glioma progression by positively regulating the expression of SP2 (Fig. 5).

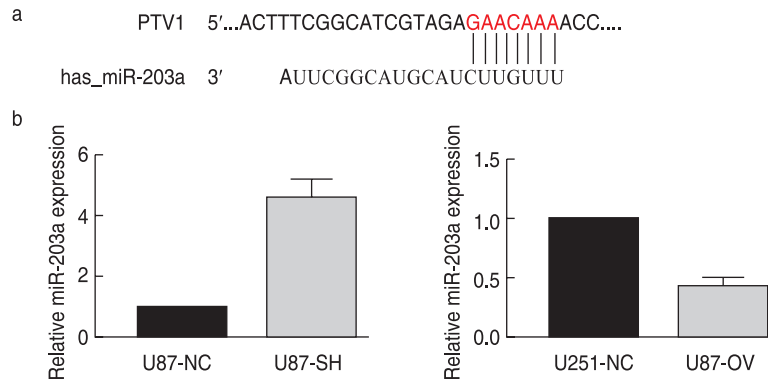


**Fig. 3** PTV1 lncRNA can target miR-203a. (a) Site of interaction between lncRNA PTV1 and miR-203a; (b) Expression of miR-203a in U87 and U251 cell lines.

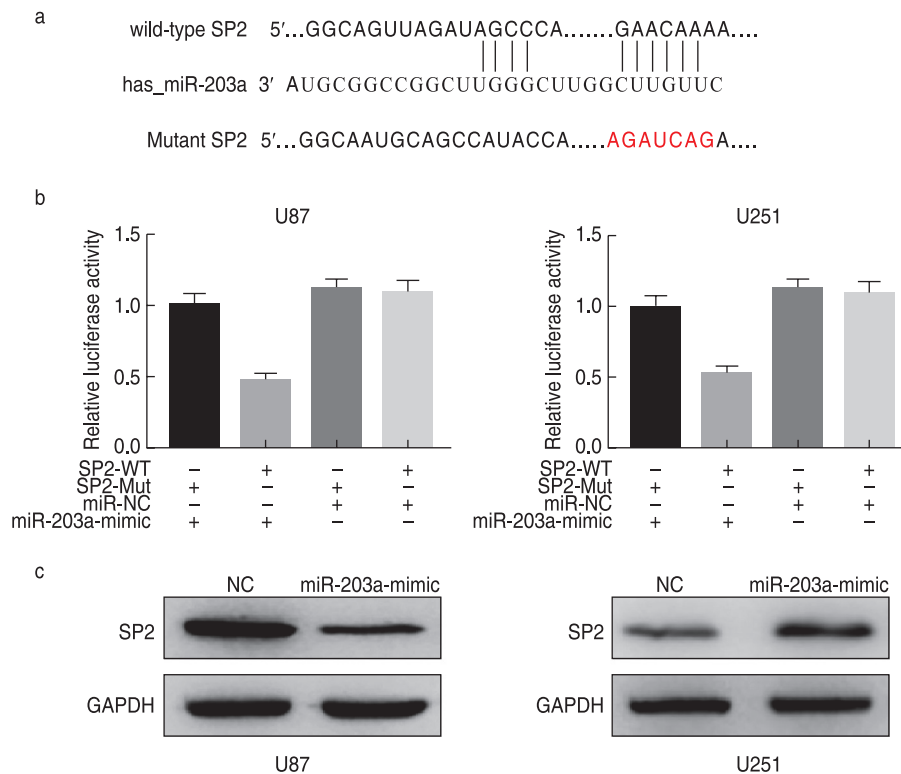


**Fig. 4** miR-203a directly targets SP2 in glioma cells. (a) Site of interaction between SP2 and miR-203a; (b) Double luciferase reporting experiment; (c) Western blot assays for SP2

### miR-203a targeting by lncRNA PTV1 upregulates the expression of SP2 in glioma cells

miR-203a inhibitor was used to treat u87-sh, while miR-203a mimic was used to treat u251-ov. Western blotting showed that the expression of SP2 protein in u87-sh cells was significantly higher than that in the corresponding control group, while the expression of SP2 protein in u251-ov was significantly lower ( $P < 0.05$ ; Fig. 6).

### lncRNA PTV1 targeting miR-203a upregulates SP2 expression in transplanted tumor

Compared with the control group, the tumor volume of mice in u87-sh group was significantly smaller and the positive rate of SP2 in tumor tissue was significantly lower. After treatment with the miR-203a inhibitor, the tumor volume increased gradually and the positive rate of SP2 increased significantly. Compared with mice in the control group, the mice in u251-ov group exhibited

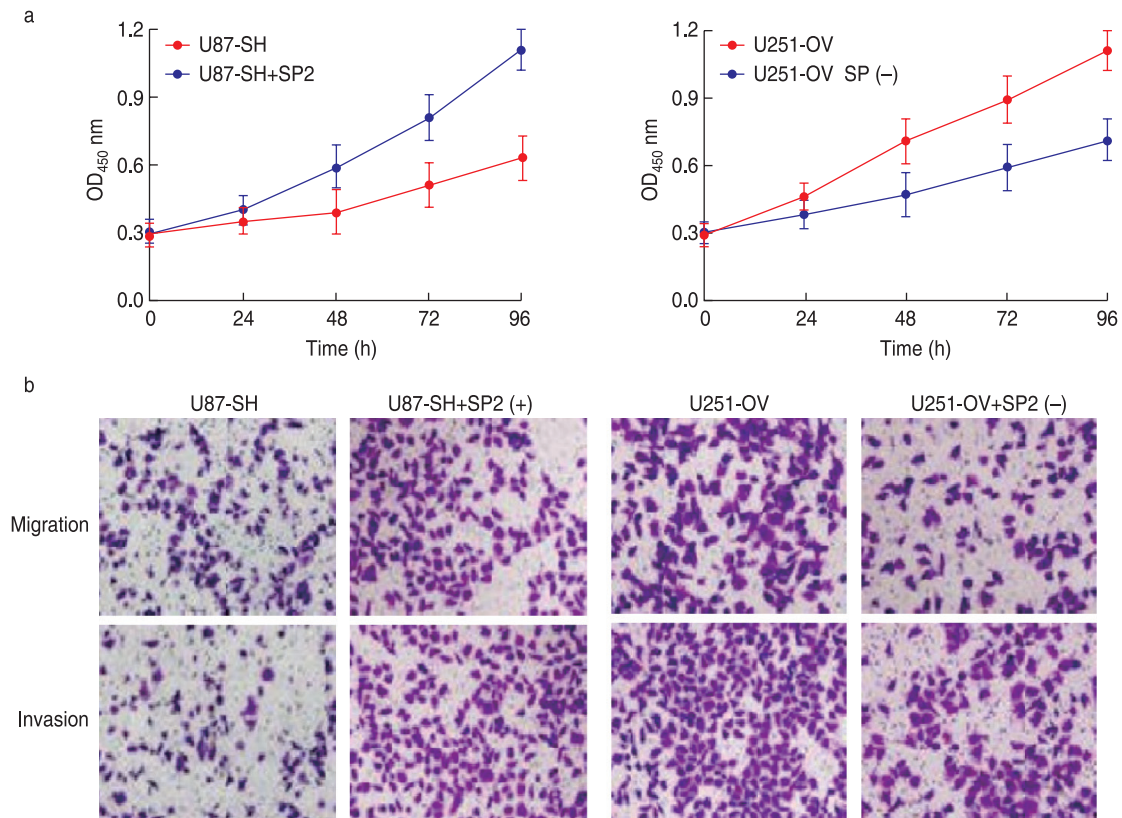


**Fig. 5** Positive regulation of SP2 expression by lncRNA PTV1 promotes glioma cell growth. (a) SP2 promotes the proliferation ability of U87 and U251. (b) Migration and invasion experiment of U87 and U251 cell lines

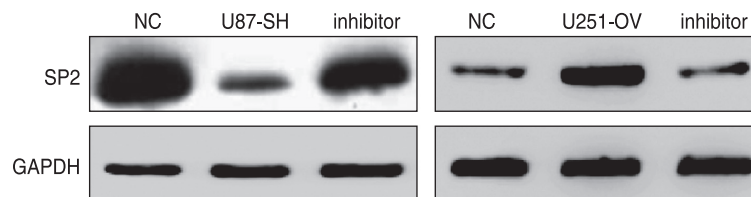


**Fig. 6** Effect of miR-203a inhibitor and mimics on the expression of SP2 protein in glioma cell lines.

significantly larger tumor volumes and the positive rate of SP2 in tumor tissue was significantly higher. Tumor volume as well as the positive rate of SP2 were significantly reduced after miR-203a mimic treatment. This indicated that PTV1 lncRNA could promote the growth of glioma through the miR-203a/SP1 axis (Fig. 7).

## Discussion

Glioma results from the interaction between congenital genetic high-risk factors and environmental carcinogenic factors. Some known genetic diseases, such as neurofibromatosis and tuberous sclerosis, predispose individuals to glioma. The risk of glioma in patients with such basic diseases is significantly higher than in the general population<sup>[8-9]</sup>. In addition, some environmental

factors may also be related to the occurrence of glioma, such as mobile phone electromagnetic radiation, but there is no evidence of a clear causal relationship between the two. Glioma, especially glioblastoma, usually has a poor prognosis, with a median survival time of less than 12 months<sup>[10]</sup>. Due to the high invasion and rapid proliferation of glioma and despite the progress in its diagnosis and even treatment, low cure rate and frequent recurrence are still the main challenges in clinical practice.

Recent studies have shown that lncRNAs can regulate the expression of downstream genes at the post-transcriptional level, thereby affecting tumor progression. In order to improve the rate of early diagnosis in glioma patients and the efficacy of targeted therapy, more biomarkers and therapeutic targets are urgently needed.

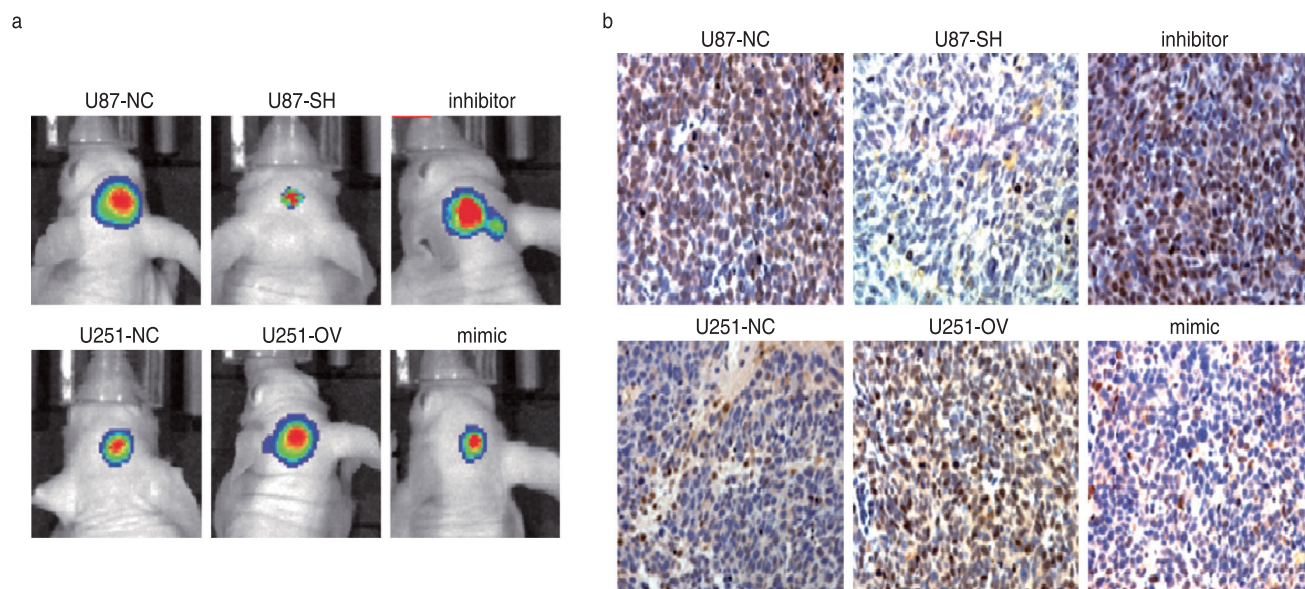


**Fig. 7** IncRNA PTV1 targeting miR-203a upregulates SP2 expression in transplanted tumor. (a) Tumorigenesis of mice treated with miR-203a; (b) Immunohistochemical detection of SP2 expression in mice tumor

IncRNA PTV1 is the first lncRNA reported to be related to tumors. It is a proto-oncogene and can stabilize the proto-oncoprotein myc, which also plays a role in promoting cancer<sup>[11]</sup>. In this study, by detecting the expression of PTV1 lncRNA in gliomas and normal brain tissues, we found that the expression of PTV1 in gliomas was significantly higher, and that the expression of PTV1 in glioblastomas was higher than that in low-grade gliomas. This indicates that PTV1 also plays an oncogenic role in glioma. In order to explore the function of PTV1 lncRNA in glioma cells, we performed a series of experiments to detect the effect of lncRNA PTV1 on the proliferation, migration, and invasion of glioma cells. The results showed that PTV1 lncRNA promoted the proliferation, migration, and invasion of glioma cells. However, the specific mechanism by which PTV1 lncRNA contributes to glioma development is not clear. lncRNA can target miRNAs to regulate mRNA expression. For example, it has been found that hcg11 lncRNA can target miR-421, which inhibits the proliferation, invasion and migration of cervical cancer cells, and induces their apoptosis by regulating the expression of matrix metalloproteinase-2 (MMP2) and E-cadherin<sup>[12]</sup>.

Previous studies have shown that miR-203a can directly target fatty acid transporter 4 (FABP4) to inhibit the proliferation and invasion of lung cancer cells<sup>[13]</sup>. Through TargetScan, we found that SP2 may also be a downstream target of miR-203a. Therefore, we speculated that PTV1 lncRNA might act by sequestering miRNA-203a to regulate the proliferation and invasion of SP2-regulated glioma cells. In order to test this

hypothesis, we have verified the relationship between PTV1 lncRNA and miR-203a by RT-PCR and luciferase reporter experiments. The results show that PTV1 lncRNA targets miR-375 and competitively modulates the expression of SP2. *In vivo* experiments in mice revealed that PTV1 lncRNA can promote the growth of glioma through the miR-203a/SP1 axis. This suggests that PTV1 lncRNA can promote the proliferation and invasion of glioma cells and play the role of ceRNA by targeting miR-375 to upregulate the expression of SP2. In addition, downregulating the expression of PTV1 lncRNA can decrease SP2 expression and slow down the growth of glioma cells. Based on the findings of this study, we hypothesize that PTV1 abnormality can be used as a biomarker for identifying glioma patients with poor prognosis, and that downregulation of PTV1 lncRNA may be a new means of inhibiting the progression of glioma.

In conclusion, *in vitro* and *in vivo* experiments show that PTV1 lncRNA can be used to interfere with miR-203a expression in order to downregulate SP2 and promote the proliferation and invasion of glioma cells. PTV1 lncRNA may be a new biomarker and therapeutic target for glioma.

### Conflicts of interest

The authors indicated no potential conflicts of interest.

### References

1. FAN K, Jia X, Zhou M, *et al.* Ferritin nanocarrier traverses the blood brain barrier and kills glioma. *Acs Nano*, 2018, 12: 4105–4115.

2. Zhao W, Geng D, Li S, *et al.* lncRNA HOTAIR influences cell growth, migration, invasion, and apoptosis via the miR-20a-5p/ HMGA2 axis in breast cancer. *Cancer Med*, 2018, 7: 842–855.
3. Ding D, Li C, Zhao T, *et al.* lncRNA H19/miR-29b-3p/PGRN axis promoted epithelial-mesenchymal transition of colorectal cancer cells by acting on Wnt signaling. *Mol Cells*, 2018, 41: 423–435.
4. Xintai Z, Zhaolin L, Shihao W, *et al.* lncRNA-SNHG7 regulates proliferation, apoptosis and invasion of bladder cancer cells. *J BUON*, 2018, 23: 776–781.
5. Zhao H, Diao C, Wang X, *et al.* lncRNA BDNF-AS inhibits proliferation, migration, invasion and EMT in oesophageal cancer cells by targeting miR-214. *J Cell Mol Med*, 2018, 22: 3729–3739.
6. Jiang X, Wu X, Chen F, *et al.* The profiles and networks of miRNA, lncRNA, mRNA, and circRNA in benzo(a)pyrene-transformed bronchial epithelial cells. *J Toxicol Sci*, 2018, 43: 281–289.
7. Guo L, Peng Y, Meng Y, *et al.* Expression profiles analysis reveals an integrated miRNA-lncRNA signature to predict survival in ovarian cancer patients with wild-type BRCA1/2. *Oncotarget*, 2017, 8: 68483–68492.
8. Yi R, Feng J, Yang S, *et al.* miR-484/MAP2/c-Myc-positive regulatory loop in glioma promotes tumor-initiating properties through ERK1/2 signaling. *J Mol Histol*, 2018, 49: 1–10.
9. Li T, Ma J, Han X, *et al.* MicroRNA-320 Enhances radiosensitivity of glioma through down-regulation of sirtuin type 1 by directly targeting forkhead box protein M1. *Transl Oncol*, 2018, 11: 205–212.
10. Jin L, Cao Y, Zhang T, *et al.* Effects of ERK1/2 S-nitrosylation on ERK1/2 phosphorylation and cell survival in glioma cells. *Int J Mol Med*, 2018, 41: 1339–1348.
11. Chai J, Guo D, Ma W, *et al.* A feedback loop consisting of RUNX2/ lncRNA-PVT1/miR-455 is involved in the progression of colorectal cancer. *Am J Cancer Res*, 2018, 8: 538–550.
12. Liu XL, Chen XY, Wang ZH, *et al.* HCG11 regulates the proliferation, apoptosis, invasion and migration of cervical cancer cells by targeting miRNA-421. *Oncol Prog*, 2020, 18: 30–34.
13. Chen JC, Wu X. miR-203 inhibits lung cancer cell metastasis by targeting fatty acid binding protein 4. *J South Med Univ*, 2018, 38: 578–583.

DOI 10.1007/s10330-020-0435-5

Cite this article as: Li Y, Bai YL, Qi Y, *et al.* Expression and role of PTV1 lncRNA in glioma cells progression. *Oncol Transl Med*, 2021, 7: 51–58.

# Differentially expressed genes analysis and target genes prediction of miR-22 in breast cancer\*

Tao Fan<sup>1</sup>, Chaoqi Wang<sup>2</sup> (Co-first author), Kun Zhang<sup>3</sup>, Hong Yang<sup>1</sup>, Juan Zhang<sup>1</sup>, Wanyan Wu<sup>1</sup>, Yingjie Song<sup>4</sup> (✉)

<sup>1</sup> Department of Oncology, The People's Hospital of China Three Gorges University, The First People's Hospital of Yichang, Yichang 443000, China

<sup>2</sup> Department of Urinary Surgery, Affiliated Hospital of Inner Mongolia University for the Nationalities, Tongliao 028007, China

<sup>3</sup> Department of Orthopedics, The People's Hospital of China Three Gorges University, The First People's Hospital of Yichang, Yichang 443000, China

<sup>4</sup> Department of General Surgery, The People's Hospital of China Three Gorges University, The First People's Hospital of Yichang, Yichang 443000, China

## Abstract

**Objective** miR-22 is highly active in breast cancer, especially in the luminal B and HER2 subtypes. However, the detailed potential of the use of target genes for miR-22 in breast cancer are still unclear. In this study, we aimed to discover potential genes and the miRNA-DEGs network of miR-22 in breast cancer using bioinformatics approaches.

**Methods** Analysis of microarray data GSE17508 (including 3 miR-22 knockout samples and 3 controls) obtained from the Gene Expression Omnibus (GEO) database was performed. Differentially expressed genes (DEGs) between the miR-22 knockout samples and the three control samples were detected using GEO2R. The gene ontology (GO) functional enrichment analysis and protein-protein interaction (PPI) network of DEGs were performed using the online tool Metascape and STRING database, separately. The miR-22 and DEG networks were obtained from the miRNet database. Cytoscape software was used to construct and analyze a merged miRNA-DEG network. The online tools database, mirDIP 4.1, was used to predict miR-22 target genes.

**Results** Certain DEGs and miRNAs may be potential targets for predicting and treating miR-22 expressed breast cancer.

**Conclusion** We constructed a prognostic model of rectal adenocarcinomas based on four immune-related lncRNAs by analyzing the data based on TCGA database, with high prediction accuracy. We also identified two biomarkers with poor prognosis (PXN-AS1 and AL158152.2) and one biomarker with good prognosis (LINC01871).

**Key words:** bioinformatics; breast cancer; MCF7 cells; MiR-22

Received: 5 October 2020

Revised: 25 October 2020

Accepted: 15 November 2020

MicroRNAs (miRNAs) are a class of noncoding single-stranded RNA molecules with a length of about 22 nucleotides encoded by endogenous genes, which coordinate multiple gene expression programs through gene regulation [1–2]. There are over 1,700 identified miRNAs in the human genome that are associated with a wide variety of human cancers, such as breast, lung, and colon cancer [2–3]. Research suggests that miRNAs may be related to the pathogenesis of cancer, tumor

growth, and metastasis, and play the role as oncogenes or tumor suppressor genes [4]. Therefore, the identification of miRNA targets is considered to be key in improving our understanding of the regulatory effects of miRNAs. miR-22 has been identified as a regulator of lipid and folic acid metabolism in breast cancer cells through the systematic integration of the molecular spectrum [5]. Song *et al.* found that miR-22 regulated breast cancer stemness and metastasis via TET (ten eleven translocation) family

✉ Correspondence to: Yingjie Song. Email: 1601340054@qq.com

\*Supported by the Joint Fund Project of Hubei Provincial Health Committee (No. WJ2019H510) and the Natural Science Foundation of Inner Mongolia Autonomous Region (No. 2015MS0877), China.

© 2021 Huazhong University of Science and Technology

dependent chromatin remodeling [6]. Experiments and clinical studies show that miR-22 promoted epithelial mesenchymal transition and tumor invasion and metastasis [7]. Hence, exploring miR-22 target genes is important for targeted therapy of breast cancer.

In this study, the differentially expressed genes (DEGs) from microarray data in the GEO database were identified between knockout or duplex miR-22 samples in human breast cancer MCF-7 cell lines. Online tools including mirDIP 4.1 software were used to predict miR-22 target genes. We aimed to explore certain differential genes, and miRNAs may be potential targets for predicting and treating miR-22 expressed breast cancer.

## Materials and methods

### Microarray data filtering eligible data set

We searched and downloaded microarray data GSE17508 (including three miR-22 knockout samples and three controls) from the GEO database ([www.ncbi.nlm.nih.gov/geo/](http://www.ncbi.nlm.nih.gov/geo/)). The datasets used human breast cancer MCF-7 cell lines. Microarray data were used to analyze the eligible data set and identify the gene expression patterns.

### DEGs' screening

DEGs were independently screened using the GEO2R online tool in the GEO database. In our study, DEGs between miR-22 knockout samples and controls were screened and selected by the cut-off point of adj. *P* value < 0.05 and  $|\log FC| > 0.5$ .

### Functional enrichment and protein-protein interaction (PPI) analysis

The functions of DEGs were further analyzed using the online tool Metascape (<http://metascape.org/gp/index.html#/main/step1>). The terms with *P*-value < 0.01, minimum count of 3, and enrichment factor > 1.5 were collected and grouped into clusters based on their membership similarities. Furthermore, we obtained the PPI of differential genes using the Search Tool in the Retrieval of Interacting Genes database (STRING, <http://string-db.org/>), and one big pairing picture was generated. In this study, DEGs with a confidence score of > 0.4 were selected to construct the PPI network.

### Established miRNA-DEG network

The DEGs and has-miR-22 were uploaded to the miRNet 2.0 database ([www.mirnet.ca/faces/home.xhtml](http://www.mirnet.ca/faces/home.xhtml)) to acquire a list of miRNA-DEG pairs, and one big pairing picture was generated. The picture was merged with the PPI picture, and a complete and huge miRNAs-DEG network was generated using the Cytoscape 3.6.1 software [8]. Then, the Molecular Complex Detection

(MCODE) plugin was used to module clustering analysis to detect the potential functional modules in the network. In the MCODE process, the cut-off value of degree was set to 2, and the cut-off value of node score was set to 0.2.

### Predicted target genes

To obtain potential target genes, hsa-miR-22 and the DEGs were uploaded to the online tools database mirDIP 4.1 ([http://ophid.utoronto.ca/mirDIP/index\\_confirm.jsp](http://ophid.utoronto.ca/mirDIP/index_confirm.jsp)). Researchers can predict target genes of miRNA with the help of this online tools database. We only selected the gene symbol whose confidence class is considered very high.

## Results

### DEG screening between miR-22 knockout samples and controls

An assessment of data normalization and cross-comparability (Table 1), and then DEGs analysis was carried out.

We applied an online tool (<http://www.heatmapper.ca/expression/>) analysis to discern the differential expression of genes. A total of 40 DEGs were identified in the profiles, including 38 upregulated and 2 downregulated DEGs in breast cancer MCF7 cells (Fig. 1).

### Gene ontology and functional enrichment analysis

Pathway and process enrichment analysis was performed using GO Biological Processes, GO Cellular Components, GO Molecular Functions, KEGG Functional Sets, and KEGG Pathway Ontology sources.

Heatmap-selected GO showed a defense response to virus (GO: 0051607) and interferon signaling (R-HSA-913531) being the top two pathways (Fig. 2a). The heatmap-selected GO parent showed a multi-organism process (GO: 0051704), immune system process (GO: 0002376), and signaling (GO: 0023052) as the top three pathways (Fig. 2b).

### Construction of miRNA-DEG network analysis

Taking the selected 40 DEGs and has-miR-22 into account, we identified 393 PPI pairs using the STRING database as well as a large network of 284 genes and 751 miRNAs using miRNet. Two big pairing pictures mentioned above were merged using Cytoscape software to obtain a complete miRNA-DEG network in Cytoscape. The MCODE plugin in Cytoscape was used to perform the module clustering of the miRNA-DEG network mentioned above, and then the key functional modules of the network were evaluated.

Two modules were identified and showed certain differential genes (Fig. 3 and 4), such as PARP14 (Poly-

**Table 1** Data normalization and cross-comparability

ID	miR-22 knockout			miR-22 duplex		
	GSM436499	GSM436500	GSM436501	GSM436502	GSM436503	GSM436504
1405_i_at	0.671169	2.09665	1.6046	191.673	83.8896	143.034
1555895_at	61.5801	42.5199	44.7025	5.12442	5.76263	5.50906
201641_at	299.389	255.064	267.642	1764.3	1416.32	1435.47
201649_at	189.132	169.375	173.936	2753.45	1971.27	2119.3
202411_at	231.34	254.555	170.62	5884.85	4094.31	4084.7
202446_s_at	746.161	585.523	633.731	4041.83	3528.97	3308.84
202863_at	147.238	136.453	132.913	809.03	896.412	745.35
202869_at	204.487	181.35	139.1	2422.99	1932.6	1909.51
203595_s_at	147.951	142.789	138.859	932.521	756.007	840.578
203964_at	205.023	135.525	185.118	2314.57	1679.31	1899.64
204972_at	26.7859	19.5057	9.41348	1287.85	814.213	1048.49
205660_at	68.5446	40.9388	46.0824	1289.54	794.51	1163.13
208012_x_at	280.53	273.367	246.022	1606.66	1515.08	1492.88
209417_s_at	82.8806	86.9507	91.2375	1103.68	771.531	831.984
209969_s_at	222.731	254.367	227.426	1324.41	1401.89	1295.05
213293_s_at	0.930746	2.59175	1.11313	149.973	79.6659	105.26
214329_x_at	21.8184	19.769	21.3362	229.147	157.749	167.125
218400_at	302.368	241.323	240.435	2008.15	1504.66	1623.47
218543_s_at	111.989	95.0014	115.551	1077.07	792.782	864.665
218943_s_at	112.554	104.418	127.537	1023.37	822.671	978.666
218986_s_at	26.0235	35.4281	33.9382	576.956	616.786	542.616
219209_at	69.2003	90.0639	64.2059	637.783	646.895	599.096
219211_at	76.3393	65.6202	45.6518	1113.93	893.935	944.552
219863_at	25.5529	25.9988	30.3203	435.618	270.39	445.39
223220_s_at	117.359	100.177	95.087	1108.72	949.663	830.072
224701_at	69.3057	45.6731	66.2717	747.816	526.984	605.155
226702_at	32.3924	43.4558	35.3575	1516.01	1143.79	1376.78
226757_at	28.6421	16.0251	25.8946	1015.75	864.11	1089.9
228152_s_at	29.6723	24.0253	19.3472	429.784	281.131	393.66
228230_at	37.0041	35.0767	46.5385	292.262	209.932	258.172
228531_at	28.14	25.3732	22.6905	413.528	307.086	378.416
228617_at	21.1541	14.1225	20.0689	1040.53	693.619	801.349
229450_at	23.0721	30.9242	40.6104	3772.66	2927.48	3140.0
234987_at	63.3734	40.6403	54.9785	494.176	445.555	481.173
235684_s_at	16.245	15.971	19.0761	3.1126	3.62215	3.08859
236156_at	1.32972	0.587631	1.35526	25.3288	24.3493	33.6445
38241_at	1.0171	0.639231	0.931997	28.4628	16.7508	19.8981
53720_at	51.1619	48.4386	40.9648	367.055	295.637	312.053

adenosine diphosphate-ribose polymerase 14), SAMHD1 (Sterile alpha motif and histidine/aspartic acid domain-containing protein 1), CCL5 (C-C chemokine ligand 5), and TNFSF10 (Tumor Necrosis Factor superfamily 10).

The four DEGs, PARP14, SAMHD1, CCL5, and TNFSF10, in these modules also occurred in the GO terms enriched above, which were associated with multi-organism immune processes and signaling pathways. PARP14 and SAMHD1 targeted miRNAs, such as miR-21-3p, miR-138-5p, miR-130a-3p, miR-155-5p, miR-452-5p, and miR-124-3p. We also observed a key hub, miR-146a-5p, that interacted with CCL5 and TNFSF10.

**Predicted target genes**

We identified that upregulated OAS1 and downregulated DEGs may be potential target genes of miR-22-3p. These were predicted using the online tools database mirDIP 4.1, with the confidence class selected as very high (Table 2).

**Discussion**

Breast cancer is the most common malignant tumor in women worldwide, and metastasis is the main cause of death. Increasing evidence indicates that miR-22 is

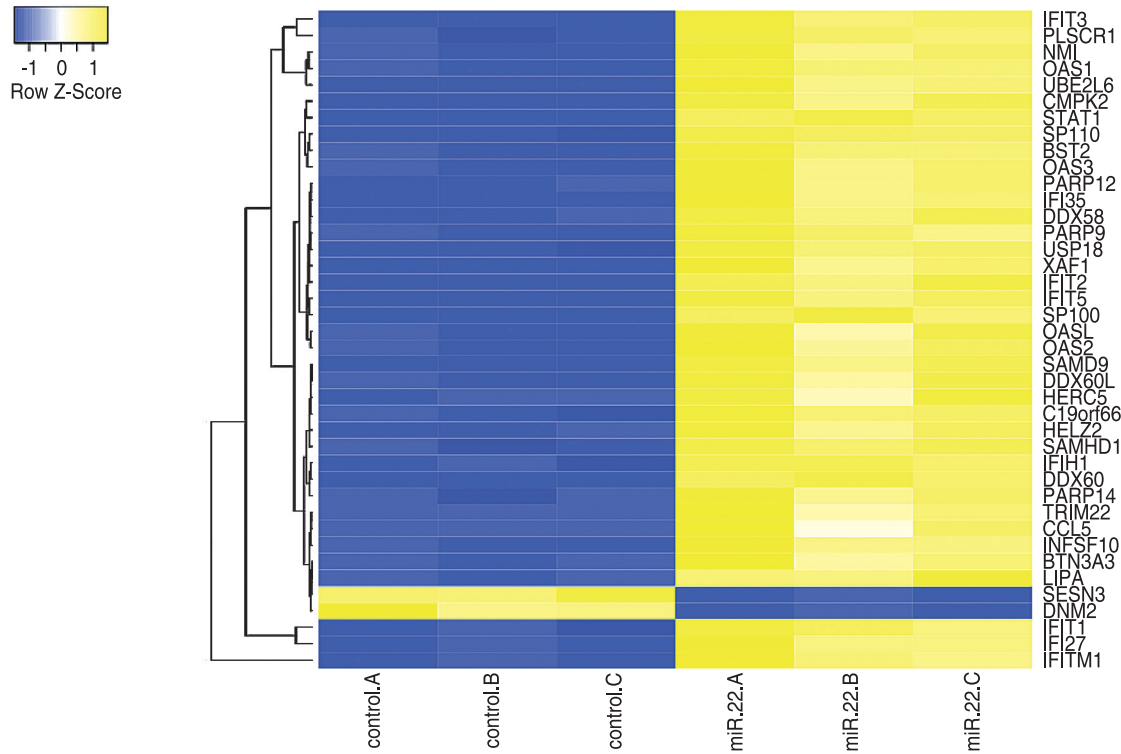


Fig. 1 DEGs expression profiling in breast cancer MCF7 cells.

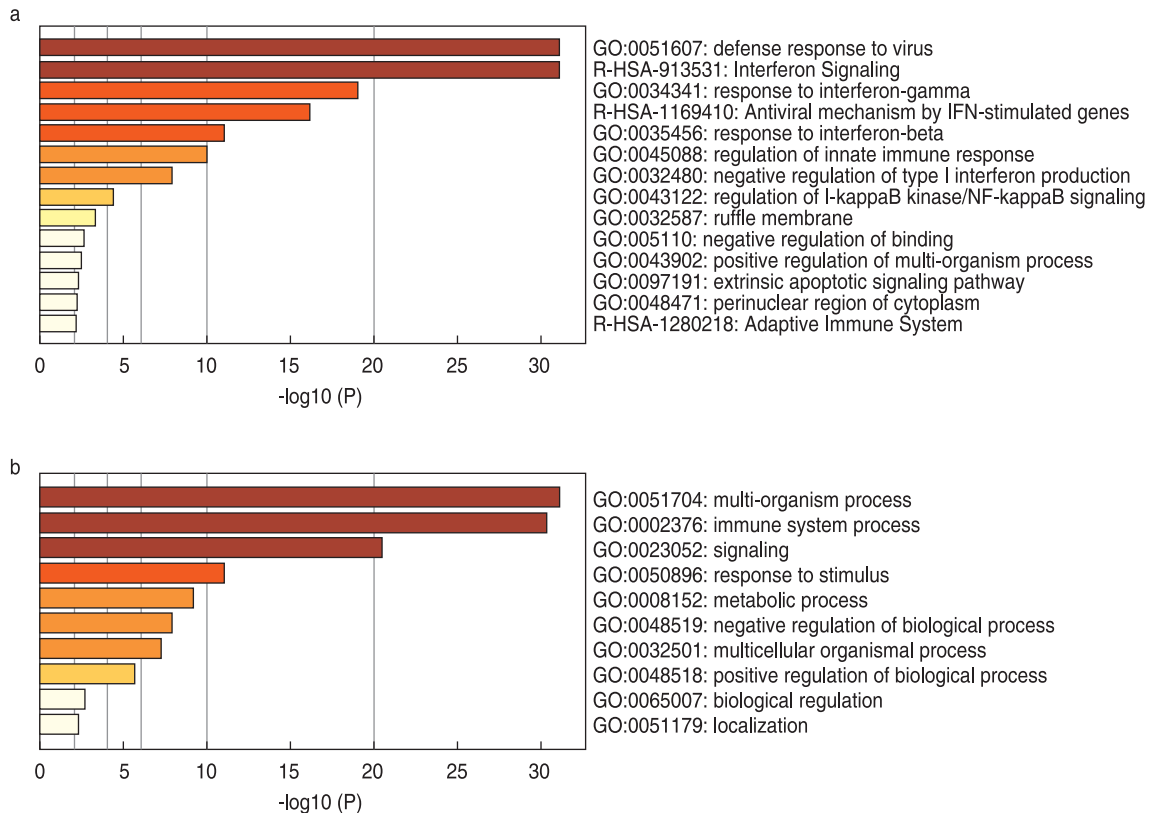
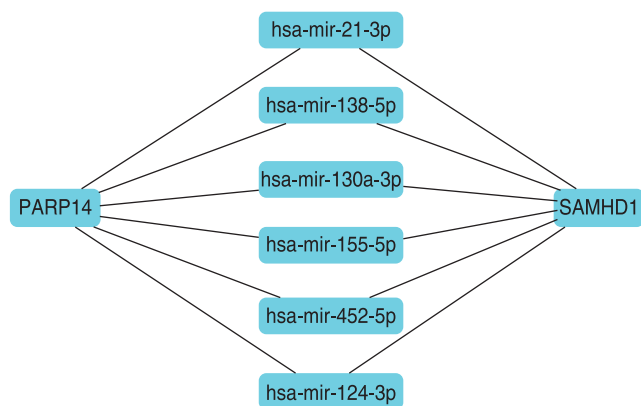


Fig. 2 Distribution of gene ontology terms for the DEGs. (a) heatmap-selected GO; (b) heatmap-selected GO parent

**Table 2** The predicted target genes of hsa-miR-22-3p

Gene	Uniprot	MicroRNA	Rank	Source	Confidence score	Confidence class
OAS1	P00973	hsa-miR-22-3p	0.2208986	microrna.org	0.1054261	Very High
SES3	P58005	hsa-miR-22-3p	0.090834	miRcode	0.1209991	Very High



**Fig. 3** An outstanding hub of DEGs, PARP14 and SAMHD1, interacting with their miRNAs.

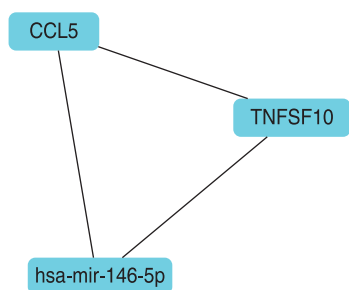


**Fig. 4** Another outstanding hub of DEGs, CCL5 and TNFSF10, interacting with miR-146a-5p.

upregulated in breast tumors compared to its marginal non-tumor counterparts, which are associated with poor overall survival [9–10]. However, the detailed potential target genes of miR-22 in breast cancer are still unclear. Thus, it is very important to study the molecular mechanism of breast cancer metastasis and progression to develop a therapeutic strategy for breast cancer patients.

As the miRNA-DEG network analysis showed, expression of miR-22 was closely related to the PARP14, SAMHD1, CCL5, and TNFSF10 genes in breast cancer MCF7 cells. PARP14 uses nicotinamide adenine dinucleotide (NAD<sup>+</sup>) as a metabolic substrate to modify the target protein by single ADP ribosylation, which is involved in cellular reactions and signaling pathways in the immune system. SAMHD1 is considered an intrinsic viral limiting factor that inhibits the process of viral infection, including retrovirus replication, packaging,

and transmission. Several studies have demonstrated that PARP14 and SAMHD1 are associated with the development of multiple types of cancer, such as lung, colon, breast, myeloma, and pancreatic cancer among others [11–12]. In the present study, through MCODE analysis, we found that PARP14 and SAMHD1 interact with some miRNAs, such as miR-21-3p, miR-138-5p, miR-130a-3p, miR-155-5p, miR-452-5p, and miR-124-3p. We found that miR-21-3p may be the core of the module because the survival analysis of miRNAs shows that the overexpression of miR-21 can significantly reduce the overall survival rate of breast cancer patients [13].

CCL5 is secreted by breast cancer cells and rarely expressed in epithelial cells of normal ducts or benign breast masses [14]. Increasing studies showed that the CCL5/CCR5 axis is involved in tumor growth, migration and angiogenesis in different tumor types, including breast cancer. In addition, CCL5/CCR5 is closely related to the recruitment of tumor-associated immune-suppressive cells and promoting the construction of the tumor microenvironment [14]. We found that CCL5 may also be the core of the module, through MCODE analysis, CCL5 interacts with TNFSF10 and miR-146a-5p. Moreover, in order to predict the target gene of miR-22 in DEGs, through the use of the online tools database mirDIP 4.1, we found that upregulated OAS1 and downregulated SESN3 may be potential target genes of miR-22-3p.

### Conclusion

In summary, certain DEGs and miRNAs may be potential targets and biomarkers for predicting and treating miR-22 expressed breast cancer. However, further studies such as disease models and PCR experiments are necessary to verify these findings.

### Conflicts of interest

The authors indicated no potential conflicts of interest.

### References

- Kim VN. MicroRNA biogenesis: coordinated cropping and dicing. *Nat Rev Mol Cell Biol*, 2005, 6: 376–385.
- Denli AM, Tops BB, Plasterk RH, *et al*. Processing of primary microRNAs by the microprocessor complex. *Nature*, 2004, 432: 231–235.
- He K, Li WX, Guan DG, *et al*. Regulatory network reconstruction of five essential microRNAs for survival analysis in breast cancer

- by integrating miRNA and Mrna expression datasets. *Funct Integr Genomics*, 2019, 19: 645–658.
4. Meltzer PS. Cancer genomics: small RNAs with big impacts. *Nature* 2005, 435: 745–746.
  5. Koufaris C, Valbuena GN, Pomyen Y, *et al.* Systematic integration of molecular profiles identifies miR-22 as a regulator of lipid and folate metabolism in breast cancer cells. *Oncogene*, 2016, 35: 2766–2776.
  6. Song SJ, Ito K, Ala U, *et al.* The oncogenic microRNA miR-22 targets the TET2 tumor suppressor to promote hematopoietic stem cell self-renewal and transformation. *Cell Stem Cell*, 2013; 13: 87–101.
  7. Farazi TA, Ten HJJ, Brown M, *et al.* Identification of distinct miRNA target regulation between breast cancer molecular subtypes using AGO2-PAR-CLIP and patient datasets. *Genome Biol*, 2014, 15: R9.
  8. Saito R, Smoot ME, Ono K, *et al.* A travel guide to cytoscape plugins. *J Nat Methods*, 2012, 9: 1069–1076.
  9. Damavandi Z, Torkashvand S, Vasei M, *et al.* Aberrant expression of breast development-related MicroRNAs, miR-22, miR-132, and miR-212, in breast tumor tissues. *J Breast Cancer*, 2016, 19: 148–155.
  10. Pandey AK, Zhang Y, Zhang S, *et al.* TIP60-miR-22 axis as a prognostic marker of breast cancer progression. *Oncotarget*, 2015, 6: 41290–41306.
  11. Qin W, Wu HJ, Cao LQ, *et al.* Research progress on PARP14 as a drug target. *Front Pharmacol*, 2019, 10: 172.
  12. Zhang Z, Zheng L, Yu Y, *et al.* Involvement of SAMHD1 In dNTP homeostasis and the maintenance of genomic Integrity and oncotherapy (Review). *Int J Oncol*, 2020, 56: 879-888.
  13. He K, Li WX, Guan DG, *et al.* Regulatory network reconstruction of five essential microRNAs for survival analysis in breast cancer by integrating miRNA and mRNA expression datasets. *Funct Integr Genomics*, 2019, 19: 645–658.
  14. Aldinucci D, Borghese C, Casagrande N. The CCL5/CCR5 axis in cancer progression. *Cancers (Basel)*, 2020; 12: 1–30.

**DOI 10.1007/s10330-020-0458-8**

**Cite this article as:** Fan T, Wang CQ, Zhang K, *et al.* Differentially expressed genes analysis and target genes prediction of miR-22 in breast cancer. *Oncol Transl Med*, 2021, 7: 59–64.

# Study on the antitumor effects of autologous and allogeneic CIK cells in patients with breast cancer\*

Xia Chen<sup>1</sup>, Zhijian Dai<sup>2</sup>, Xiangji Lu<sup>3</sup>, Meng Ren<sup>2</sup>, Zhenshan Guo<sup>2</sup>, Yanwei Gao<sup>2</sup> (✉)

<sup>1</sup> Department of Apheresis, Inner Mongolia Red Cross Blood Center, Hohhot 010010, China

<sup>2</sup> Department of Surgical Oncology, Inner Mongolia People's Hospital, Hohhot 010017, China

<sup>3</sup> Department of General Surgery, Inner Mongolia Armed Police Hospital, Hohhot 010010, China

## Abstract

**Objective** This study aimed to compare the anti-tumor effects of cytokine-induced killer (CIK) cells induced by autologous cytokines in patients with breast cancer and those of allogeneic CIK cells from healthy adults.

**Methods** We used conventional methods to induce CIK cells originating from two peripheral blood mononuclear cell types (from patients with breast cancer and healthy adults). Killing activity was detected using an LDH assay, immunophenotypic changes were analyzed by flow cytometry, and the IFN- $\gamma$  level of culture supernatants was detected by ELISA.

**Results** The results showed that the proliferative capacity of the allogeneic CIK cells was significantly higher than that of the autologous CIK cells. Compared with autologous CIK cells, the allogeneic CIK cells had significantly enhanced anti-tumor activity against SKBR-3 cells ( $P < 0.01$ ) and IFN- $\gamma$  secretion ( $P < 0.05$ ); moreover, they increased the ratio of CD3+ CD56+ cells and CD3+ CD8+ cells ( $P < 0.05$ ).

**Conclusion** Healthy adult-derived induced CIK cells exhibited a stronger anti-tumor effect than induced CIK cells derived from patients with breast cancer. The results of this study could provide experimental evidence for the clinical application of CIK cells.

**Key words:** CIK cells; autologous; allogeneic; cellular immunotherapy; breast cancer

Received: 24 February 2021

Revised: 12 March 2021

Accepted: 15 April 2021

As a new model for treatment following surgery, radiotherapy, and chemotherapy, biological treatment of tumors is gradually being accepted by a majority of patients due to its safety, effectiveness, and low level of side effects. It has been widely used in the treatment of cancer patients on both national and international levels, achieving good results. At the beginning of 2014, *Science*, an authoritative American magazine, even rated tumor immunotherapy among “the top ten technological breakthroughs in 2013”<sup>[1]</sup>.

CIK cell adoptive immunotherapy is an important method of tumor biotherapy. CIK cells are immunocompetent cells that can be obtained by separating mononuclear cells from peripheral blood, bone marrow, or cord blood and culturing them in the presence of multiple cytokines for a certain period<sup>[2,3]</sup>. At present, the common treatment method in China is to induce CIK cells from the peripheral blood of tumor patients and then reintroduce them into the patient

for immunotherapy. Certain studies have revealed that tumor patients have under-functioning immunity and immune cells, which potentially affect the treatment effect. Moreover, it was suggested that the healthy lineal relatives of tumor patients should be considered as treatment cell donors<sup>[4]</sup>. In this study, we compared the antitumor effects of autologous and allogeneic CIK cells in patients with breast cancer to determine the more effective CIK cell adoptive immunotherapy.

## Materials and methods

### Case selection

We randomly selected 61 patients with breast cancer from the Department of oncology, people's Hospital of Inner Mongolia Autonomous Region, from June 2019 to May 2020. One month after the operation (without radiotherapy, chemotherapy, and other adjuvant treatment), peripheral venous blood was taken from the

✉ Correspondence to: Yanwei Gao. Email: gaoyw0518@163.com

\*Supported by a grant from the National Natural Sciences Foundation of Inner Mongolia (No. 2012MS1102).

© 2021 Huazhong University of Science and Technology

patients and their lineal relatives (with no history of malignant tumor and the same ABO blood group as the patients).

### CIK cell induction

Peripheral blood mononuclear cells (PBMCs) were obtained from the peripheral blood of patients with breast cancer and their lineal relatives by density gradient centrifugation using the human lymphocyte separation solution. We used RPMI1640 medium containing 10 % calf serum to culture the cells at 37 °C and 5% CO<sub>2</sub> in an incubator for 2 h; we collected non-adherent cells and placed them in a new culture flask. After adjusting the cell density to  $1 \times 10^6$ /mL, the cells were supplemented with IFN- $\gamma$  (1000 U/mL), CD3 monoclonal antibody (50  $\mu$ g/mL), IL-2 (300 U/mL), and IL-1  $\alpha$  (100 U/mL). Then, the cells were counted every 3 days and supplemented with a fresh medium containing 300 U/mL IL-2.

### Tumor cell culture

SKBR-3 cells were cultured in an RPMI1640 medium containing 10 % calf serum at 37°C and 5 % CO<sub>2</sub>. Cells in the logarithmic growth phase were sampled for use in the experiment.

### Immunophenotypic detection of CIK cells

We collected autologous and allogeneic CIK cells from patients with breast cancer on day 15 of culture and analyzed them by flow cytometry with direct immunofluorescence labeling.

### Detection of secretory cytokines

We investigated the IFN- $\gamma$  secretion levels of autologous and allogeneic CIK cells from patients with breast cancer on day 15 of culture using the ELISA double antibody sandwich method.

### Cytotoxicity test

We used SKBR-3 cells in the logarithmic growth phase as target cells and autologous and allogeneic CIK cells as effector cells. The specific cytotoxicity was detected using the LDH release method. The effector and target cells were incubated in RPMI1640 medium containing 10 % FBS at 37 °C for 4 h. We detected the LDH release level of the cells using an ELISA kit and calculated the target cell lysis rate.

### Statistical analysis

We used the SPSS 18.0 software to analyze the results. The results are expressed as the mean  $\pm$  SD. We used the *t*-test to compare the different groups and considered  $P < 0.05$  as indicative of statistical significance.

## Results

### CIK cell proliferation ability analysis

Fig. 1 shows the proliferation rate comparison of the two CIK cell groups cultured on days 2, 5, 8, 11, and 14. The two groups of CIK cells began to proliferate on culture days 3-4 and were in the active growth phase by days 6-7. The proliferation rate of the allogeneic CIK cells was significantly higher than that of the autologous CIK cells in patients with breast cancer.

### CIK cell immunophenotype detection

On culture day 15, the proportion of allogeneic CD3<sup>+</sup>CD8<sup>+</sup> and CD3<sup>+</sup>CD56<sup>+</sup> double-positive CIK cells was significantly higher than that of the autologous CIK cells of the patients with breast cancer under the same conditions (Fig. 2).

### Detection of cytokines secreted by the CIK cells

Fig. 3 shows the results of the ELISA, which detected the level of IFN- $\gamma$  secreted by the CIK cells in the two groups. The level of IFN- $\gamma$  secreted by the CIK cells ( $1 \times 10^6$ ) in the allogeneic group on culture day 15 was significantly higher than that secreted by the CIK cells in the autologous group.

### Detection of the antitumor activity of the CIK cells

The cytotoxicity of the two cell groups against human breast cancer SKBR-3 cells was detected by a non-radioactive 4-hour LDH release assay. The dissolution rates of target cells with different target-to-effector ratios are shown in Fig. 4. The results showed that, with the increase in the effector-to-target ratio, the killing

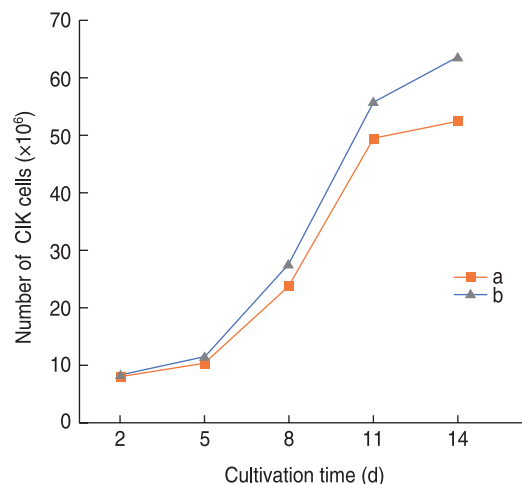
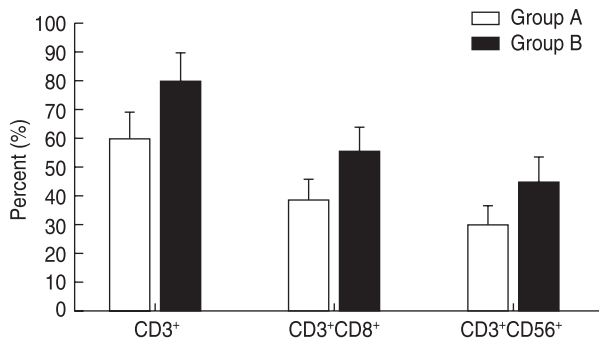
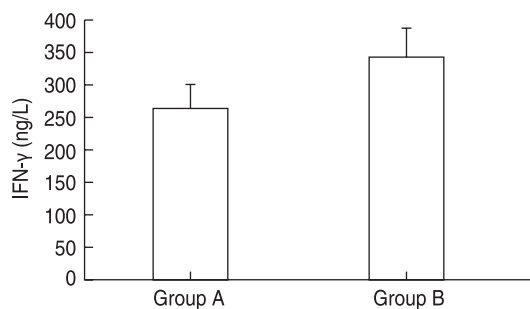


Fig. 1 Analysis of CIK cell proliferation. Lines a and b represent the autologous CIK cells of patients with breast cancer and allogeneic CIK cells of their healthy lineal relatives, respectively



**Fig. 2** Immunophenotype detection of the two CIK cell groups. Groups A and B represent the autologous CIK cells of patients with breast cancer and allogeneic CIK cells of their healthy lineal relatives, respectively



**Fig. 3** Detection of IFN-γ secreted by the two CIK cell groups. Groups A and B represent the autologous CIK cells of patients with breast cancer and allogeneic CIK cells of their healthy lineal relatives, respectively

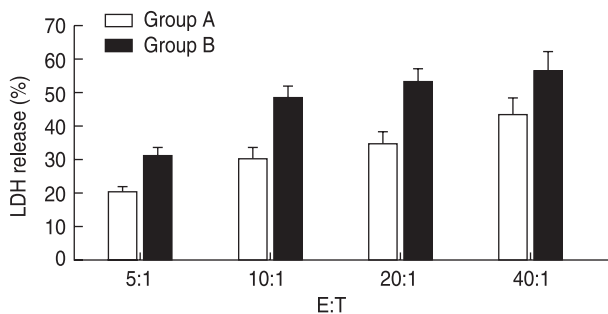


**Fig. 4** The lysis rates of the two groups of CIK cells for SKBR-3 cells. Groups A and B represent the autologous CIK cells of patients with breast cancer and allogeneic CIK cells of their healthy lineal relatives, respectively

activity of the two effector cell groups also increased. At the same effector-to-target ratio, the killing activity of the allogeneic CIK cells was higher than that of the autologous CIK cells ( $P < 0.01$ ).

## Discussion

Tumor biotherapy is considered to be the only way to cure cancer. As a new treatment approach after surgery,

radiotherapy, and chemotherapy, tumor biotherapy is gradually being accepted by a majority of patients, due to its safety, effectiveness, and low level of side effects. It is widely used in the treatment of tumor patients both nationally and internationally, and has given good results. Adoptive cellular immunotherapy is the most common and effective approach for tumor biotherapy. It mainly enhances the anti-tumor effect of the immune system by stimulating cultured immune cells *in vitro* to inhibit or eliminate tumors [1, 5]. Several national and international clinical studies have confirmed that adoptive cellular immunotherapy has obvious therapeutic effects on a variety of malignant tumors, including breast cancer; malignant tumors of the digestive, urinary, and hematological systems; and gynecological malignant tumors and malignant melanoma. Adoptive cell immunotherapy mainly uses immune cells, such as lymphokine-activated killer cells (LAK), tumor-infiltrating lymphocytes (TIL), and cytokine-induced killer cells (CIK), of which CIK cells are the most widely used [6-7].

The first CIK cell phase I clinical trial conducted was that by Schmidt wolf *et al.* The authors transfused autologous CIK cells back into 10 patients with malignant tumors, which confirmed the efficacy and safety of CIK cells for clinical treatment for the first time. Subsequently, due to the advantages of CIK cells and the progress of the *in vitro* induction and amplification technology, CIK cells became widely used in the clinical treatment of a variety of malignant tumors. It is worth mentioning here, that, although early CIK cell research originated from the United States and Europe, clinical application of CIK cells in other countries is far less significant than that in China. At present, hundreds of scientific research institutions and hospitals in China have carried out CIK cell-related clinical research and treatment. The results of these scientific and medical efforts provide significant clinical data to further progress the CIK cell induction and treatment technology in the world, representing an important contribution [8-10].

The clinical application of CIK cells mainly includes the following aspects: (1) Elimination of small residual lesions in patients with a complete response and survival prolongation. (2) Combination with traditional tumor treatment methods (such as surgery, radiotherapy, and chemotherapy) to treat malignant tumors. (3) Use, alone, in patients with advanced malignant tumors who cannot tolerate other treatment options. CIK cells yield excellent results in terms of minimizing side effects. To date, no serious adverse reactions and death events related to CIK cell therapy have been reported in clinical application. Very few patients showed mild adverse reactions, such as fever or fatigue, most of which were relieved on their own, and only a few patients needed simple symptomatic

treatment<sup>[11]</sup>.

At present, CIK cells used in clinical treatment nationally and internationally are mostly induced using the autologous peripheral blood mononuclear cells of tumor patients. The reason for using this approach is that autologous CIK cells might recognize the surface markers of tumor cells and have strong tumor antigen activity. However, in recent years, certain researchers brought attention to the low level of immunity and poor activity of immune cells in tumor patients, which could affect the therapeutic effect of autologous CIK cells<sup>[12]</sup>. In this study, we compared various activities (including proliferation, cytokine secretion, and anti-tumor effect) of autologous CIK cells and allogeneic CIK cells (induced by peripheral blood mononuclear cells from healthy lineal relatives) in 61 patients with breast cancer. The results showed that the proliferation ability of CIK cells in healthy adults was significantly higher than that of autologous CIK cells in breast cancer patients, and the ratio of CD3 + CD8 + and CD3 + CD56 + cells in healthy adults was significantly higher than that of autologous CIK cells in breast cancer patients ( $P < 0.05$ ). At the same culture time-point, the level of IFN- $\gamma$  secreted by allogeneic CIK cells was higher than that secreted by autologous CIK cells ( $P < 0.05$ ). In vitro killing experiments confirmed that the anti-tumor activity of healthy human CIK cells against tumor cells was stronger than that of autologous CIK cells of tumor patients under the same effector-to-target ratio ( $P < 0.01$ ), and this anti-tumor activity increased with the increase of the effector-to-target ratio.

Patients with malignant tumors often have impaired immune function, which affects the anti-tumor effect of autologous CIK cells. The breast cancer patients selected in this study had just finished surgery, without chemotherapy, radiotherapy, or other adjuvant therapies that might have caused myelosuppression, and the number of peripheral blood mononuclear cells in them was relatively high. The number and biological activity of autologous CIK cells induced in patients after chemotherapy and other treatments may be even lower. The CIK cells of healthy people have stronger anti-tumor activity *in vitro*, have a wide range of sources, and proliferate faster; thus, they can greatly shorten the patient's waiting time for treatment while exerting anti-tumor effects. With the development of research on the isolation and purification of CIK cells and tumor

antigens, adoptive immunotherapy using CIK cells will be more widely accepted and play an important role in the comprehensive treatment of malignant tumors.

### Conflicts of interest

The authors indicated no potential conflicts of interest.

### References

1. McNutt M. Cancer immunotherapy. *Science*, 2013, 342: 1432–1433.
2. Gao YW, Chen X, Gao WS, *et al.* A study on melanoma treatment using dendritic cells loaded with antigens purified from melanoma cell lines. *Oncol Transl Med*, 2020, 6: 9–13.
3. Zhang Z, Wang LP, Luo ZZ, *et al.* Efficacy and safety of cord blood derived cytokine-induced killer cells in treatment of patients with malignancies. *Cytotherapy*, 2015, 17: 1130–1138.
4. Zhang YH, Wang SB, Yang BB, *et al.* Adjuvant treatment for triple-negative breast cancer: a retrospective study of immunotherapy with autologous cytokine-induced killer cells in 294 patients. *Cancer Biol Med*, 2019, 16: 350–360.
5. Shou CC, Wu AW. Application of biotherapy in recurrent or metastatic gastric cancer. *Zhonghua Wei Chang Wai Ke Za Zhi*, 2011, 14: 569–572.
6. Timalansa S, Lamichhane PP. Cytokine induced killer (CIK) cells based adoptive immunotherapy. *J-GMC-N*, 2017, 2: 58–63.
7. Lee HK, Kim YG, Kim JS, *et al.* Cytokine-induced killer cells interact with tumor lysate-pulsed dendritic cells via CCR5 signaling. *Cancer Lett*, 2016, 378: 142–149.
8. Schmidt-Wolf IG, Negrin RS, Kiem HP, *et al.* Use of a SCID mouse/human lymphoma model to evaluate cytokine-induced killer cells with potent antitumor cell activity. *J Exp Med*, 1991, 174: 139–149.
9. Schmidt-Wolf IG, Finke S, Trojaneck B, *et al.* Phase I clinical study applying autologous immunological effector cells transfected with the interleukin-2 gene in patients with metastatic renal cancer, colorectal cancer and lymphoma. *Br Cancer J*, 1999, 6: 1009–1016.
10. Mata-Molanes JJ, Sureda González M, Valenzuela Jiménez B, *et al.* Cancer immunotherapy with cytokine-Induced killer cells. *Target Oncol*, 2017, 12: 289–299.
11. Meng Y, Yu Z, Wu Y, *et al.* Cell-based immunotherapy with cytokine-induced killer (CIK) cells: From preparation and testing to clinical application. *Hum Vaccin Immunother*, 2017, 13: 1–9.
12. Hayes C. Cellular immunotherapies for cancer. *Ir J Med Sci*, 2021, 90: 41–57.

DOI 10.1007/s10330-021-0483-3

Cite this article as: Chen X, Dai ZJ, Lu XJ, *et al.* Study on the antitumor effects of autologous and allogeneic CIK cells in patients with breast cancer. *Oncol Transl Med*, 2021, 7: 65–68.

# KIF15 expression characteristics: Relevance to neo-adjuvant chemotherapy efficacy in breast cancer\*

Mengting Dong, Chunyang Li, Patiguli-Jiapaer, Xiaofei Li, Xiaohong Xue, Ke Jiang(✉), Jiayu Sheng (✉)

Department of Breast Diseases, Yueyang Hospital of Integrated Traditional Chinese and Western Medicine, Shanghai University of Traditional Chinese Medicine, Shanghai, China

## Abstract

**Objective** The relationship between the expression of kinesin family member 15 (KIF15) and clinicopathological features in breast cancer (BC) remains controversial. In this study, we aimed to explore the influence of KIF15 expression on the efficacy of neoadjuvant chemotherapy (NAC) and evaluate its clinical value in predicting prognosis for BC patients.

**Methods** Immunohistochemistry was used to detect KIF15 expression in 93 BC patients undergoing NAC to analyze the relationship between KIF15 expression and clinical efficacy and analytical parameters.

**Results** Of the 93 BC patients enrolled, 24.73% who underwent NAC had higher KIF15 expression levels, showing positive correlations with ER, HER-2, Ki67, and lymph node metastasis ( $P < 0.05$ ). The clinical benefit of NAC was 70.97%, and the major histological response (MHR) rate was 61.29%. The effective therapeutic rate in patients with high KIF15 expression was 95.65%, while the MHR rate was 65.22%. Various molecular BC subtypes with varied clinical and pathological responses exhibited correlation to a large extent. Of all the BC patients studied, 84% of the triple-negative breast cancer (TNBC) patients were evaluated as clinically effective, and 52% of the TNBC patients were evaluated as pathologically effective, and these values were significantly higher than those of the other molecular types ( $P < 0.05$ ). The expression of KIF15 in 25 TNBC patients showed positive correlations with lymph node metastasis.

**Conclusion** Overexpression of KIF15 was shown to increase BC sensitivity to chemotherapy and demonstrated better outcomes.

**Key words:** breast cancer; neoadjuvant chemotherapy; KIF15; molecular subtypes

Received: 13 January 2021

Revised: 31 January 2021

Accepted: 1 March 2021

Breast cancer (BC) is the leading malignancy that seriously threatens the health of women [1–3]. Approximately 35% of the therapy failures in BC patients are attributed to tumor chemoresistance [4]. At present, there are no predictive biomarkers identified for assessing the therapeutic effects of adjuvant chemotherapy in BC patients. There is a certain degree of uncertainty in choosing chemotherapy regimens, and thus, we sought to identify an effective marker that might be a potential therapeutic target in BC and predict responses to

chemotherapy.

Kinesin family member 15 (KIF15) belongs to the kinesin superfamily of proteins. Previous studies have reported that the overexpression of KIF3C, KIF5A, and KIF12 plays a role in mediating resistance to the chemotherapeutic agent docetaxel [5]. In BC, KIF15 is associated with poor prognosis [6–7], and therefore, KIF15 is expected to be a new marker of chemosensitivity and a target with therapeutic potential. Patients with locally advanced BC generally receive neoadjuvant

✉ Correspondence to: Ke Jiang. Email: surgeonjk@163.com

Jiayu Sheng. Email: sjy1983sh@163.com

\* Supported by grants from the National Natural Science Foundation of China (No. 82004240), the Scientific Research Program of Shanghai Science and Technology Commission (No. 17401935300), Special Research Projects for Graduate Student Innovation and Training of Shanghai University of Traditional Chinese Medicine (No. Y20200073), the Shanghai Municipal Health and Family Planning Commission (No. 2018LQ020) and the Shanghai Office of Traditional Chinese Medicine Development (No. ZY2018- 2020-RCPY-2009).  
© 2021 Huazhong University of Science and Technology

chemotherapy (NAC) to shrink breast tumors prior to surgical removal. Another important role of NAC is in the evaluation of the effects of NAC regimens for guiding the selection of postoperative chemotherapy approaches [8-9]. Hence, in this study, the expression levels of KIF15 in tumor tissues of 93 BC patients were analyzed, and relationships involving KIF15 and clinicopathological parameters as well as NAC efficacy were evaluated.

## Materials and methods

### Patient cohort

Ninety-three primary invasive breast carcinoma specimens were obtained from the Yueyang Hospital of Integrated Traditional Chinese and Western Medicine, Shanghai University of Traditional Chinese Medicine (Shanghai, China) between 2016 and 2018. The inclusion criteria were as follows: (1) all patients with histopathological diagnosis of invasive BC; (2) all BC patients for whom immunohistochemical staining of KIF15 was performed for their tumors; (3) all patients who were at stage II or III according to the American Joint Committee on Cancer (AJCC) TNM staging system for BC (7th edition); and (4) patients with an Eastern Cooperative Oncology Group performance status of 0 or 2. The exclusion criteria were as follows: (1) patients with incomplete clinical data; (2) with distant metastasis; (3) who underwent NAC previously, and who received any anti-tumor therapy; and (4) with severe abnormality of liver and kidney function before undergoing NAC.

A total of 93 patients with a median age of 56 years (ranging between 28 and 75 years) were included. All women enrolled had single unilateral invasive BC lesions. All patients had primary lesions and none had undergone chemotherapy, radiotherapy, or endocrine therapy before surgical intervention. Estrogen receptor (ER), progesterone receptor (PR), HER2, and KI67 status was determined by immunostaining core-needle biopsy samples of BC tissues obtained before the initiation of NAC. Among the 93 patients, 92 had invasive ductal cancer (98.9%) and 1 patient (1.08%) had invasive apocrine adenocarcinoma. Molecular typing revealed 26 luminal A (28.0%), 21 luminal B (22.6%), 25 triple negative (26.9%) and 21 HER2-positive (22.6%) cases. Clinical staging before NAC showed that 49 patients were at stage II (52.7%) and 47 were at stage III (50.5%). This study was approved by the Institutional Review Board of the Yueyang Hospital of Integrated Chinese and Western Medicine affiliated with the Shanghai University of Traditional Chinese Medicine. All patients provided signed informed consent.

For all patients, paclitaxel (80 mg/m<sup>2</sup>) was administered weekly starting from day 1 for 16 weeks, and cisplatin 25 mg/m<sup>2</sup> was given weekly on days 1, 8, and 15 every 28

days for four cycles as an NAC therapy regimen. HER2 positive patients could have trastuzumab concurrently with the chemo therapy in the neoadjuvant setting. The trastuzumab was given every week at 4 mg/kg (cycle 1), followed by 2 mg/kg, and used for a year. Postoperative chemotherapy for non-pCR patients was left to the discretion of the attending physician. Planned surgery was sequentially provided after neoadjuvant therapy. All procedures performed in this study involving human participants were done in accordance with the ethical standards of the institutional and/or national research committee and with the 1964 Helsinki declaration and its later amendments or comparable ethical standards.

### Immunohistochemistry (IHC)

ER, PR, Ki-67, HER2, and KIF15 levels were evaluated using paraffin-embedded tumor samples obtained via biopsy. ER, PR, HER2, and Ki-67 were detected using rabbit monoclonal antibodies SP1, EE2, 4B5 (Hoffmann-La Roche Ltd., Switzerland), and MIB1 (Leica Biosystems Newcastle Ltd., UK). KIF15 was detected using a goat anti-KIF15 monoclonal antibody (Abcam, USA).

IHC staining results were judged by two independent pathologists from the Department of Pathology of our hospital. Positive ER and PR were defined as > 1% positive nuclear staining, and Ki-67 levels were recorded as a continuous value. HER2 assessments were conducted according to the American Society of Clinical Oncology (ASCO)/College of American Pathologists (CAP) recommendations, 2013 [10]. KIF15 evaluation was performed according to the following criteria. The percentage of positively-stained tumor cells was graded based on a four-point scale, which was as follows: (1) percentage of positive cells ≤ 10%; (2) 11% < percentage of positive cells ≤ 50%; (3) 51% < percentage of positive cells ≤ 75%; and (4) 76% < percentage of positive cells. IHC intensity scores were graded as follows: 0, no staining; 1, weak staining: light yellow; 2, moderate staining: yellow brown; and 3, strong staining: brown. According to the above two indicators, the results were divided into four levels: 0-3 (-), 4-5 (+), 6-7 (++), and ≥ 8 (+++). A score of 0-7 indicated low expression (-), and scores of ≥ 8 indicated high expression (+).

### Efficacy evaluation

Efficacy evaluations included clinical and histopathological evaluations of BC lesions. Tumor assessment was performed every two months by physical examination, mammary magnetic resonance imaging (MRI), and ultrasonography. Clinical efficacy was ranked according to the Response Evaluation Criteria in Solid Tumors (RECIST 1.1) guidelines [11]. Clinical efficacy evaluation was performed according to the World Health Organization (WHO) tumor lesion classification and

curative effect evaluation, including complete remission (CR), partial response (PR), no change (SD), and progress (PD). Effective chemotherapy refers to patients with CR or PR, and ineffective chemotherapy refers to patients with SD or PD.

Final pathological responses were assessed using the Miller-Payne grading system [11], in which pathological responses are divided into five grades based on tumor cellularity comparisons involving pre-NAC core biopsies and postoperative surgical specimens. Miller-Payne response grade 3 to 5 was considered as good pathological responses (GPRs), while grades 1 and 2 were considered as poor pathological responses (PPRs).

### Statistical analysis

SPSS v.22.0 software was used for statistical analysis. Chi-square analysis, Fisher's exact probability test, and Spearman correlation coefficient analysis methods were used for investigation of KIF15 expression, clinicopathological parameters, and differences between subtypes. Statistical tests were two-sided with a significance level of  $P < 0.05$ .

## Results

### KIF15 expression and clinicopathological features

Expression of KIF15 in BC tumor tissues of patients who underwent NAC was detected by IHC (200 ×)

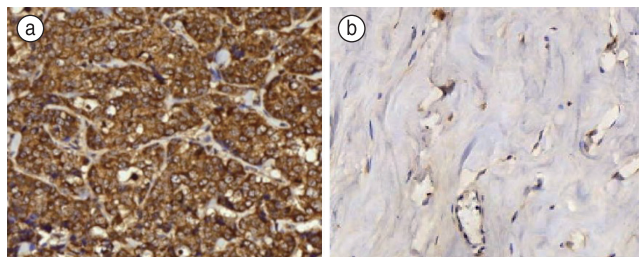


**Fig. 1** Different expressions of KIF15 immunohistochemistry staining. (a) High expression; (b) Low expression

(Fig. 1). The results showed that the expression of KIF15 was upregulated in 23 patients (23/93, 24.73%). Potential correlation between KIF15 expression and clinicopathological characteristics in BC patients was then analyzed. KIF15 exhibited positive correlations with ER ( $P = 0.028$ ,  $r = 0.228$ ), HER-2 ( $P = 0.042$ ,  $r = 0.211$ ), and KI67 expression ( $P = 0.040$ ,  $r = 0.213$ ). Furthermore, lymph node involvement ( $P = 0.031$ ,  $r = 0.224$ ) acted as a predictive factor of KIF15 expression. However, there was no significant correlation with age ( $P = 0.980$ ,  $r = 0.037$ ) or tumor size ( $P = 0.862$ ,  $r = 0.018$ ; Table 1).

### KIF15 expression and the clinical efficacy of NAC

Of the 93 patients, eight showed CR (8.60%), 58 showed PR (62.37%), 23 showed SD (24.73%), and four showed PD (4.30%). The total effective rate (CR + PR) was 70.97% (66/93). The effective chemotherapy rate of NAC in patients with high KIF15 expression was 95.65% (22/23), whereas the effective chemotherapy rate in BC patients with negative or low KIF15 expression was 62.86% (44/70), showing statistically significant differences ( $P = 0.003$ ,  $r = 0.312$ ). Furthermore, HER2 gene amplification ( $P = 0.047$ ,  $r = 0.206$ ) and high Ki-67 proliferation ( $P = 0.048$ ,  $r = 0.205$ ) were also found to be predictive factors of clinical efficacy in NAC therapy (Table 2).

### KIF15 expression and histopathological evaluation of NAC

Of the 93 patients, six had MP1 (6.45%), 51 had MP2 (54.84%), 20 had MP3 (21.51%), 5 had MP4 (5.38%), and 11 had MP5 (11.83%). The GPR (MP3~5) was 61.29% (36/93), and the GPR rate in the high KIF15 expression NAC group was 65.22% (15/23). The GPR rate in the high KIF15 expression group was significantly higher than that in the low KIF15 expression group, and the difference was statistically significant ( $P = 0.003$ ,  $r = 0.312$ ). Furthermore, HER2 amplification ( $P = 0.006$ ,  $r = 0.285$ ) also acted as a predictive factor for histopathological evaluation of NAC (Table 3).

**Table 1** Correlation between KIF15 expression and clinicopathological features of patients with BC receiving neoadjuvant chemotherapy [n (%)]

Variables	n	Age (years)		Lymph node involvement		Tumor size (cm)		ER		HER2		Ki-67	
		> 40	≤ 40	> 0	= 0	> 5	≤ 5	Positive	Negative	Positive	Negative	>14%	≤14%
High expression	23	19 (82.61)	4 (17.39)	21 (91.30)	2 (8.70)	6 (26.09)	17 (73.91)	19 (82.61)	4 (17.39)	18 (78.26)	5 (21.74)	20 (86.96)	3 (13.04)
Low expression	70	60 (85.71)	8 (14.29)	46 (68.57)	22 (31.43)	17 (24.29)	53 (75.71)	40 (57.14)	30 (42.86)	38 (54.29)	32 (45.71)	45 (64.29)	25 (35.71)
$\chi^2$		0.001		4.673		0.030		4.841		4.154		4.228	
P		0.980		0.031		0.862		0.028		0.042		0.040	
r		0.037		0.224		0.018		0.228		0.211		0.213	

**Table 2** Correlation between KIF15 expression and the clinical efficacy of neoadjuvant chemotherapy in BC [n (%)]

Variables	n	Clinical effectiveness						$\chi^2$	P	r
		CR	PR	SD	PD	Effective	Ineffective			
ER										
Positive	41	2 (4.88)	24 (58.54)	11 (26.83)	4 (9.76)	26 (63.41)	15 (36.59)	2.030	0.154	-0.148
Negative	52	6 (11.54)	34 (65.38)	12 (23.08)	0 (0.00)	40 (76.92)	12 (23.08)			
HER2										
Positive	56	6 (10.71)	38 (67.86)	11 (19.64)	1 (1.79)	44 (78.57)	12 (21.43)	3.950	0.047	0.206
Negative	37	2 (5.41)	20 (54.05)	12 (32.43)	3 (8.11)	22 (59.46)	15 (40.54)			
Ki-67										
>14%	74	8 (10.81)	48 (64.86)	16 (21.62)	2 (2.70)	56 (75.68)	18 (24.32)	3.897	0.048	0.205
≤14%	19	0 (0.00)	10 (52.63)	7 (36.84)	2 (10.53)	10 (52.63)	9 (47.37)			
KIF15										
High expression	23	5 (21.74)	17 (73.91)	0 (0.00)	1 (4.35)	22 (95.65)	1 (4.35)	9.037	0.003	0.312
Low expression	70	3 (4.29)	41 (58.57)	23 (32.86)	3 (4.29)	44 (62.86)	26 (37.14)			
All	93	8 (8.60)	58 (62.37)	23 (24.73)	4 (4.30)	66 (70.97)	27 (29.03)			

**Table 3** Correlation between KIF15 expression and histopathological evaluation of neoadjuvant chemotherapy in BC [n (%)]

Variables	n	Histopathological evaluation							$\chi^2$	P	r
		MP1	MP2	MP3	MP4	MP5	GPR	PPR			
ER											
Positive	43	2 (4.65)	23 (53.49)	5 (11.63)	5 (11.63)	8 (18.60)	18 (41.86)	25 (58.14)	0.335	0.563	0.060
Negative	50	4 (8.00)	28 (56)	15 (30.00)	0 (0.00)	3 (6.00)	18 (36.00)	32 (64.00)			
HER2											
Positive	56	2 (3.57)	26 (46.43)	19 (33.93)	3 (5.36)	6 (10.71)	28 (50.00)	28 (50.00)	7.563	0.006	0.285
Negative	37	4 (10.81)	25 (67.57)	1 (2.70)	2 (5.41)	5 (13.51)	8 (21.62)	29 (78.38)			
Ki-67											
>14%	74	5 (6.76)	42 (56.76)	16 (21.62)	3 (5.36)	8 (10.81)	27 (36.49)	47 (63.51)	0.755	0.385	0.090
≤14%	19	1 (5.26)	9 (47.37)	4 (21.05)	2 (5.41)	3 (15.79)	9 (47.37)	10 (52.63)			
KIF15											
High expression	23	2 (8.70)	6 (26.09)	7 (30.43)	2 (4.05)	6 (26.09)	15 (65.22)	8 (34.78)	9.050	0.003	0.312
Low expression	70	4 (5.71)	45 (64.29)	13 (18.57)	3 (10.53)	5 (7.14)	21 (30.00)	49 (70.00)			
All	93	6 (6.45)	51 (54.84)	20 (21.51)	5 (5.38)	11 (11.83)	36 (38.71)	57 (61.29)			

### Molecular subtypes of BC and efficacy of NAC

No significant differences were observed in terms of age, tumor size, and lymph node metastasis in four different subtypes of BC among patients. Correlations between molecular subtypes and clinical efficacy of NAC in BC ( $P = 0.035$ ,  $r = 0.358$ ). The effective rate (CR + PR) in TNBC patients was 84% (21/25), which was higher than that of the other three molecular subtypes. Histopathological evaluations also showed similar results, in which the GPR rate remained the highest in TNBC patients (52%, 13/25). In addition, KIF15 expression levels exhibited associations with the four different subtypes of BC. Elevated expression of KIF15 was detected in 44% (11/25) of the TNBC patients. Compared with the other three types of molecular typing, the difference was statistically significant ( $P = 0.031$ ,  $r = 0.148$ ) (Table 4).

### KIF15 expression and NAC efficacy in TNBC patients

Results for 25 TNBC patients from the 93 patients who underwent NAC were analyzed. KIF15 was positively correlated with lymph node involvement ( $P = 0.042$ ,  $r = 0.435$ ) and histopathological evaluation ( $P = 0.015$ ,  $r = 0.529$ ) (Table 5). In the high KIF15 expression group, 10 patients (90.91%) had lymph node metastases, and this number was higher than that of the low KIF15 expression group. In addition, the GPR rate in the high KIF15 expression group (81.82%, 9/11) was higher than that in the low KIF15 expression group (28.57%, 4/13). However, there was no significant correlation with clinical effectiveness ( $P = 0.105$ ,  $r = 0.387$ ) and tumor size ( $P = 0.056$ ,  $r = 0.445$ ; Table 5).

**Table 4** Correlation between the molecular subtypes of BC and the efficacy of neoadjuvant chemotherapy [n (%)]

Variables	n	Age		Lymph node involvement		Tumor size		Clinical effective		Histopathological evaluation		KIF15 expression	
		> 40	≤ 40	> 0	= 0	> 5 cm	≤ 5 cm	Effective	Ineffective	GPR	PPR	High	Low
Luminal A	26	20 (76.92)	6 (23.08)	21 (80.77)	5 (19.23)	6 (23.08)	20 (76.92)	13 (50.00)	13 (50.00)	4 (15.38)	22 (84.62)	7 (26.92)	19 (73.08)
Luminal B	21	19 (90.48)	2 (9.52)	17 (80.95)	4 (19.05)	3 (14.29)	18 (85.71)	17 (80.95)	4 (19.05)	10 (47.62)	11 (52.38)	2 (9.52)	19 (90.48)
HER2	21	20 (95.24)	1 (4.76)	14 (66.67)	7 (33.33)	8 (38.10)	13 (61.90)	15 (71.43)	6 (28.57)	9 (42.86)	12 (57.14)	3 (14.29)	18 (85.71)
TNBC	25	20 (80.00)	5 (20.00)	17 (68.00)	8 (32.00)	6 (24.00)	19 (76.00)	21 (84.00)	4 (16.00)	13 (52.00)	12 (48.00)	11 (44.00)	14 (56.00)
$\chi^2$		4.437		2.210		3.291		8.627		8.678		8.893	
P		0.218		0.530		0.349		0.035		0.034		0.031	
r		-0.046		0.067		-0.062		0.246		0.258		0.148	

**Table 5** Correlation between the KIF15 expression of the TNBC and the efficacy of neoadjuvant chemotherapy [n (%)]

Variables	n	Age		Lymph node involvement		Tumor size (cm)		Clinical effective		Histopathological evaluation	
		> 40	≤ 40	> 0	= 0	> 5	≤ 5	Effective	Ineffective	GPR	PPR
High expression	11	7 (63.64)	4 (36.36)	10 (90.91)	1 (9.09)	5 (45.45)	6 (54.55)	11 (100.00)	0 (0.00)	9 (81.82)	2 (18.18)
Low expression	14	13 (92.86)	1 (7.14)	7 (50.00)	7 (50.00)	1 (7.14)	13 (92.86)	10 (71.43)	4 (28.57)	4 (28.57)	10 (71.43)
P		0.133		0.042		0.056		0.105		0.015	
r		0.363		0.435		0.445		0.387		0.529	

## Discussion

Mitotic spindle checkpoint genes were previously considered as targets of anticancer therapies. Studies have shown that taxanes inhibit the proliferation of tumor cells by targeting key components of rivet mitotic spindle-microtubules. As is known, disruption of microtubule assembly is equivalent to inhibition of cell proliferation<sup>[9, 10]</sup>. Eg5 is one of the key mitotic microtubule motors, and 38 Eg5-targeted therapies, including paclitaxel treatment, have been shown to exert certain anti-tumor effects<sup>[13]</sup>. However, tumor cell spindles always contribute to resistance and dose restriction whether they are innate or acquired. Therefore, exploring other key spindle components may provide promising targets, which is essential.

Mitotic kinesin, which is a key transducer in cellular mitosis, may act as a novel target with potential roles in cancer therapy. It has been demonstrated that overexpression of tumor-related KIFs is correlated with poorer outcomes in BC patients, and thus, these KIFs can work as potential prognostic biomarkers<sup>[14]</sup>. KIF15 is a member of the Kinesin superfamily and is usually involved in various biological activities such as endocytotic trafficking, cell signaling, and assembly of cellular structures, and it can also serve as a biomarker of various tumors<sup>[15-18]</sup>. Interestingly, KIF15 also serves as a functional alternative to Eg5 under defined conditions. Its overlapping functions with these two proteins might lead to the promotion of tumor cell proliferation<sup>[15]</sup>. Emma<sup>[16]</sup> reported that the Eg5 blockers K5Is can inhibit

mitotic spindle formation; however, in follow-ups, cultured cells were found to be resistant to K5Is. Further studies have suggested that high KIF15 expression is not only related to high migratory activity of tumor cells but also results in the emergence of drug-resistant strains of K5Is. In addition, KIF15 can induce cells to develop into KIF15-dependent K5I drug-resistant strains and adapt to alterations to the cytoarchitecture to break the bottle-neck of tissue development, which is otherwise induced by K5Is. Therefore, it is believed that small-molecule KIF15 inhibitors might enhance the biological activities of K5Is in tumor cells and decrease resistance to paclitaxel and other Eg5 inhibitors. In our previous studies, KIF15 expression in BC tissues was found to be significantly higher than that in tumor-adjacent normal tissues, as determined using tissue microarrays containing 163 BC samples<sup>[17-18]</sup>. According to the aforementioned findings from the present studies, we consider increased KIF15 expression as a biomarker of high-risk breast tissue and KIF15 expression might also correlate with chemotherapy-resistant breast cancer (related to the resistance of taxanes). Thus, KIF15 was selected as the research subject, and we observed the expression status of KIF15 in 93 BC patients receiving NAC to analyze the relationship between the expression of KIF15 and efficacy of NAC and explored the role of this protein in BC development.

Relationships between clinicopathological features in BC and KIF15 expression were observed in our study. The results of Chi-square tests showed higher expression of KIF15, increased numbers of metastatic lymph nodes, and

elevated expression of ER, HER-2, and KI67 ( $P < 0.05$ ), indicating that high KIF15 expression was associated with poor prognosis in BC patients. Conversely, a positive correlation was revealed between KIF15 expression and pCR in BC patients receiving NAC. The efficacy and safety of this 4-cycle NAC regimen of paclitaxel plus cisplatin has been proved in many recent clinical studies<sup>[19–20]</sup>, which is the reason why we choose it as a unified protocol. These results showed that tumors expressing high levels of KIF15 protein were more likely to achieve pCR after NAC. The pathological benefit rate in the high KIF15 expression group was 65.22%, which was significantly higher than that in the low KIF15 expression group ( $P < 0.05$ ). The evaluation results of pathological and clinical benefits remained largely similar. In subgroup analyses, a similar trend was observed in TNBC patients. TNBC patients are the most sensitive to NAC and demonstrated the best pathological and clinical outcomes (84% and 52%) when compared to other subtypes ( $P < 0.05$ ). In our separate analyses involving TNBC cases, patients with lymph node metastasis exhibited elevated KIF15 expression and presented better clinical efficacy outcomes. These results corroborated our previous bioinformatic analysis results based on TCGA database<sup>[18]</sup>.

From this, KIF15 might be suggested as a molecular marker with potential diagnostic and treatment value. Also might become a potential target for reversing the chemoresistance of BC. Nevertheless, our study could not demonstrate the difference of KIF15 expression between various regimen of chemotherapy. Studies have proved that kinesins may contribute greatly to the modulation of breast cancer cell sensitivity to paclitaxel, but not to doxorubicin, carboplatin, or gemcitabine<sup>[21–22]</sup>. From these experimental results and our review of the literature, we propose that KIF15 might be a promising biomarker for the resistance of taxanes, while the relationship between KIF15 and cisplatin responses remains unknown. Triple-negative tumors, which obtained best efficacy from NAC of all molecular subtypes in our study, however, are known to respond well to carboplatin in previous studies<sup>[23–24]</sup>. This means we were unable to determine which of these chemotherapeutics singly or together was responsible for the positive effects of the intervention, especially in TNBC. Therefore, more clinical and basic studies are needed in order to find out the possible mechanism of KIF15 inducing chemoresistance and its association between different chemotherapeutic agents. Further follow-ups of survival in the future are also needed to confirm and refine the current results. .

### Conflicts of interest

The authors indicated no potential conflicts of interest.

## References

1. McKenna MT, Weis JA, Brock A, *et al.* Precision medicine with imprecise therapy: computational modeling for chemotherapy in breast cancer. *Transl Oncol*, 2018, 11: 732–742.
2. Siegel RL, Miller KD, Fuchs HE, *et al.* Cancer Statistics, 2021. *CA Cancer J Clin*, 2021, 71: 7–33.
3. Polk A, Svane IM, Andersson M, *et al.* Checkpoint inhibitors in breast cancer-Current status. *Cancer Treat Rev*, 2018, 63: 122–134.
4. Lydiatt WM, Patel SG, O'Sullivan B, *et al.* Head and neck cancers-major changes in the American Joint Committee on cancer eighth edition cancer staging manual. *CA Cancer J Clin*, 2017, 67: 122–137.
5. Luketich JD, Pennathur A, Franchetti Y, *et al.* Minimally invasive esophagectomy: results of a prospective phase II multicenter trial-the eastern cooperative oncology group (E2202) study. *Ann Surg*, 2015, 261: 702–707.
6. Baihong Z, Hongyun Y. Brief introduction of response evaluation criteria in solid tumors. *J Int Oncol*, 2016, 43: 845–847.
7. Zeng H, Li T, Zhai D, *et al.* ZNF367-induced transcriptional activation of KIF15 accelerates the progression of breast cancer. *Int J Biol Sci*, 2020, 16: 2084–2093.
8. Wentao Y, Hong B. Expert consensus on pathological diagnosis of breast cancer after neoadjuvant chemotherapy. *Chin J Pathol*, 2015, 44: 232–236.
9. Yount AL, Zong H, Walczak CE. Regulatory mechanisms that control mitotic kinesins. *Exp Cell Res*, 2015, 334: 70–77.
10. Wolff AC, Hammond ME, Hicks DG, *et al.* Recommendations for human epidermal growth factor receptor 2 testing in breast cancer: American Society of Clinical Oncology/College of American Pathologists clinical practice guideline update. *J Clin Oncol*, 2013, 31: 3997–4013.
11. Eisenhauer EA, Therasse P, Bogaerts J, *et al.* New response evaluation criteria in solid tumours: revised RECIST guideline (version 1.1). *Eur J Cancer*, 2009, 45: 228–247.
12. Pérez-Melero C. KSP inhibitors as antimetabolic agents. *Curr Top Med Chem*, 2014, 14: 2286–2311.
13. Myers SM, Collins I. Recent findings and future directions for inter-polar mitotic kinesin inhibitors in cancer therapy. *Future Med Chem*, 2016, 8: 463–489.
14. Li TF, Zeng HJ, Shan Z, *et al.* Overexpression of kinesin superfamily members as prognostic biomarkers of breast cancer. *Cancer Cell Int*, 2020, 20: 123.
15. Kavallaris M. Microtubules and resistance to tubulin-binding agents. *Nat Rev Cancer*, 2010, 10: 194–204.
16. Sturgill EG, Norris SR, Guo Y, *et al.* Kinesin-5 inhibitor resistance is driven by kinesin-12. *J Cell Biol*, 2016, 213: 213–227.
17. Sheng J, Xue X, Jiang K. Knockdown of Kinase family 15 inhibits cancer cell proliferation and its Clinical relevance in Triple-Negative Breast Cancer. *Curr Mol Med*, 2019, 19: 147–155.
18. Sheng J, Li C, Dong M, Jiang K. Identification by Comprehensive Bioinformatics Analysis of KIF15 as a Candidate Risk Gene for Triple-Negative Breast Cancer. *Cancer Manag Res*, 2020, 12: 12337–12348.
19. Bayarmaa B, Wu Z, Peng J, *et al.* Association of LncRNA MEG3 polymorphisms with efficacy of neoadjuvant chemotherapy in breast cancer. *BMC Cancer*, 2019, 19: 877.
20. Wu Z, Zhang L, Xu S, *et al.* Predictive and prognostic value of ZEB1 protein expression in breast cancer patients with neoadjuvant chemotherapy. *Cancer Cell Int*, 2019, 19: 78.

21. Tan MH, De S, Bebek G, *et al.* Specific kinesin expression profiles associated with taxane resistance in basal-like breast cancer. *Breast Cancer Res Treat*, 2012, 131: 849–858.
22. Singel SM, Cornelius C, Zaganjor E, *et al.* KIF14 promotes AKT phosphorylation and contributes to chemoresistance in triple-negative breast cancer. *Neoplasia*, 2014, 16: 247–256.
23. Sharma P, López-Tarruella S, García-Saenz JA, *et al.* Pathological Response and Survival in Triple-Negative Breast Cancer Following Neoadjuvant Carboplatin plus Docetaxel. *Clin Cancer Res*, 2018, 24: 5820–5829.
24. Loibl S, Weber KE, Timms KM, *et al.* Survival analysis of carboplatin added to an anthracycline/taxane-based neoadjuvant chemotherapy and HRD score as predictor of response-final results from GeparSixto. *Ann Oncol*, 2018, 29: 2341–2347.

**DOI 10.1007/s10330-021-0478-8**

**Cite this article as:** Dong MT, Li CY, Jiapaer P, *et al.* KIF15 expression characteristics: Relevance to neo-adjuvant chemotherapy efficacy in breast cancer. *Oncol Transl Med*, 2021, 7: 69–75.

# Application of endoscopic nasobiliary cutting in the treatment of hilar cholangiocarcinoma

Shujuan Jiang, Zhongyin Zhou (✉)

Department of Gastroenterology, Renmin Hospital of Wuhan University, Wuhan 430060, China

## Abstract

**Objective** The aim of the study was to study the clinical efficacy and prognosis of endoscopically cutting the nasobiliary duct and leaving its residual segment as a biliary stent in the treatment of hilar cholangiocarcinoma (HC).

**Methods** The clinical data of 55 patients with HC treated by endoscopic biliary drainage at the Gastrointestinal Endoscopy Center of our hospital (Renmin Hospital of Wuhan University, China) from August 2017 to August 2019 were retrospectively analyzed. According to different drainage schemes, patients were divided into the endoscopic nasobiliary cutting group ( $n = 26$ ) and the endoscopic retrograde biliary drainage (ERBD) group ( $n = 29$ ). The postoperative liver function indexes, incidence of postoperative complications, median patency period of stents, and median survival time of patients were compared between the two groups.

**Results** Liver function indexes (total bilirubin, direct bilirubin, alanine aminotransferase, aspartate aminotransferase, alkaline phosphatase, gamma-glutamyl transpeptidase) were significantly decreased in 55 patients a week postoperatively ( $P < 0.05$ ), and decreases in liver function indexes in the endoscopic nasobiliary cutting group were more significant than those in the ERBD group ( $P < 0.05$ ). The incidence of biliary tract infection in the endoscopic nasobiliary cutting group was significantly lower than that in the ERBD group (15.40% vs. 41.4%,  $P < 0.05$ ). In the endoscopic nasobiliary cutting subgroups, there were 1 and 3 cases of biliary tract infection in the gastric antrum cutting group ( $n = 21$ ) and duodenal papilla cutting group ( $n = 5$ ), respectively, and 0 cases and 2 cases of displacement, respectively; there was a statistically significant difference in terms of complications between the two subgroups ( $P < 0.05$ ). The median patency period (190 days) and median survival time (230 days) in the nasobiliary duct cutting group were higher than those (169 days and 202 days) in the ERBD group, but there was no significant difference ( $P > 0.05$ ).

**Conclusion** The nasobiliary duct was cut by using endoscopic scissors in Stage II after the bile was fully drained through the nasobiliary duct. The residual segment could still support the bile duct and drain bile. The reduction of jaundice and the recovery of liver enzymes were significant, and the incidence of biliary tract infection was low. Cutting off the nasobiliary duct at the duodenal papilla results in a higher incidence of biliary tract infection, and the residual segment of the nasobiliary duct is more likely to be displaced. Endoscopic nasobiliary-cutting drainage is an effective, simple, and safe method to reduce jaundice in the palliative treatment of HC.

**Key words:** hilar cholangiocarcinoma (HC); endoscopic nasobiliary drainage; endoscopic nasobiliary cutting; endoscopic retrograde biliary drainage (ERBD); biliary stent

Received: 13 October 2020  
Revised: 20 November 2020  
Accepted: 27 December 2020

Hilar cholangiocarcinoma (HC) is a kind of malignant tumor with poor prognosis, which originates from the ductuli hepaticus communis, left and right hepatic ducts, and its confluence bile duct epithelium, accounting for approximately 50% to 70% of all cholangiocarcinomas [1]. Currently, surgical resection remains to be the main radical treatment for HC [2]. However, due to its special

anatomical structure and biological characteristics, the surgical resection rate is low, and the 5-year survival rate is less than 10% [3–5]. Most patients have insidious onset and are in an advanced stage when they seek medical treatment, thus losing the opportunity for radical surgery. For patients who are unable or unwilling to undergo radical surgery, it is important to choose an

appropriate and effective palliative jaundice reduction therapy to improve their quality of life and prolong their survival<sup>[6-8]</sup>. Currently, the palliative treatment of HC is mainly biliary drainage, which can be performed by using endoscopic, percutaneous, and surgical methods, among which endoscopic biliary drainage is considered to be the best non-surgical treatment at present<sup>[9-10]</sup>. Endoscopic biliary stenting (EBS) and endoscopic nasobiliary drainage (ENBD) could achieve internal and external biliary drainage, respectively. In clinical practice, EBS and ENBD have advantages and disadvantages.

As early as in 2002, Uchida *et al*<sup>[11]</sup> proposed for the first time that the nasobiliary duct could be cut under endoscopy, and its residual section could be retained to serve as a biliary stent to make nasobiliary drainage change from external drainage to internal drainage, thus alleviating the discomfort of patients' nasophary and improving their quality of life. In 2003, Uchida *et al*<sup>[12]</sup> implemented the same drainage scheme for four patients, and followed them up after discharge. One patient had a stent patency period of 62 days, which preliminarily showed that this method could replace the hilar bile duct plastic stent implantation, which provided us with a third choice that combined the advantages of biliary stent and nasobiliary duct. Currently, there are few reports on this treatment scheme at home and abroad. To further explore the feasibility of this drainage scheme, from August 2017 to August 2019, the author treated 55 HC cases through two drainage schemes, namely ENBD via endoscopic retrograde cholangiopancreatography (ERCP) in Stage I, followed by endoscopic nasobiliary cutting and leaving the residual segment of the nasobiliary duct as biliary stent in Stage II or direct endoscopic retrograde biliary drainage (ERBD) via ERCP, and achieved certain results.

## Patients and methods

### Patients

From August 2017 to August 2019, continuous 55 patients with HC, including 31 men and 24 women, aged 34–85 years, with an average age of  $(66.46 \pm 11.26)$  years, were treated with endoscopic biliary drainage at the Gastrointestinal Endoscopy Center, Renmin Hospital of Wuhan University, China. All patients were diagnosed with HC according to preoperative clinical data and imaging examinations [computer tomography (CT), magnetic resonance cholangiopancreatography (MRCP), ERCP] with a Bismuth-Corlette classification type of Stenosis IV. Among them, there were 26 and 29 cases in the endoscopic nasobiliary cutting and ERBD groups, respectively. There was no significant difference between the two groups in the preoperative general characteristics of the patients ( $P > 0.05$ ), as presented in Table 1. Chest

radiography, electrocardiogram, echocardiography, blood routine examination, coagulation function, and liver and kidney functions were examined routinely preoperatively to assess the risk of surgery. This study was approved by the Ethics Committee of the Renmin Hospital of Wuhan University, China.

### Equipment preparation

The Olympus TJF-240 and TJF-260 electronic duodenoscopes, electronic gastroscope, duodenal papillotomy knife, zebra guidewire, bile duct dilatation probe, dilatation balloon, nasobiliary [all 7Fr size and made in the same manufacturer (Boston Scientific, Boston, MA, USA)] and plastic biliary stents (all 7Fr size and made by the same manufacturer), nasal guide tube, and Zhang's scissors were used.

### Operation method

Routine endoscopic preparation was performed, including routine fasting for 8–12 h preoperatively; intravenous injections of diazepam (10 mg), pethidine hydrochloride (100 mg), and anisodamine (20 mg) were performed to calm and relieve pain preoperatively, and a diclofenac sodium suppository of 50 mg was inserted into the anus to prevent postoperative pancreatitis (PEP); the patient was in the left prone position and received oxygen inhalation and electrocardiograph (ECG) monitoring during the operation.

The papillae opening was exposed under the electronic duodenoscope and a small amount of contrast media was injected to confirm the obstruction position and dilatation condition of the intrahepatic bile duct after successful intubation with papillotomy knives and guidewires. If necessary, papillae dilation or papillae sphincterotomy is performed with biliary dilatation balloons. Guidewires were placed in the main drainage areas of left and right hepatic ducts under digital subtraction angiography (DSA) fluoroscopy. If bilateral intrahepatic bile ducts could not be super-selected, drainage was performed on one side, and the ductuli hepaticus communis and stenosis sections of left and right hepatic ducts were fully expanded along the reserved guidewires with expansion probes.

In the ERBD group, the plastic biliary stent was implanted directly along the guidewire. In the endoscopic nasobiliary cutting group, the nasobiliary duct was inserted into biliary duct along the guidewire for ENBD at Stage I. After we confirmed that there were no complications such as cholangitis and pancreatitis, and the nasobiliary duct was confirmed to be in good position by X-ray fluoroscopy, the duodenoscope or gastroscope was inserted, and the nasobiliary duct was sent into the stomach for about 20 cm. The endoscope was introduced to the duodenal papilla gently, and the scope was straightened. After the nasobiliary duct was confirmed

**Table 1** Preoperative general characteristics and liver function indexes of the patients a week after operation

Index	Endoscopic nasobiliary cutting group ( <i>n</i> = 26)	Endoscopic retrograde biliary drainage group ( <i>n</i> = 29)	Statistic	<i>P</i> value
Male/Female, <i>n</i>	14/12	17/12	$\chi^2 = 0.127$	0.721
Age, years (median $\pm$ SD)	66.19 $\pm$ 8.94	66.52 $\pm$ 13.12	$t = -0.106$	0.916
Biliarytract infection, with/without, <i>n</i>	8/18	11/17	$\chi^2 = 0.311$	0.577
Preoperative general characteristics				
TBIL, $\mu\text{mol/L}$ (median, range)	111.09 (11.65, 352.77)	140.92 (11.91, 536.35)	$Z = -1.854$	0.064
DBIL, $\mu\text{mol/L}$ (median, range)	83.50 (3.60, 289.30)	103.50 (5.70, 398.00)	$Z = -1.796$	0.073
ALT, U/L (median, range)	72.50 (11.00, 489.00)	94.00 (7.00, 526.00)	$Z = -0.868$	0.385
AST, U/L (median, range)	93.00 (23.00, 849.00)	82.00 (17.00, 348.00)	$Z = -0.413$	0.680
ALP, U/L (median, range)	413.00 (63.00, 1193.00)	295.00 (86.00, 1230.00)	$Z = -0.565$	0.572
GGT, U/L (median, range)	379.50 (32.00, 2414.00)	405.00 (45.00, 2546.00)	$Z = -0.126$	0.899
A week after operation				
TBIL, $\mu\text{mol/L}$ (median, range)	46.80 (16.70, 186.10)*	54.23 (15.74, 243.70)*	$Z = -2.868$	0.035
DBIL, $\mu\text{mol/L}$ (median, range)	39.10 (4.60, 161.60)*	44.00 (4.60, 185.50)*	$Z = -2.877$	0.029
ALT, U/L (median, range)	40.00 (12.00, 104.00)*	63.00 (12.00, 209.00)*	$Z = -3.914$	0.000
AST, U/L (median, range)	44.00 (17.00, 195.00)*	60.00 (17.00, 208.00)*	$Z = -2.395$	0.017
ALP, U/L (median, range)	213.00 (67.00, 698.80)*	323.00 (74.00, 757.00)*	$Z = -1.919$	0.048
GGT, U/L (median, range)	200.00 (23.00, 900.00)*	295.00 (16.00, 1015.00)*	$Z = -2.063$	0.043
The decrease in TBIL, $\mu\text{mol/L}$ (median $\pm$ SD)	110.86 $\pm$ 21.22	57.92 $\pm$ 15.88	$t = -2.241$	0.026
The decrease in DBIL, $\mu\text{mol/L}$ (median $\pm$ SD)	82.19 $\pm$ 15.88	38.31 $\pm$ 11.96	$t = -2.524$	0.029
The decrease in ALT, U/L (median $\pm$ SD)	76.08 $\pm$ 20.60	58.90 $\pm$ 17.40	$t = -3.585$	0.021
The decrease in AST, U/L (median $\pm$ SD)	86.96 $\pm$ 32.08	35.55 $\pm$ 13.96	$t = -2.732$	0.031
The decrease in ALP, U/L (median $\pm$ SD)	144.74 $\pm$ 42.56	105.85 $\pm$ 51.78	$t = -1.991$	0.048
The decrease in GGT, U/L (median $\pm$ SD)	299.44 $\pm$ 75.05	209.35 $\pm$ 94.26	$t = -2.168$	0.035

Note: \*, denotes postoperative indexes compared with preoperative indexes of the same group ( $P < 0.05$ ).  $P < 0.05$  was considered to indicate a statistically significant difference. TBIL: total bilirubin, DBIL: direct bilirubin, ALT: alanine aminotransferase, AST: aspartate aminotransferase, ALP: alkaline phosphatase, GGT: gamma-glutamyl transpeptidase

to be in good position by fluoroscopy once again, the nasobiliary duct was cut off at the gastric antrum or duodenal papilla with Zhang's scissors, and its residual section was retained as a biliary stent. After ensuring that the stent drainage is unobstructed by observing the stent drainage and the stent position was confirmed to be good by fluoroscopy, the duodenoscope or gastroscope was withdrawn and the operation was finished. The operation of cutting the nasobiliary duct at the gastric antrum is depicted in Fig. 1.

### Postoperative observation and treatment

After ERCP, patients were treated with routine fasting and water deprivation, appropriate fluid infusion, broad-spectrum antibiotics for anti-infection, inhibition of gastric acid and pancreatin, liver protection, nutrition and other symptomatic support treatment, and the patient's body temperature and abdominal signs were observed closely. Blood routine and pancreas biochemistry were reexamined at 3 h and 24 h postoperatively. Postoperative complications (pancreatitis, biliary tract infection, hemorrhage, perforation, etc.) were focused on. If complications occurred, they were treated according to

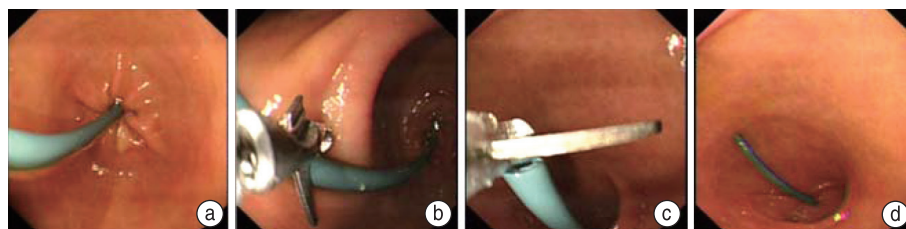


**Fig. 1** Endoscopic images of nasobiliary duct cutting off in gastric antrum. (a) endoscopic image of the gastric antrum before nasobiliary duct cutting; (b and c) endoscopic images of cutting off the nasobiliary duct in the gastric antrum; (d) endoscopic image of the gastric antrum after nasobiliary duct cutting

the corresponding diagnosis and treatment standards; if abdominal signs were normal, the diet was opened gradually in combination with the indexes of blood amylase and lipase. Liver function was reexamined a week postoperatively, and related indexes were recorded. The patients were discharged from the hospital after their condition became stable and were followed up by telephone.

**Statistical analysis**

Statistical software (SPSS 22.0, IBM Corp., Armonk, NY, USA) was used to analyze the data. The measurement data conforming to normal distribution were expressed as mean ± SD, and were compared by Student’s *t*-test, while those not conforming to normal distribution were expressed as median and range, and were compared by a rank sum test; counting data were expressed by rates (%) and number of cases, and were compared by the rank sum and Fisher’s exact probability tests, respectively. The median survival time was analyzed by a Kaplan-Meier analysis, and the difference in the cumulative survival rate between groups was estimated using thelog-rank test. A *P*-value < 0.05 was considered to indicate statistical significance.

**Results**

**Operation condition**

All 55 patients were successfully treated with ERBD or nasobiliary drainage through ERCP. In the nasobiliary cutting group, the nasobiliary duct was cut by using Zhang’s scissors under a gastroscope or duodenoscope 3–19 days after ENBD, and its residual segment was retained as a biliary stent; conversion from external biliary drainage to internal biliary drainage was achieved with a success rate of 100%. There was no significant difference between the two groups in terms of unilateral and bilateral drainage (*P* > 0.05), as shown in Table 2. In the endoscopic nasobiliary cutting group, the nasobiliary duct was cut at the gastric antrum in 21 cases, and at the

duodenal papilla in 5 cases.

**Jaundice reduction and changes of liver function indicators**

There was no significant difference in total bilirubin (TBIL), direct bilirubin (DBIL), alanine aminotransferase (ALT), aspartate aminotransferase (AST), alkaline phosphatase (ALP), gamma-glutamyl transpeptidase (GGT) levels between the two groups preoperatively (*P* > 0.05). TBIL, DBIL, ALT, AST, ALP, and GGT levels decreased significantly in the two groups a week postoperatively. Among them, TBIL, DBIL, ALT, AST, ALP and GGT decreased by 110.86 μmol/L, 82.19 μmol/L, 76.08 U/L, 86.96 U/L, 144.74 U/L and 299.44 U/L, respectively, in the endoscopic nasobiliary cutting group a week postoperatively, and TBIL, DBIL, ALT, AST, ALP and GGT decreased by 57.92 μmol/L, 38.31 μmol/L, 58.90 U/L, 35.55 U/L, 105.85 U/L and 209.35 U/L respectively in the ERBD group a week postoperatively; the difference between the two groups was statistically significant (*P* < 0.05), indicating that the endoscopic nasobiliary cutting group was superior to the ERBD group in reducing jaundice and recovering liver function, as shown in Table 1.

**Complications**

Among the 55 patients, biliary tract infection occurred in 16 patients (29.10%). In the nasobiliary duct cutting group, biliary tract infection occurred in 4 cases (15.40%). The incidence of biliary tract infection in ERBD group was 41.40%, which was significantly higher than that in the nasobiliary duct cutting group; the difference was statistically significant (*P* < 0.05), indicating that the nasobiliary duct cutting group has obvious advantages over the ERBD group in controlling biliary tract infection. There was no significant difference in pancreatitis, biliary bleeding, perforation, or displacement between the two groups (Table 2). There was no significant difference in sphincterotomy and the types of nasobiliary drainage tubes between the gastric antrum cutting group (group A)

**Table 2** Comparison of intraoperative situation and postoperative complications between the two groups

Index	Endoscopic nasobiliary cutting group (n = 26)	Endoscopic retrograde biliary drainage group (n = 29)	Statistic	P value
Unilateral/bilateral, n	12/14	17/12	χ <sup>2</sup> = 0.857	0.355
Sphincterotomy, n (with/without)	20/6	24/5	χ <sup>2</sup> = 0.291	0.589
<b>Complications</b>				
Pancreatitis, n (%)	3 (11.5)	4 (13.8)	χ <sup>2</sup> = 0.000	1.000
Biliary tract infection, n (%)	4 (15.4)	12 (41.4)	χ <sup>2</sup> = 4.491	0.034
Hemorrhage, n (%)	0 (0)	0 (0)		
Perforation, n (%)	0 (0)	0 (0)		
Dislocation, n (%)	2 (7.7)	1 (3.4)	χ <sup>2</sup> = 0.009	0.922
Total complications, n (%)	8 (30.8)	15 (51.7)	χ <sup>2</sup> = 2.474	0.116

Note: *P* < 0.05 was considered to indicate a statistically significant difference

**Table 3** Comparison of intraoperative situation and postoperative complications between the two cutting sites

Index	Gastric antrum ( <i>n</i> = 21)	Duodenal papilla ( <i>n</i> = 5)	<i>P</i> value
Sphincterotomy, <i>n</i> (with/without)	15/6	5/5	0.298
Pigtail-type nasobiliary duct / $\alpha$ -typernasobiliaryduct, <i>n</i>	19/2	5/0	1
Biliary tractinfection, <i>n</i> (with/without)	1/20	3/2	0.014
Dislocation, <i>n</i> (with/without)	0/21	2/3	0.031

Note:  $P < 0.05$  was considered to indicate a statistically significant difference

and the duodenal papilla cutting group (group B). There was one case and three cases of biliary tract infection in groups A and B, respectively, and two cases of biliary tract displacement in group B, and the difference was statistically significant ( $P < 0.05$ ), which indicated that biliary tract infection and residual stent displacement were more likely to occur when the nasobiliary duct was cut off at the duodenal papilla than at the gastric antrum, as shown in Table 3.

### Median patency of stent and median survival time postoperatively

The overall median survival time of the 55 patients was 202 days. The median patency periods of the endoscopic nasobiliary cutting and ERBD groups were 190 and 169 days, respectively, with no statistical difference ( $\chi^2 = 2.644$ ,  $P = 0.104 > 0.05$ ). The median survival times of the endoscopic nasobiliary cutting and ERBD groups were 230 and 202 days, respectively, with no significant difference ( $\chi^2 = 2.308$ ,  $P = 0.129 > 0.05$ ). The survival curves are shown in Fig. 2.

## Discussion

In recent years, with the development of endoscopic technology, endoscopic biliary drainage for the palliative treatment of HC has attracted increasing attention. Currently, biliary stents are currently considered the most effective treatment for biliary drainage [13]. To reduce the psychological, physiological, and economic burden of patients, studies on the replacement of plastic biliary stents with modified nasobiliary stents and the conversion of external biliary drainage to internal drainage have been reported at home and abroad in recent years, but the clinical efficacy and prognosis of this method are unclear [14-17]. In this study, ENBD was performed under ERCP in Stage I, and the nasobiliary duct was cut under a gastroscope or duodenoscope, and its residual segment was retained as a biliary stent for biliary drainage in Stage II, with a success rate of 100%. In terms of operation, as the operation of cutting the nasobiliary duct only requires to cut the nasobiliary duct directly under a gastroscope or duodenoscope, compared with the traditional procedure of pulling the nasobiliary duct through ERCP and then placing a stent,

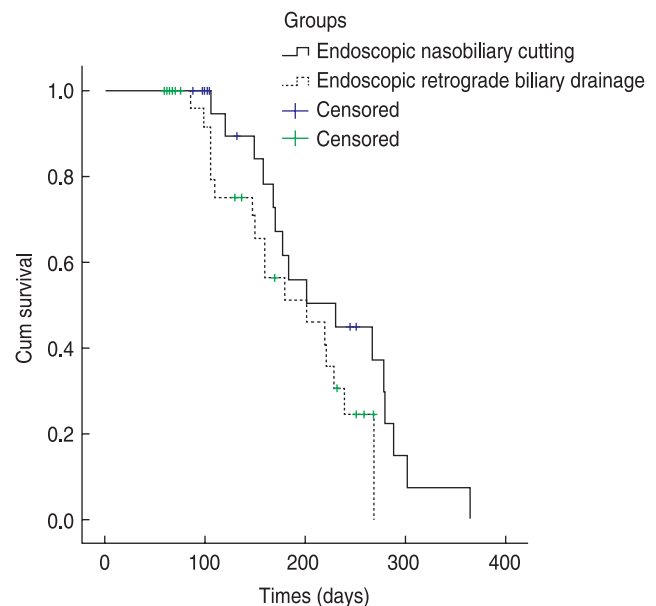


**Fig. 2** Analysis of the Kaplan-Meier survival curves of the two groups

the number of ERCPs required is reduced by one; this reduces the risk of the pollution of the contrast medium and equipment, such as the guidewire to the bile duct and pancreatic duct system, and the postoperative infection rate; simultaneously, the whole operation is relatively simple and easy, and the operation time is short, which can reduce intraoperative anesthesia accidents, relieve the postoperative discomfort of patients, and improve patients' benefits significantly. This drainage scheme controls the risk and cost of ERCP operation effectively and simplifies the operation efficiently and safely.

By comparing the data of liver function indexes pre- and post-operatively, the author found that the drainage scheme of endoscopic nasobiliary cutting can significantly reduce bilirubin and liver enzymes, and that the short-term curative effect is remarkable; some studies [18] have shown that ENBD and EBS have no significant difference in the drainage effect under the condition of biliary tract patency, and both can achieve ideal drainage effect; however, in this study, the nasobiliary cutting group had obvious advantages over the ERBD group in reducing jaundice and improving liver function. To investigate the reason for this phenomenon, the author believes that the

nasobiliary duct has the following advantages: first, there are many lateral holes in the nasobiliary duct, and the drainage area is wide. Moreover, the nasobiliary duct is soft, which causes little compression or damage to the adjacent non-drainage bile duct and organs<sup>[19]</sup>. Nasobiliary ducts can be placed in the left and right hepatic ducts respectively, further improving the drainage efficiency. Secondly, the nasobiliary duct is connected externally, and the curative effect can be analyzed directly by observing the drainage volume and bile characteristics to guide the next treatment; if the drainage effect is not good, the blockage and displacement of the nasobiliary drainage tube and poor drainage area can be considered, and then suction, irrigation or ERCP intervention can be conducted again. Finally, the external drainage of the nasobiliary duct reduces the chance of retrograde infection. The bile drainage of the intrahepatic bile duct can be promoted by flushing the bile duct and connecting the external negative pressure drainage device, which is also beneficial in treating jaundice and toward the improvement of liver function.

In this study, the incidence of biliary tract infection in the ERBD group was 41.40%, which was higher than that (15.40%) in the endoscopic nasobiliary cutting group, with statistical significance ( $P < 0.05$ ). This is because the endoscopic nasobiliary cutting drainage scheme is controllable in the occurrence of biliary tract infection. In the control of biliary tract infection, the nasobiliary duct has many lateral holes, achieve sufficient drainage, and causes little compression or obstruction to other peripheral bile ducts. It can also be sampled through the nasobiliary duct for bacteriological examination to guide the selection of clinical antibiotics, and can be flushed and drained, including antibiotic flushing, to improve the treatment effect. This study showed that biliary tract infection and displacement of the residual segment of the nasobiliary duct are more likely to occur when the nasobiliary duct is cut off at the duodenal papilla than at the antrum, and the difference between the gastric antrum cutting group and the duodenal papilla cutting group was statistically significant ( $P < 0.05$ ). By analyzing the reasons, the author found that due to the anatomical structure of gastrointestinal biliary tract, when the nasobiliary duct is cut off at duodenal papilla intestinal bacteria are more likely to retrograde into the bile duct through the cut end of the residual stent of the nasobiliary duct, compared with at gastric antrum, resulting in retrograde biliary tract infection, and the cut end of the residual stent of the nasobiliary duct is more likely to displace to the intestine. The number of the postoperative complications of the duodenal papilla cutting group involved in this study seems to be higher than that of the gastric antrum cutting group, but the number of the included patients was too small, and might

affect the results, which need further clinical studies, that include larger sample sizes, to be confirmed.

It has been reported that the displacement of the modified nasobiliary stent is related to the type of nasobiliary duct and duodenal papillary sphincterotomy. Compared with the  $\alpha$ -type nasobiliary duct, the pigtail-type nasobiliary duct structure is easier to fix in the target drainage area; additionally, duodenal papillary sphincterotomy makes the stent displaced to the intestinal tract easily through the damaged papilla, discharged with stool, or left in the intestinal tract, causing intestinal obstruction and even intestinal perforation<sup>[12]</sup>. In this study, due to the limited sample size, the occurrence of residual stent displacement after endoscopic nasobiliary cutting has no significant correlation with the type of nasobiliary duct stent and duodenal papillary myotomy, which needs further clinical studies to confirm in the future.

Wang *et al*<sup>[20]</sup> in China studied the modification of a nasobiliary stent, which is cutting a nasobiliary stent directly, and placing it as a common plastic biliary stent to treat hilar bile duct stenosis. Research shows that it is superior to the common plastic biliary stent in improving clinical symptoms and postponing patency time. In this study, the median patency period (190 days) and median survival period (230 days) in the endoscopic biliary cutting group were not significantly different from those (169 and 202 days) in the ERBD group ( $\chi^2 = 2.644$ ,  $P = 0.104$ ;  $\chi^2 = 2.308$ ,  $P = 0.129$ ), which also shows that the clinical symptoms of patients can be relieved for a long time, which further shows the feasibility of resecting the nasobiliary duct and retaining its residual segment as a biliary stent in the treatment of HC.

In conclusion, for patients with obstructive jaundice due to high malignant biliary stenosis in HC, ENBD was performed under ERCP in Stage I, and the nasobiliary duct was cut off by using endoscopic scissors through the nasobiliary duct in Stage II after fully draining the bile, and the residual segment of the nasobiliary duct can still support the bile duct, and drain the bile. Compared with ERBD, the effects of jaundice reduction and liver enzyme improvement in endoscopic nasobiliary cutting drainage are significant, and the incidence of biliary tract infection is low, and there is no significant difference in the median patency period and median survival time between the two drainage schemes. Compared with cutting off the nasobiliary duct at the gastric antrum, the incidence of biliary tract infection is higher in the duodenal papilla, and the stent of the residual segment of the nasobiliary duct is easier to displace. It is safe and feasible to adopt an endoscopic nasobiliary cutting drainage scheme for the palliative treatment of the hilar bile duct stenosis. Of course, this study is a single-center non-randomized controlled retrospective study, and the small sample size

is limiting, meaning that the results of this study still need further comparative researches and multi-center randomized controlled experiments with large samples to be confirmed.

### Conflicts of interest

The authors indicated no potential conflicts of interest.

### References

1. Capobianco I, Rolinger J, Nadalin S. Resection for Klatskin tumors: technical complexities and results. *Transl Gastroenterol Hepatol*, 2018, 3: 69.
2. Yang M, Zhang YH, Cui MH, *et al*. Value of partial hepatectomy for the treatment of hilar cholangiocarcinoma: a Meta-analysis study. *Oncol Transl Med*, 2019, 5: 268–277.
3. Bergquist A, von Seth E. Epidemiology of cholangiocarcinoma. *Best Pract Res Clin Gastroenterol*, 2015, 29: 221–232.
4. Doherty B, Nambudiri VE, Palmer WC. Update on the diagnosis and treatment of cholangiocarcinoma. *Curr Gastroenterol Rep*, 2017, 19: 2.
5. Lee H, Han YM, Kim JR, *et al*. Preoperative biliary drainage adversely affects surgical outcomes in periampullary cancer: a retrospective and propensity score-matched analysis. *J Hepatobiliary Pancreat Sci*, 2018, 25: 206–213.
6. Hashimoto S, Ito K, Koshida S, *et al*. Risk factors for post-endoscopic retrograde cholangiopancreatography (ERCP) pancreatitis and stent dysfunction after preoperative biliary drainage in patients with malignant biliary stricture. *Intern Med*, 2016, 55: 2529–2536.
7. Moole H, Dharmapuri S, Duvvuri A, *et al*. Endoscopic versus percutaneous biliary drainage in palliation of advanced malignant hilar obstruction: A meta-analysis and systematic review. *Can J Gastroenterol Hepatol*, 2016, 2016: 4726078.
8. Shim DJ, Gwon DI, Han K, *et al*. Percutaneous metallic stent placement for palliative management of malignant biliary hilar obstruction. *Korean J Radiol*, 2018, 19: 597–605.
9. Blumgart LH, Hadjis NS, Benjamin IS, *et al*. Surgical approaches to cholangiocarcinoma at confluence of hepatic ducts. *Lancet*, 1984, 1: 66–70.
10. Miao L, Fan ZN, Ji GZ, *et al*. Endoscopic stent for palliation of malignant and benign biliary obstruction. *Chin J Endosc (Chinese)*, 2004, 10: 11–14.
11. Uchida N, Ezaki T, Fukuma H, *et al*. Conversion of endoscopic nasobiliary drainage to internal drainage by means of endoscopic scissor forceps. *Endoscopy*, 2002, 34: 180.
12. Uchida N, Tsutsui H, Ezaki T, *et al*. Conversion from external nasobiliary drainage to internal drainage using endoscopically available scissor forceps. *Hepatogastroenterology*, 2003, 50: 1891–1893.
13. Rerknimitr R, Angsuwatcharakon P, Ratanachu-ek T, *et al*. Asia-Pacific consensus recommendations for endoscopic and interventional management of hilar cholangiocarcinoma. *J Gastroenterol Hepatol*, 2013, 28: 593–607.
14. Xia T, Yao J, Shen Z, *et al*. Gastrointestinal: first report of conversion of nasopancreatic drainage to internal drainage by endoscopic scissor forceps. *J Gastroenterol Hepatol*, 2019, 34: 9.
15. Yane K, Katanuma A, Maguchi H. Endoscopic cutting technique using scissors forceps after temporary endoscopic naso-gallbladder drainage for acute cholecystitis (with videos). *J Hepatobiliary Pancreat Sci*, 2015, 22: 244–245.
16. He KJ, Cheng CS, Zhang Q, *et al*. Clinical application of improved biliary stent by endoscopic biliary stent insertion. *Chin J Endosc (Chinese)*, 2011, 17: 113–115.
17. Zhang Y, Huang J, Qian Y, *et al*. A preliminary exploration of modified nasal bile duct stent combined with plastic stent to treat hilar bile duct stricture. *Chin J Dig Endosc (Chinese)*, 2013, 30: 696–698.
18. Li YT, Lin YF, Liu Y, *et al*. Therapeutic effect of endoscopic retrograde biliary drainage and nasal biliary drainage for hilar cholangiocarcinoma. *Chin J Dig Endosc (Chinese)*, 2017, 34: 466–469.
19. Kawakubo K, Kawakami H, Kuwatani M, *et al*. Lower incidence of complications in endoscopic nasobiliary drainage for hilar cholangiocarcinoma. *World J Gastrointest Endosc*, 2016, 8: 385–390.
20. Wang JL, Yu TT, Zhang W, *et al*. Application value of nasobiliary stent reconstruction in hilar cholangiocarcinoma. *Chin J Dig Endosc (Chinese)*, 2018, 35: 275–277.

DOI 10.1007/s10330-020-0461-1

Cite this article as: Jiang SJ, Zhou ZY. Application of endoscopic nasobiliary cutting in the treatment of hilar cholangiocarcinoma. *Oncol Transl Med*, 2021, 7: 76–82.

# Analyses of the clinical characteristics of 49 cases of malignancy with multiple bone lesions as the first manifestation

Yu Huang, Ping Peng, Peng Zhang, Lei Zhou, Yingying Wu (✉)

Department of Oncology, Tongji Hospital, Tongji Medical College, Huazhong University of Science and Technology, Wuhan 430030, China

## Abstract

**Objective** To investigate the clinical features of several cases of malignancy with multiple bone lesions as the first manifestation.

**Methods** Forty-nine cases of malignancy with multiple bone lesions as the first manifestation were retrospectively analyzed from May 2018 to July 2019. All patients complained of “pain at the site of bone lesion” upon admission. Baseline patient information, such as age, gender, location of bone lesions, etiology, diagnosis method, time of onset was collected.

**Results** The median age of the patients was 56 years old, of which 83.7% (41/49) were aged  $\geq 50$  years. The median time of onset was 2 months. Among the cases, 40 were confirmed as solid tumor bone metastasis, whereas the remaining 9 cases as hematological system tumor. Lung cancer and multiple myeloma were the main tumor types, accounting for 40.8% (20/49) and 16.3% (8/49), respectively. Other common causes were seven cases of cancer affecting the digestive system (three cases of liver cancer, three cases of gastric cancer, and one case of esophageal cancer), as well as seven cases of unknown primary cancer. Half of the solid tumors had only multiple bone metastases but no other distant metastasis.

**Conclusion** Multiple bone lesions accompanied by pain may be the first clinical manifestation in various malignant tumors. The common tumor types were lung cancer, multiple myeloma, and digestive system tumor. It is more common in people aged 50 years and older. Multiple bone lesions might be the only metastasis site of some solid tumors, and its mechanism needs further investigation.

**Key words:** Bone lesions, malignancy, bone metastasis, clinical characteristics

Received: 17 January 2021

Revised: 4 March 2021

Accepted: 15 April 2021

The incidence of malignant tumors has been increasing annually, and advanced malignant tumors are one of the most common causes of deaths<sup>[1]</sup>. Bones are one of the most common metastatic sites of malignant tumors<sup>[2]</sup>. The onset of some malignant tumors is occult, and patients may not show the symptoms of primary lesions. Multiple bone metastases or multiple bone diseases may only be detected when the tumor affects the bone and causes bone pain. Hence, bone pain may be the only or the first manifestation of the tumor, and it can often be misdiagnosed and mistreated.

With the continuous development of tumor treatment, the survival time of advanced malignant tumor is prolonged. Early detection and intervention of advanced

malignant tumor will help to improve the overall survival of patients. At the same time, bone metastasis may lead to bone related events, multiple bone destruction is more prone to bone related events, and seriously affect the quality of life of patients. Early detection and intervention will significantly improve the quality of life of patients. Many types of malignant tumors have multiple bone destruction as the initial manifestation, but no systematic clinical report has been published on the clinical characteristics and diagnosis of this kind of disease.

In this study, 49 cases with multiple bone destruction as the first manifestation were treated and analyzed in our oncology department. The clinical characteristics of

✉ Correspondence to: Yingying Wu. Email: 704887324@qq.com

© 2021 Huazhong University of Science and Technology

these diseases were preliminarily discussed. We hope to provide a new direction for the diagnosis and treatment of such diseases.

## Materials and methods

A retrospective analysis was made on 49 cases with multiple bone destruction as the first manifestation in the oncology department of Tongji Hospital from May 2018 to July 2019.

All cases met the following criteria: (1) The chief complaint was “pain at the bone destruction site”, and multiple bone destruction was the first manifestation of the patient. (2) The patients had at least three bone destruction sites that have not been directly invaded by the same mass. (3) Malignant tumor was confirmed by pathology or cytology. (4) The patients had no history of tumor.

The patients were examined via positron emission computed tomography (PET-CT) or conventional imaging examination methods, such as CT, MRI, and radionuclide bone scan (ECT). One or more examinations, such as biopsy of bone lesions, biopsy of primary focus, puncture cytology, or bone marrow biopsy, were performed to confirm the diagnosis.

Baseline patient information, such as age, gender, bone lesion location, etiology, diagnosis method, onset time, imaging examination methods used, and other information, was collected. The onset time of the patient was defined as the time from the onset of pain symptoms to the examination of multiple bone destruction.

## Results

### Patients' characteristics

The clinical data of 49 patients were analyzed. All patients complained of “pain”, and the first manifestation was multiple bone destruction. Among them, 27 were males and 22 were females, and the male-to-female ratio was 1.23. The median age of the patients was 56 years (34–79 years), and 41 patients (83.7%) were over 50 years old. The median onset time was 2 months (ranging from 10 days to 1 year);  $\leq 2$  months for 28 cases, 2–6 months for 18 cases, and 7 months up to 1 year for 3 cases. Laboratory examination revealed that 29 cases (59.1%) had elevated alkaline phosphatase, and 19 cases (38.8%) had anemia, including 17 cases of mild anemia (hemoglobin 90 g/L to lower limit of normal value) and 2 cases of moderate anemia (hemoglobin 60–90 g/L). The common bone-related events were spinal cord compression in 3 cases, pathological fracture in 11 cases, hypercalcemia in 2 cases, bone metastasis radiotherapy in 10 cases, and spinal surgery in 2 cases (Table 1).

Twenty cases of solid tumor had only multiple bone

**Table 1** Clinical characteristics of 49 patients

Variables	No. of patients ( <i>n</i> = 49)
Gender	
Male	27
Female	22
Age (years)	
< 40	3
40–49	5
50–59	20
$\geq 60$	21
Onset times (months)	
$\leq 2$	28
$>2$ and $\leq 6$	18
$> 6$	3
ALP	
$> \text{ULN}$	29
Anemia	
Mild	17
Middle	2
Skeletal related events	
Spinal cord compression	3
Pathologic fractures	11
Hypercalcemia	2
Radiation to bone	10
Surgery to bone	2
Metastasis to other organ	
Regional lymph node	16
Distant metastasis	20

ALP: Alkaline phosphatase; ULN: Upper limit of normal value

metastases and no other distant metastasis (accounting for 50% of solid tumors). Sixteen cases of solid tumor had regional lymph node metastasis.

Given that the biopsy tissue was small, only 12 cases of solid tumor were classified by analyzing pathologic differentiation degree. Among them, 11 cases were poorly differentiated carcinoma, and 1 case was highly differentiated carcinoma.

### Etiology of bone destruction

The diagnosis of primary tumor was confirmed via imaging examination, cytology, and pathology. The diagnosis of multiple myeloma also required routine laboratory examination. A total of 25 patients were examined via PET. The final diagnosis of 19 patients was largely consistent with the judgment of the primary disease via PET, and the coincidence rate was 76%.

Forty cases of solid tumors, including 20 cases of lung origin (13 cases of adenocarcinoma, 3 cases of squamous cell carcinoma, 1 case of small cell, and 3 cases of undetermined pathological classification), 7 cases of digestive tract origin (3 cases of liver cancer, 3 cases of gastric cancer, and 1 case of esophageal cancer), and 7 cases of unknown primary tumor metastasis (4 cases of

adenocarcinoma, 2 cases of undetermined pathological type, and 1 case of neuroendocrine carcinoma). The other types of tumors were 4 cases of prostate cancer, 1 case of nasopharyngeal carcinoma, and 1 case of mediastinal neuroendocrine carcinoma. There were 9 cases of hematological tumors: 8 cases of multiple myeloma, and 1 case of lymphoma bone marrow infiltration (Table 2).

**Bone metastasis pattern**

PET/CT, SPECT, CT, and MRI are all effective detection methods for malignant bone lesions. In this study, four patients were assessed via CT scan only, whereas the rest were examined via two or more of the aforementioned methods. Malignant bone lesions involved multiple skeletons in the whole body, including spine, pelvis, sternum, ribs, femur, humerus, scapula, skull, and clavicle. The most common sites of bone destruction were thoracic vertebrae (73.5%), lumbar vertebrae (71.4%), ribs (65.3%), and pelvis (69.4%). Twenty-three cases (46.9%) had five or more bone metastasis sites (Table 3).

**Table 2** Etiology of the patients

Primary tumors	No. of patients (%) (n = 49)
Lung cancer	20 (40.8%)
Adenocarcinoma	13
Small cell lung cancer	1
Squamous cell carcinoma	3
Others	3
Digestive system cancer	7 (14.3%)
Liver cancer	3
Gastric cancer	3
Esophageal cancer	1
Other solid tumor	13 (26.5%)
Prostatic cancer	4
Nasopharyngeal carcinoma	1
Mediastinal tumor	1
Unknown primary origin	7
Hematological tumors	9 (18.4%)
Multiple myeloma	8
Lymphoma	1

**Table 3** Location of bone lesions

Metastatic site	No. of patients (%) (n = 49)
Cervical vertebra	19 (38.8)
Thoracic vertebra	36 (73.5)
Lumbar vertebra	35 (71.4)
Sacral vertebrae	22 (44.9)
Ribs	32 (65.3)
Pelvis	34 (69.4)
Humerus	17 (34.7)
Femur	18 (36.7)
Sternum	15 (30.6)
Scapula	10 (20.4)
More than 5 metastatic sites	23 (46.9)

**Discussion**

Bones are often invaded by malignant solid tumors and multiple myeloma. Bone destruction due to bone metastasis or bone involvement can cause pain and other bone-related events that seriously affect the quality of life of patients [3-4]. Some of the patients who were recently diagnosed with bone metastases had bone metastasis after the primary malignant tumor was confirmed, but they did not have symptoms of bone metastasis. In the other part patients, bone pain due to bone metastasis is the first manifestation. In these patients, bone pain was often not accompanied by primary tumor symptoms. The diagnosis of multiple bone metastases is often delayed. Timely detection of multiple bone destruction lesions and identification of the primary cause may avoid misdiagnosis and mistreatment of such diseases. Doing so will help in improving the quality of life of patients and in increasing their survival rate.

All the patients in this study were diagnosed with bone destruction due to bone pain, and multiple bone destruction was found at the initial diagnosis. The median time from bone pain to the diagnosis of multiple bone destruction was 2 months (ranging from 10 days to 1 year). Among the patients, 83.7% were over 50 years old. According to previous studies, the incidence of bone metastasis in advanced malignant tumors is 65%–75% in breast cancer, 65%–75% in prostate cancer, 67%–75% in nasopharyngeal carcinoma, 30%–40% in lung cancer, 14%–45% in melanoma, 13%–41% in liver cancer, 1%–7% in colorectal cancer, and 13% in gastric cancer [4]. In this study, we found that the solid tumors with multiple bone destruction as the first manifestation were lung cancer and gastrointestinal tumor. Prostate cancer was observed in four cases, and nasopharyngeal carcinoma was noted in one case. No one among the patients had breast cancer. This result was not consistent with the reported incidence of bone metastasis of advanced tumors. We analyzed two possible reasons that explain this discrepancy. First, breast cancer, prostate cancer, and nasopharyngeal carcinoma are more likely to have primary lesion symptoms, and thus the primary tumors are easily confirmed. Second, the previous reports included not only newly diagnosed bone metastases but also diagnosed bone metastases after disease progression. In this study, patients with bone metastasis or osteopathy as the first manifestation were included. The clinical characteristics and pathogenesis between early multiple bone metastases and late bone metastases (after disease progression) must be further studied. Kim et al reported that the overall survival after the diagnosis of metastatic or recurrent gastric cancer (MRGC) is substantially shorter in the initial BM group ((BM present at initial diagnosis of MRGC) than in the late bone metastasis group [5]. Therefore, malignant tumors

with multiple bone metastases as the first manifestation may have different biological behaviors. The study of these phenomena will provide a new direction for the treatment of these diseases. At the same time, 12 cases of the above carcinoma were classified by pathologic degree. We found that 11 cases (91.7%) were poorly differentiated and only 1 case was well differentiated. This suggests that poorly differentiated cancer is more likely to have distant bone metastasis.

In this study, the most common primary tumor with multiple bone destruction was lung cancer, accounting for 40.8% of all cases and 50% of solid tumors. Lung adenocarcinoma was the most important pathological type. In China, the incidence of lung cancer in men and women is increasing every year. In the whole population, lung cancer is the most common malignant tumor in the country and also the main cause of cancer-related deaths [6]. Bone metastasis is one of the most common metastatic sites of lung cancer. Some studies reported that the bone is the most common distant metastatic site in newly diagnosed stage IV NSCLC [7]. He *et al* [8] found that lung adenocarcinoma is the most important pathological type in patients with lung cancer with initial bone metastasis, and the prognosis of patients with bone metastasis from lung adenocarcinoma is better than that of patients with squamous cell carcinoma. With the continuous improvement of lung cancer treatment methods and technologies, the expected survival rate of patients with advanced lung cancer can be prolonged. The detection of patients with lung cancer with bone metastasis should be timely to improve the quality of life and prolong the survival of patients. Therefore, patients with unexplained bone and joint pain or bone destruction, especially those over 50 years old, should be considered for routine lung CT screening. Nevertheless, this proposal must be explored further.

The second most common bone destruction tumor found in this study was multiple myeloma. This tumor is closely related to the clinical characteristics of mm. About 70%–90% of patients with multiple myeloma may have bone damage accompanied with bone pain and other bone-related events, and about two-thirds may suffer from bone pain. Multiple myeloma is often complicated with hypercalcemia, renal insufficiency, anemia, and other symptoms. Routine blood biochemical examination of patients with multiple myeloma shows elevated globulin levels. PET/CT has a high value in the differential diagnosis of solid tumor bone metastasis and MM [9]. Nevertheless, the final diagnosis should be combined with blood tests, urine tests, bone marrow tests, and imaging examination. The risk of multiple myeloma is much higher in older age groups. The relative 5-year survival rate was about 45% in the period 2019–2020 [10]. Bone pain is a common symptom in elderly patients.

Multiple myeloma may be one of the causes of occult disease. Therefore, timely examination and diagnosis can help to improve the diagnosis rate of this kind of disease and improve the overall survival of patients.

Another common tumor type found in this study was digestive system tumors, including liver cancer and gastric cancer. This result suggested that the origin of digestive tract, especially the liver and stomach, for multiple bone metastases of unknown origin should be considered. Bae *et al* reported a rare case of small solitary HCC, presenting multiple bone involvement as a first manifestation of extrahepatic metastasis in patient with no cirrhotic liver [11]. Gastric cancer with initial bone metastasis has been reported in some studies, and the prognosis is poor. Gomi *et al* also suggest that gastric cancer should be considered in the differential diagnosis in patients initially presenting with single or multiple bone metastases [12].

Moreover, this study found seven cases of patients with unknown primary metastatic carcinoma, of which the most common pathological type was adenocarcinoma, which was consistent with the study of unknown primary metastatic carcinoma. Previous studies established that adenocarcinoma is the most common pathological type of unknown primary metastatic carcinoma [13].

Malignant bone lesions often involve the spine, pelvis, ribs, skull, and femur [4]. Our study revealed that in patients with multiple bone destruction as the first manifestation, the spine, ribs, and pelvis were the most common metastatic sites. Furthermore, about half of the patients with solid tumors only had multiple bone metastases and no other distant metastases. Therefore, further study on the clinical characteristics and pathogenesis of malignant tumors with multiple bone metastases as the first manifestation will help to improve our understanding of this disease. Multiple bone metastases are more prone to bone-related events [14–15]. This study had 11 cases of pathological fracture, 2 cases of hypercalcemia, 10 cases of bone metastasis radiotherapy, and 2 cases of spinal surgery. Therefore, patients with newly diagnosed multiple bone destruction diseases should be given active treatment as soon as possible and educated on the prevention of bone-related events. Bone destruction can be examined via ECT or PET-CT, CT or MRI, And X-ray examination [16–17]. The patients in our group were mostly examined via PET/CT, ECT, and CT/MRI. These methods can detect bone destruction earlier than X-ray examination, Moreover, through these methods, multiple bone destruction lesions can be easily spotted. PET/CT is one of the most important methods for examining unknown primary metastatic carcinoma [18]. In this study, the coincidence rate of PET in the diagnosis of primary disease was 76%.

## Conclusion

Multiple bone destruction with bone pain is one of the first manifestations of various malignant tumors. Diagnosis of this condition is often delayed. Imaging examination should be promptly conducted. The most common tumors associated with this disease are lung cancer, multiple myeloma, and digestive system tumors. It can occur at different ages, but it is more common in people aged 50 years and older. Targeted examination should be performed to determine the cause in time. Routine lung CT examination will be helpful to the screening of lung cancer in patients with bone pain as the first manifestation. Multiple bone destructions are more likely to be associated with bone-related events. Thus, patients should be educated on pathological fractures. This study was retrospective in nature, and the sample size was small. Solid tumors with multiple bone destruction as the initial manifestation may have unique biological behaviors that should be explored in prospective studies and related basic research.

## Conflicts of interest

The authors indicated no potential conflicts of interest.

## References

- Chen WQ, Zheng RS, Baade PD, *et al.* Cancer statistics in China, 2015. *CA Cancer J Clin*, 2016, 66: 115–132.
- Papachristou DJ, Basdra EK, Papavassiliou AG. Bone metastases: molecular mechanisms and novel therapeutic interventions. *Med Res Rev*, 2012, 32: 611–636.
- Terpos E, Morgan G, Dimopoulos MA, *et al.* International Myeloma Working Group recommendations for the treatment of multiple myeloma-related bone disease. *J Clin Oncol*, 2013, 31: 2347–2357.
- Yu SY, Jiang ZF, Zhang L, *et al.* Chinese expert consensus statement on clinical diagnosis and treatment of malignant tumor bone metastasis and bone related diseases. *Chinese-German J Clin Oncol*, 2010, 9: 1–12.
- Kim YJ, Kim SH, Kim JW, *et al.* Gastric cancer with initial bone metastasis: a distinct group of diseases with poor prognosis. *Eur J Cancer*, 2014, 50: 2810–2821.
- Chen W, Sun K, Zheng R, *et al.* Cancer incidence and mortality in China, 2014. *Chin J Cancer Res*, 2018, 30: 1–12.
- Li FH, Lu B, Fu HY, *et al.* Metastasis features of 546 patients with stage IV non-small cell lung cancer at first visit and the significance in radiotherapy. *Chin J Radiat Oncol (Chinese)*, 2012, 21: 122–125.
- He YF, Luo HQ, Wang W, *et al.* Clinical features and rognosis-associated factors of non-small cell lung cancer exhibiting symptoms of bone metastasis at the time of diagnosis. *Oncol Lett*, 2015, 9: 2706–2712.
- Li XJ, Zheng JS, Sun JM, *et al.* Diagnostic value of 18F-FDG PET/CT for differentiating multiple myeloma from bone metastases with undetermined origin. *Chin J Nucl Med Mol Imaging (Chinese)*, 2015, 35: 284–288.
- Gerecke C, Fuhrmann S, Striffler S, *et al.* The diagnosis and treatment of multiple myeloma. *Dtsch Arztebl Int*, 2016, 113: 470–476.
- Bae SY, Kim HJ, Oh HH, *et al.* Multiple bone metastases as the first manifestation of hepatocellular carcinoma in patient with noncirrhotic liver. *Case Rep Oncol Med*, 2015, 2015: 512849.
- Daisuke G, Toshirou F, Takashi K, *et al.* Gastric cancer initially presenting as bone metastasis: Two case reports and a literature review. *Oncol Lett*, 2018, 16: 5863–5867.
- Economopoulou P, Mountzios G, Pavlidis N, *et al.* Cancer of unknown primary origin in the genomic era: Elucidating the dark box of cancer. *Cancer Treat Rev*, 2015, 41: 598–604.
- He Q, Zang SZ, Bao QY, *et al.* The risk factors of skeletal-related events and their influence on survival in breast cancer patients with bone metastases. *Chin J Anat Clin (Chinese)*, 2019, 24: 245–249.
- Imura Y, Yamamoto S, Wakamatsu T, *et al.* Clinical features and prognostic factors in patients with esophageal cancer with bone metastasis. *Oncology Lett*, 2020, 19: 717–724.
- Lukaszewski B, Nazar J, Goch M, *et al.* Diagnostic methods for detection of bone metastases. *Contemp Oncol (Pozn)*, 2017, 21: 98–103.
- Bannas P, Kroger N, Adam G, *et al.* Modern imaging techniques in patients with multiple myeloma. *Rofo*, 2013, 185: 26–33.
- Sève P, Billotey C, Broussolle C, *et al.* The role of 2-deoxy-2-[F-18] fluoro-D-glucose positron emission tomography in disseminated carcinoma of unknown primary site. *Cancer*, 2007, 109: 292–299.

DOI 10.1007/s10330-021-0479-9

Cite this article as: Huang Y, Peng P, Zhang P, *et al.* Analyses of the clinical characteristics of 49 cases of malignancy with multiple bone lesions as the first manifestation. *Oncol Transl Med*, 2021, 7: 83–87.

# Analysis of the adverse reactions of atezolizumab: A real-world study based on FAERS database

Hao Liu<sup>1</sup>, Yujing Zhang<sup>1</sup>, Jingyi Li<sup>2</sup>, Rong Yan<sup>1</sup> (✉)

<sup>1</sup> Department of Surgical Oncology, The First Affiliated Hospital of Xi'an Jiaotong University, Xi'an 710061, China

<sup>2</sup> College of Stomatology, Xi'an Jiaotong University, Xi'an 710061, China

## Abstract

**Objective** In this study, we aimed to determine the incidence of adverse drug reactions (ADRs) of atezolizumab, identify ADR signals that are significantly related to atezolizumab, and provide a reference for the rational use of atezolizumab in the clinic through the statistical analysis of its adverse drug events (ADEs) reported in the American Food and Drug Administration (FDA) Adverse Event Reporting System (FAERS) database.

**Methods** In total, 4796 cases of atezolizumab ADEs reported in the American FAERS database from 2017 to 2019 were retrospectively analyzed.

**Results** The top three ADEs were febrile neutropenia (3.7%), anemia (2.9%), and acute renal failure (2.3%). In addition, the incidence rates of some ADEs were significantly different according to sex and age. The systematic organ classification of atezolizumab ADEs involved 32 systems, among which the top three were blood and lymphatic system disorders (585 cases, 12.2%), gastrointestinal disorders (433 cases, 9.0%), and infections and infestations (401 cases, 8.4%). The reporting odds ratio (ROR) method was used to detect the ADR signals of atezolizumab. The ROR (95% confidence interval) of the top ADE, febrile neutropenia, was 39.236 (33.757–45.604). In addition, we found 121 cases of complications associated with immune-related ADEs.

**Conclusion** The ADRs of atezolizumab reported in the FAERS database were consistent with those mentioned in the instructions for atezolizumab use, suggesting that atezolizumab has an acceptable and controllable drug effect.

**Key words:** atezolizumab; adverse reactions; Food and Drug Administration (FDA) Adverse Event Reporting System (FAERS) database; rational drug use

Received: 13 July 2020

Revised: 21 December 2020

Accepted: 15 January 2021

Currently, three main global databases are used worldwide to collect information about adverse drug events (ADEs): the World Health Organization (WHO)-Vigibase, the European Information System for Suspected Drug Adverse Reactions (Eudravigilance), and the US Food and Drug Administration (FDA) Adverse Event Reporting System (FAERS). The FAERS database has been open to the public since 2004, and data are updated quarterly. The large amount of data included in the FAERS database can be effectively used for post-market safety monitoring and risk evaluation. In addition, the number of ADE cases as well as detailed information about the ADEs for each drug, including age, gender, combination therapy, and outcome, can be found in the

FAERS database. The mining and analysis of large-scale ADE databases allow us to determine the incidence rate of several ADEs and provide a reference for the rational clinical drug use. Because of its rich content, extensive coverage, and large scale, the FAERS database has an important research value in drug safety evaluation<sup>[1]</sup>.

Atezolizumab is the first clinically approved synthetic immunoglobulin (Ig) G1 monoclonal antibody developed against programmed death-ligand 1 (PD-L1). Because of its favorable safety and efficacy, it was approved by the US FDA in 2016 as a second-line treatment for advanced non-small-cell lung carcinoma (NSCLC) and urothelial bladder cancer<sup>[2–4]</sup>. Fig. 1 shows the top 20 indications for atezolizumab use among 4796 cases of atezolizumab

✉ Correspondence to: Rong Yan. Email: ronresearch@xjtu.edu.cn

© 2021 Huazhong University of Science and Technology

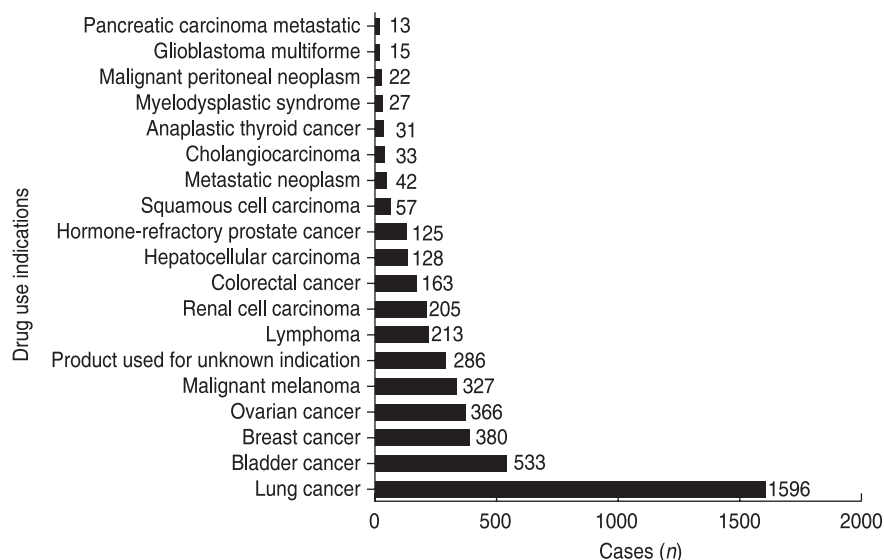


**Fig. 1** Distribution of the top 20 indications for atezolizumab use. For a more intuitive impression, we unified small cell lung cancer and non-small cell lung cancer as lung cancer

**Table 1** Four-grid table of the ratio imbalance measurement method

Drugs	Number of target adverse event reports	Number of other adverse event reports	Total
Target drug	a	b	a + b
Other drugs	c	d	c + d
Total	a + c	b + d	n = a + b + c + d

ADEs reported in the FAERS database. These data may indirectly reflect the worldwide use of atezolizumab for the treatment of various tumors. However, with the increasingly widespread use of atezolizumab in clinical practice, concerns about the adverse drug reactions (ADRs) associated with its use have gradually emerged. In this study, we aimed to reveal the incidence of atezolizumab ADRs, identify the ADR signals that are significantly related to atezolizumab, and provide a reference for its rational use in the clinic. We analyzed a total of 4796 atezolizumab ADE cases reported in the US FAERS database from 2017 to 2019.

## Methods

### Data sources and processing

Data used in this study were obtained from the US FAERS database. The US FAERS database is a spontaneous reporting system database that does not require a reporter to prove the causal relationship between drugs and reported ADEs and does not require the report to include sufficient information to evaluate the causal relationship between drugs and ADEs.

The generic name of the target drug is “atezolizumab” (Tecentriq®). We exported the atezolizumab ADE

reports for the period from the first quarter of 2017 to the fourth quarter of 2019 from the FAERS database, removed duplicate data, and used the Medical Dictionary for Regulatory Activities (MedDRA) terminology to standardize the ADR description in the report. After data cleaning, a total of 4796 reports of atezolizumab ADEs were obtained for statistical analysis.

### Signal detection and analysis

In this study, descriptive statistical analysis was used to analyze the 4796 reports of atezolizumab ADEs extracted from the US FAERS database. The data included clinical manifestations, organs and systems involved, and major ADR signals. The reporting odds ratio (ROR) method, which is widely used for ADR signal mining, was employed to detect the main ADRs related to atezolizumab. This method has a high sensitivity and can eliminate a large number of deviations. The algorithm was based on a four-grid table as listed in Table 1. The formula used for calculating the ROR is as follows:  $ROR = (a/c)/(b/d)$ ;  $ROR\ 95\% \text{ confidence interval (95\% CI)} = e^{\ln(ROR) \pm 1.96 \sqrt{\frac{1}{a} + \frac{1}{b} + \frac{1}{c} + \frac{1}{d}}}$ . The signal detection standard was set as follows: the ROR value should be  $\geq 3$ , and the lower limit of ROR 95% CI should be  $> 1$  to indicate a suspicious signal. The stronger the ADR signal, the stronger the correlation between the drug and the ADR.

## Results

### ADE overview

Of the 4796 ADE reports included, 4787 included the source region; among these, 1298 reports (27%) were from the United States and remaining were from Japan (539 cases), France (413 cases), Spain (387 cases), and China

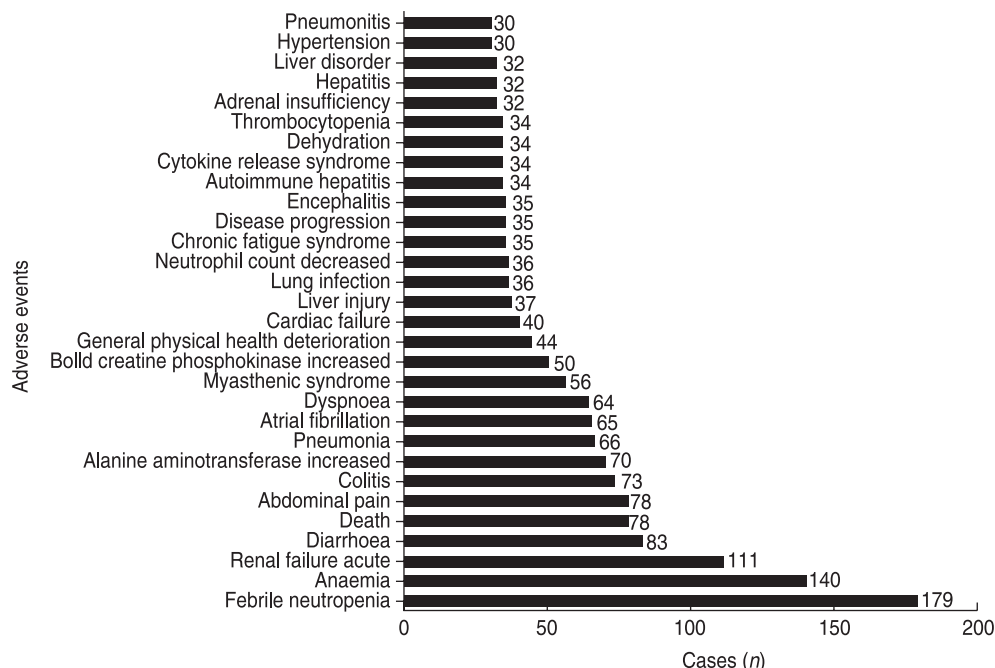


**Fig. 2** The top 20 ADEs associated with atezolizumab use

(309 cases). The vast majority of reports (approximately 70%) were from economically developed Western countries, whereas the remaining reports were mainly from Southeast Asia, followed by South America. No reports were obtained from Africa and the Middle East. This difference in the source of ADE reports might be attributed to differences in the frequency of atezolizumab use and the development of the ADE reporting systems in different regions.

In 2017, the number of reported ADEs of atezolizumab in the four quarters was 322, 320, 244, and 299, respectively; in 2018, there were 344, 389, 447, and 501 reports, respectively; and in 2019, there were 465, 435, 447, and 583 reports, respectively. Therefore, the annual atezolizumab ADEs reported in the FAERS database showed a year-on-year upward trend from 2017 to 2019, whereas the quarterly distribution was more uniform. However, potential differences in the quarterly distribution of ADE reports require further investigation.

Among the 4796 ADE reports, sex was effectively recorded in 4702 reports (98%), including 2597 males (55.23%) and 2123 females (45.15%). In addition, age was recorded in 4601 reports (95%) and could be divided into four groups: 8 cases < 18-years old, 532 cases between 18- and 50-years old (including 18-years old), 1761 cases between 50- and 65-years old (including 50-years old), and 2300 cases  $\geq$  65-years old, indicating that most of the reported atezolizumab ADEs occurred in patients aged more than 50-years old. However, this did not necessarily imply that men or individuals aged more than 50-years old are more likely to have ADRs related to atezolizumab

use because the incidence of atezolizumab use might differ according to sex and age, in addition to the presence of other potential confounding factors.

### Reporting frequency of the major atezolizumab ADEs

The reporting frequency of ADEs can reveal the incidence rate of ADRs and reflect the impact of ADRs on the patients' health, thus indicating the key direction for risk management [2]. In this study, 4796 cases of ADEs related to atezolizumab use were analyzed. Based on the number of ADEs, the top 20 reported ADEs included febrile neutropenia (179 cases), anemia (140 cases), acute renal failure (111 cases), diarrhea (83 cases), death (78 cases), colitis (73 cases), and elevated alanine aminotransferase (70 cases; Fig. 2). Notably, 51 cases of skin-related ADRs with similar nature but different names, including rash, dermatitis, eczema, and empyema, were reported.

In addition, we used the unique identification codes of ADEs, the number of ADEs, sex, age, country and region, indications, adverse reaction outcomes, and other indicators to exclude data that might be reported by the same person at different times; however, very few records of ADEs reported by the same person to the FAERS database could not be excluded because some individuals might have used atezolizumab at different ages. Accordingly, 4023 cases of atezolizumab-related ADEs were included in this analysis and divided into three age groups: 532 reports between 18- and 50-years old (including 18-years old), 1761 cases between 50- and

**Table 2** Differences in the incidence rate of the top 20 ADEs by sex

ADE	Sig	P value	Indication*
Febrile neutropenia	7.433	0.006	F > M
Anaemia	4.195	0.041	M > F
Renal failure acute	3.135	0.077	
Diarrhoea	0.982	0.322	
Death	0.108	0.743	
Abdominal pain	0.332	0.564	
Colitis	0.008	0.928	
Alanine aminotransferase increased	3.018	0.082	
Pneumonia	1.533	0.216	
Atrial fibrillation	4.456	0.035	M > F
Dyspnoea	0.013	0.910	
Myasthenic syndrome	1.266	0.261	
Blood creatine phosphokinase increased	2.655	0.103	
General physical health deterioration	0.509	0.476	
Cardiac failure	0.840	0.359	
Liver injury	0.587	0.443	
Lung infection	2.478	0.115	
Neutrophil count decreased	14.476	0.000	F > M
Chronic fatigue syndrome	11.811	0.001	F > M
Disease progression	9.334	0.002	M > F
Encephalitis	2.619	0.106	
Autoimmune hepatitis	0.016	0.901	
Cytokine release syndrome	2.064	0.151	
Dehydration	1.531	0.216	
Thrombocytopenia	8.004	0.005	F > M
Adrenal insufficiency	0.444	0.505	
Hepatitis	0.424	0.515	
Liver disorder	0.210	0.647	
Hypertension	5.386	0.020	F > M
Pneumonitis	0.959	0.327	

Notes: Chi-squared test cross-table composition of sex differences: if the number of adverse drug events in males is  $\chi_1$  and that in females is  $\chi_2$ , the positive number of adverse drug events in males in the cross table is  $\chi_1$ , and the negative number is total -  $\chi_1$ ; the positive number of adverse reaction events in females is  $\chi_2$ , and the negative number is total -  $\chi_2$ . \*, F > M indicates that the incidence of the ADE in females is higher than that in males, and M > F indicates that the incidence of the ADE in males is higher than that in females

65-years old (including 50-years old), and 2300 cases ≥ 65-years old. The difference in the incidence of ADEs according to different ages and sex was analyzed using chi-squared test (Tables 2 and 3).

In addition, chi-squared test was performed using the three age groups for each ADE and showed significant differences among different age groups (Table 4).

### Involved organs and systems

The MedDRA is a multi-axial, five-tiered hierarchical terminology used by regulatory authorities and biopharmaceutical industry for the coding (classification) of clinical data in ADE/ADR reports. Therefore, it has become an international standard terminology for ADR reports<sup>[5]</sup>. According to the MedDRA terms, a total of 4796

**Table 3** Differences in the incidence rate of the top 20 ADEs by age

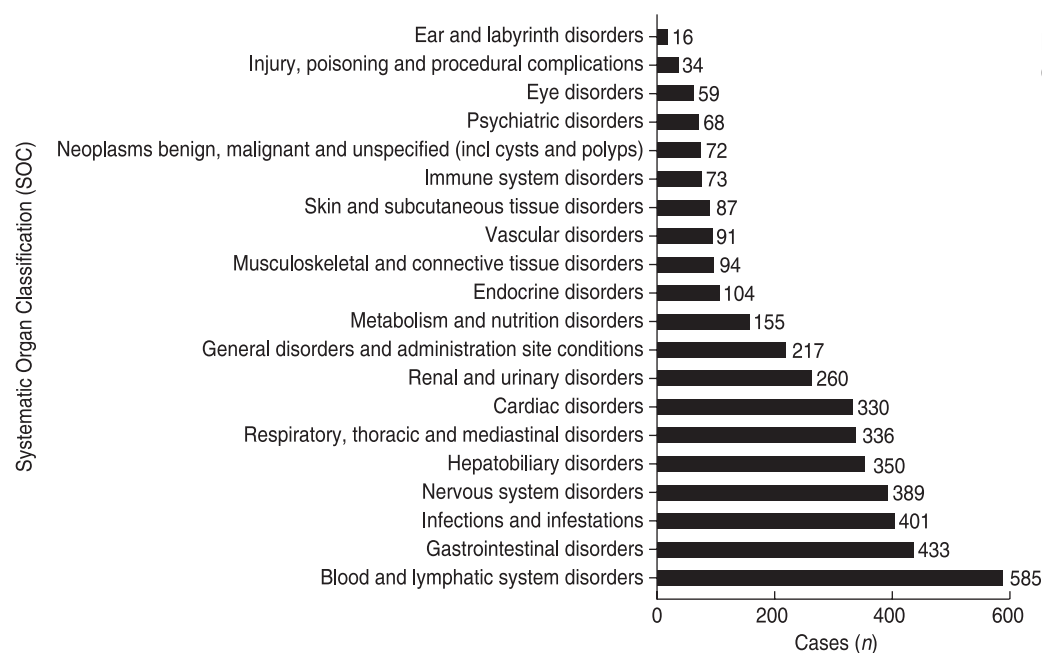
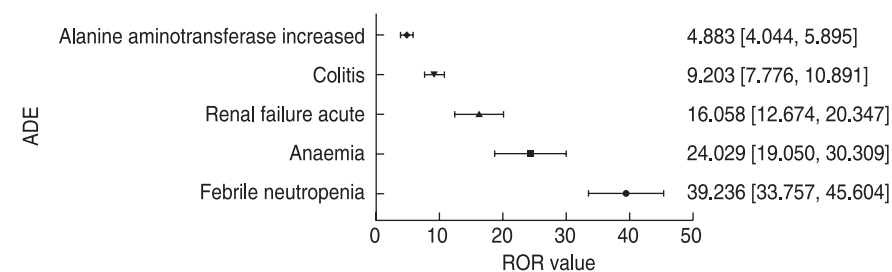
PT	Sig	P value	Significant difference*
Febrile neutropenia	12.904	0.002	y
Anaemia	2.318	0.314	n
Renal failure acute	6.232	0.044	y
Diarrhoea	2.260	0.323	n
Death	6.142	0.046	y
Abdominal pain	2.253	0.324	n
Colitis	0.879	0.645	n
Alanine aminotransferase increased	0.265	0.876	n
Pneumonia	0.211	0.900	n
Atrial fibrillation	11.947	0.003	y
Dyspnoea	1.146	0.564	n
Myasthenic syndrome	6.862	0.032	y
Blood creatine phosphokinase increased	3.806	0.149	n
General physical health deterioration	1.518	0.468	n
Cardiac failure	8.599	0.014	y
Liver injury	14.324	0.001	y
Lung infection	1.769	0.413	n
Neutrophil count decreased	6.166	0.046	y
Chronic fatigue syndrome	5.508	0.064	n
Disease progression	3.469	0.176	n
Encephalitis	0.620	0.734	n
Autoimmune hepatitis	0.206	0.902	n
Cytokine release syndrome	10.985	0.004	y
Dehydration	15.047	0.001	y
Thrombocytopenia	2.471	0.291	n
Adrenal insufficiency	4.333	0.115	n
Hepatitis	5.850	0.054	n
Liver disorder	4.357	0.113	n
Hypertension	1.088	0.580	n
Pneumonitis	4.488	0.106	n

Notes: Chi-square test cross-table composition of age differences: if the number of ADEs in the 18–49 age group is  $\chi_1$ , the number of ADEs in the 50–64 age group is  $\chi_2$ , and the number of ADEs in the ≥ 65 age group is  $\chi_3$ , the positive number of ADE in the 18–49 age group in the cross table is  $\chi_1$ , the negative number is 4023 -  $\chi_1$ ; the positive number of ADEs in the 50–64 age group is  $\chi_2$ , the negative number is 4023 -  $\chi_2$ ; the positive number of ADEs in the ≥ 65 age group is  $\chi_3$ , and the negative number is 4023 -  $\chi_3$ . \*, y indicates that the occurrence of an adverse reaction in each age group is statistically significant. If the difference is significant, the probability of an ADE in the three age groups is not equal

atezolizumab ADEs were recorded and classified using the ADE Preferred Terminology (PT) and Systematic Organ Classification (SOC) codes. The details of the ADEs of each SOC that contained PT > 100 are shown in Fig. 3 and Table 5 (the percentage base of “proportion” in Table 5 is 4796 ADEs). The number of “product usage problems” and “incorrect product management approaches” was 9. There was no relevant description in the MedDRA, which might be because of terminology changes due to the MedDRA biannual updates<sup>[2,6]</sup>. The ROR method was used to detect the signal strength of ADEs, and five ADEs with strong ADR signals were selected from the top ten

**Table 4** Incidence rate of each ADE in the three age groups

ADE	18–49 and 50–64 years			18–49 and > 64 years			50–64 and > 64 years		
	Sig	P value	Indication	Sig	P value	Indication	Sig	P value	Indication
Febrile neutropenia	12.173	0.000	18–49 > 50–64	8.366	0.004	18–49 > 64	0.662	0.416	n
Renal failure acute	0.695	0.405	n	3.857	0.050	64 > 18–49	3.684	0.055	n
Atrial fibrillation	1.563	0.120	n	6.253	0.012	64 > 18–49	6.140	0.013	64 > 50–64
Myasthenic syndrome	0.962	0.327	n	3.581	0.058	n	2.702	0.100	n
Death	2.879	0.090	n	3.832	0.050	64 > 18–49	3.832	0.050	64 > 18–49
Cardiac failure		0.017	50–64 > 18–49		0.018	64 > 18–49	0.006	0.940	n
Liver injury	4.351	0.037	18–49 > 50–64	15.329	0.000	18–49 > 64	4.006	0.045	50–64 > 64
Neutrophil count decreased	1.434	0.231	n	6.397	0.011	18–49 > 64	2.410	0.121	n
Cytokine release syndrome	2.979	0.084	n	11.854	0.001	18–49 > 64	3.584	0.058	n
Dehydration		0.356	n		0.007	64 > 18–49	7.090	0.008	64 > 50–64

**Fig. 3** The systematic organ classification (SOC) of ADEs**Fig. 4** ADE signal detection value (ROR, 95% CI). Notes: Data on the right side of the graph show the ROR values with 95% CI of each ADR

ADEs: febrile neutropenia, anemia, renal failure acute, colitis, and elevated alanine aminotransferase (Fig. 4).

### IrAEs-related complications

There have been some reports of atezolizumab-related autoimmune pancreatitis and hepatitis. Although these adverse reactions are uncommon, they pose a great threat to the patient life. Therefore, we extracted the immune-

related ADE (irAE)-related complications from the 4796 reports of ADRs. We found that the incidence of irAE-related complications was low. In particular, a total of 121 cases of 14 irAEs-related complications were reported (Fig. 5). In addition, there were several ADEs that might indicate irAEs-related complications, including nine cases of amylase increase that might indicate pancreatitis and three cases of hepatitis.

**Table 5** The major ADEs of each SOC

SOC	Number of cases/proportion	Cases (n)
Blood and lymphatic system disorders	585/12.2%	Febrile neutropenia (178), Anaemia (140), Thrombocytopenia (34), Neutrophil count decreased (34)
Gastrointestinal disorders	433/9.0%	Diarrhoea (83), Colitis (73), Ascites (27)
Infections and infestations	401/8.4%	Pneumonia (66), Lung infection (36), Bronchitis (21), Sepsis(20)
Nervous system disorders	389/8.1%	Myasthenic syndrome (56), Encephalitis (35), Syncope (21), Cerebral infarction (20)
Hepatobiliary disorders	350/7.3%	Alanine aminotransferase increased (70), Liver injury (37), Autoimmune hepatitis (34), Hepatitis (32), Liver disorder (32), Hyperbilirubinaemia (19)
Cardiac disorders	330/6.9%	Atrial fibrillation (65), Cardiac failure (40), Myocarditis (21), Pericardial effusion (20), Acute myocardial infarction (20)
Respiratory, thoracic and mediastinal disorders	336/7.0%	Dyspnoea (64), Pneumonitis (30), Respiratory failure (28), Interstitial lung disease (25), Haemoptysis (24)
Renal and urinary disorders	260/6.2%	Renal failure acute (111), Nephritis (24), Glomerulonephritis acute (24), Tubulointerstitial nephritis (17), Renal impairment (17), Renal failure (17)
General disorders and administration site conditions	217/5.4%	Death (78), General physical health deterioration (44), Chronic fatigue syndrome (35), Immediate post-injection reaction (27)
Metabolism and nutrition disorders	155/3.2%	Dehydration (34), Hyponatraemia (25), Hypercalcaemia (17), Hyperglycaemia (13), Diabetes mellitus (10)
Endocrine disorders	104/2.2%	Adrenal insufficiency (32), Hypothyroidism (17), Hyperthyroidism (14)

## Discussion

Atezolizumab has been previously shown to exhibit acceptable and controllable tolerance. Therefore, it is a valuable treatment option for patients with NSCLC, melanoma, urological tumors, and breast cancer who progress during or after chemotherapy [7-10].

As an immune checkpoint inhibitor (ICI), atezolizumab (anti-PD-L1) may subsequently lead to various autoimmune manifestations with a specific clinical spectrum called irAEs [11]. These effects result from an overall immune enhancement, and thus, they may affect any body system; however, they mainly involve the skin, colon, lungs, endocrine glands, and liver [12] and are related to the tumor types [13]. Some rare complications, such as atezolizumab-induced photo-distributed bullous pemphigoid [14], atezolizumab-related encephalitis [15], and ileal perforation secondary to atezolizumab enterocolitis [16], were also investigated in this study.

Previous studies have shown that approximately 66% of the patients treated with anti-PD-L1 or PD-L1 antibodies experience at least one ADR, whereas approximately 14% of the patients have severe ADRs. The incidence of these ADRs was not significantly different among different types of tumors [17]. In addition, the occurrence of ADRs did not affect the efficacy of treatment [18]. In a meta-analysis of clinical trials including 8730 patients [19], atezolizumab had the lowest risk of IrAEs. In addition, there was no significant difference in the risk associated with atezolizumab and avelumab. Based on the literature and reports in the FAERS database, the clinical manifestations of common ADEs of ICIs (such as navumab and pamumab) were relatively consistent and

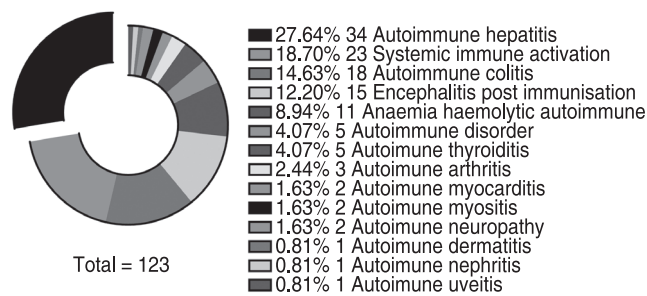


**Fig. 5** irAEs-related complications of atezolizumab

mainly concentrated in the gastrointestinal tract, skin, and respiratory system, including diarrhea, heart attack, vomiting, colitis, rash, dyspnea, and pneumonia. These reported ADEs might be considered ICI-induced IrEAs.

## Conclusion

The ADRs of atezolizumab reported in the FAERS database were consistent with those mentioned in the instructions for its use. This study suggested that physicians need to be more cautious when using atezolizumab clinically. Individuals eligible for atezolizumab treatment should be screened for a personalized treatment, thus promoting the importance of precision medicine.

Compared with cytotoxic T-lymphocyte-associated protein 4-blocking agents, PD-1/PD-L1 inhibitors are generally considered to have minor side effects [20]. However, during the course of PD-1/PD-L1 inhibitor treatment, the use of glucocorticoids to treat irAEs can result in opportunistic infections owing to temporary immunosuppression [21]. In addition, there are currently reported cases of latent/chronic infection reactivation

without irAEs during treatment with PD-1/PD-L1 inhibitors<sup>[22]</sup>. Therefore, it is necessary to fully evaluate the risks that patients with irAEs may be subject to. It should be considered that the irAEs-related complications can reduce the clinical benefit<sup>[23]</sup>. Moreover, some ADEs might occur after treatment; therefore, it is important to provide a timely treatment to reduce the risk of ADEs. In addition, some reported ADEs of ICIs might be specific to some ICIs.

At present, further studies are needed to investigate other aspects of the irAEs, including their mechanism, population characteristics, and effect on tumor treatment, as well as whether immunosuppressive therapy might affect tumor treatment efficacy. It has been suggested that cross-antigens, non-specific immune activation, and T cell diversification contribute to the pathogenesis of irAEs<sup>[24]</sup>. However, there are no prospective studies to support this hypothesis. In addition, it is essential to identify the factors related to irAEs clearly and thus help improve the screening of susceptible patients, thereby reducing the risk of ADRs. Large-scale, multi-center, randomized controlled studies should be encouraged to determine the best medication plan for immunotherapy drugs and provide a basis for the safe and reasonable medication use.

### Conflicts of interest

The authors indicated no potential conflicts of interest.

### References

- Raschi E, Parisotto M, Forcesi E, *et al.* Adverse events with sodium-glucose co-transporter-2 inhibitors: A global analysis of international spontaneous reporting systems. *Nutr Metab Cardiovasc Dis*, 2017, 27: 1098–1107.
- Li S, Feng YL, Liang CZ, *et al.* Prognostic factors for pN2 non-small cell lung cancer: a comprehensive evidence from 73 studies involving 23 772 patients. *Oncol Transl Med*, 2020, 6: 57–63.
- Shah NJ, Kelly WJ, Liu SV, *et al.* Product review on the Anti-PD-L1 antibody atezolizumab. *Hum Vaccin Immunother*, 2018, 14: 269–276.
- Cao H, Liang K, Liu P, *et al.* Efficacy and safety of anlotinib plus S-1 as thirdly-line or later-line treatment in advanced non-small cell lung cancer. *Oncol Transl Med*, 2020, 6: 10–15.
- Lin WX, Ye XF, Yao HX, *et al.* Analysis of the current adverse drug reaction terminologies. *Chin J Pharmacov (Chinese)*, 2009, 6: 713–716.
- Jiang PL, Wu J, Sun H. Association of cognitive decline, diabetes mellitus and cancer with statins use: gaining insight through the FDA pharmacovigilance database. *Chin J Clin Pharmacol Ther (Chinese)*, 2014, 19: 1132–1138.
- Dhillon S, Syed YY. Atezolizumab first-line combination therapy: A review in metastatic nonsquamous NSCLC. *Target Oncol*, 2019, 14: 759–768.
- Madden K, Kasler MK. Immune checkpoint inhibitors in lung cancer and melanoma. *Semin Oncol Nurs*, 2019, 35: 150932.
- Tripathi A, Plimack ER. Immunotherapy for urothelial carcinoma: current evidence and future directions. *Curr Urol Rep*, 2018, 19: 109.
- Basile D, Pelizzari G, Vitale MG, *et al.* Atezolizumab for the treatment of breast cancer. *Expert Opin Biol Ther*, 2018, 18: 595–603.
- Cousin S, Seneschal J, Italiano A. Toxicity profiles of immunotherapy. *Pharmacol Ther*, 2018, 181: 91–100.
- Sosa A, Cadena EL, Olive CS, *et al.* Clinical assessment of immune-related adverse events. *Ther Adv Med Oncol*, 2018, 10: 1758835918764628.
- Michot JM, Bigenwald C, Champiat S, *et al.* Immune-related adverse events with immune checkpoint blockade: a comprehensive review. *Eur J Cancer*, 2016, 54: 139–148.
- Leavitt E, Holland V. A case of atezolizumab-induced photodistributed bullous pemphigoid. *Dermatol Ther*, 2019, 32: e12924.
- Laserna A, Tummala S, Patel N, *et al.* Atezolizumab-related encephalitis in the intensive care unit: Case report and review of the literature. *SAGE Open Med Case Rep*, 2018, 6: 2050313X18792422.
- Zilliox J, DiLizia M, Schaheen B, *et al.* Ileal perforation in the setting of atezolizumab immunotherapy for advanced bladder cancer. *Can J Urol*, 2018, 25: 9525–9526.
- Wang YC, Zhou SH, Yang F, *et al.* Treatment-related adverse events of PD-1 and PD-L1 inhibitors in clinical trials: A systematic review and meta-analysis. *JAMA Oncol*, 2019, 5: 1008–1019.
- Horvat TZ, Adel NG, Dang TO, *et al.* Immune-related adverse events, need for systemic immunosuppression, and effects on survival and time to treatment failure in patients with melanoma treated with ipilimumab at Memorial Sloan Kettering Cancer Center. *J Clin Oncol*, 2015, 33: 3193–3198.
- Sonpavde GP, Grivas P, Lin Y, *et al.* Immune-related adverse events (irAEs) with single-agent PD-1 vs PD-L1 inhibitors: A meta-analysis of 8730 patients from clinical trials. *Ann Oncol*, 2019, 30 (Suppl 5): v527–v528.
- Baxi S, Yang A, Gennarelli RL, *et al.* Immune-related adverse events for anti-PD-1 and anti-PD-L1 drugs: systematic review and meta-analysis. *BMJ*, 2018, 360: k793.
- Fujita K, Kim YH, Kanai O, *et al.* Emerging concerns of infectious diseases in lung cancer patients receiving immune checkpoint inhibitor therapy. *Respir Med*, 2019, 146: 66–70.
- Picchi H, Mateus C, Chouaid C, *et al.* Infectious complications associated with the use of immune checkpoint inhibitors in oncology: reactivation of tuberculosis after anti PD-1 treatment. *Clin Microbiol Infect*, 2018, 24: 216–218.
- Michot JM, Bigenwald C, Champiat S, *et al.* Immune-related adverse events with immune checkpoint blockade: a comprehensive review. *Euro J Cancer*, 2016, 54: 139–148.
- Weber JS, Dummer R, de Pril V, *et al.* Patterns of onset and resolution of immune-related adverse events of special interest with ipilimumab: detailed safety analysis from a phase 3 trial in patients with advanced melanoma. *Cancer*, 2013, 119: 1675–1682.

DOI 10.1007/s10330-020-0444-4

Cite this article as: Liu H, Zhang YJ, Li JY, *et al.* Analysis of the adverse reactions of atezolizumab: A real-world study based on FAERS database. *Oncol Transl Med*, 2021, 7: 88–94.

# A case report of iodine-125 seed placement during operation for the treatment of advanced gallbladder carcinoma with septic shock\*

Zhuo Zhong<sup>1</sup>, Fei Gao<sup>2</sup>, Zhuo Lv<sup>1</sup>, Zhihui Zhong<sup>2</sup>, De Long<sup>1</sup> (✉)

<sup>1</sup> Department of Oncology, Guangzhou Hospital of Integrated Traditional and West Medicine, Guangzhou 510800, China

<sup>2</sup> Department of Minimally Invasive Interventional Radiology, Sun Yat-sen University Cancer Center, Guangzhou 510060, China

## Abstract

This case report describes a patient with advanced gallbladder cancer who developed septic shock associated with iodine-125 (<sup>125</sup>I) seed implantation. The treatment process is described to provide a clinical reference for similar cases. A 52-year-old woman with recurrence of advanced gallbladder cancer underwent <sup>125</sup>I seed implantation and developed postoperative sepsis with septic shock. The blood culture suggested infection with *Aeromonas caviae* and *Enterococcus faecalis*. Vancomycin and imipenem were immediately administered according to the drug sensitivity results, along with immunoglobulin therapy and vasoactive drugs. The patient's condition gradually stabilized after comprehensive treatment. Sepsis with septic shock is a rare but potentially fatal complication of <sup>125</sup>I seed implantation. Timely administration of broad-spectrum antibiotics, immunoglobulin therapy, and vasoactive drugs is very important to stabilize the patient's condition. Our treatment of this patient can serve as a reference for clinicians to manage this complication in similar cases.

Received: 25 September 2020

Revised: 13 November 2020

Accepted: 24 December 2020

**Key words:** advanced gallbladder cancer; <sup>125</sup>I seed placement; sepsis; septic shock

The pathogenesis of gallbladder cancer is complex. Studies have shown that interleukin 8, monocyte chemoattractant protein 1, and macrophage inflammatory protein 1 jointly regulate and affect the occurrence and transformation of gallbladder cancer [1]. Excision is the main treatment method [2–3]; however, the surgical effect is limited, and most cases of advanced gallbladder cancer respond poorly to chemoradiotherapy [4–5]. Gallbladder cancer is characterized by complex clinical symptoms, low quality of life, and a short survival time. Effective local control of the tumor and alleviation of clinical symptoms are the keys to prolonging survival and improving patients' quality of life. Gene sequencing, as well as targeted and comprehensive therapies, are all considered useful [6]. Radiation seed implantation brachytherapy is a type of internal radiation therapy that has recently been developed [7–8] and has the characteristics of a large radiation dose in the tumor area but causes minimal

damage to adjacent normal tissues [9]. The mechanism of radioactive seed implantation therapy involves the use of gamma rays released by a radioactive seed to continuously kill tumor cells. In recent years, satisfactory results have been achieved in the treatment of prostate cancer, pancreatic cancer, lung cancer, and head and neck tumors [10–11]. Because of the ability to administer a large dose of radiation with minimal damage to the surrounding area, radioactive seed implantation therapy may be beneficial for patients who cannot undergo routine surgery for advanced gallbladder cancer.

## Case report

A 52-year-old woman was hospitalized because of a 3-month history of abdominal pain, nausea, and vomiting. Another hospital had diagnosed and treated her for gallbladder cancer. The pathologic examination indicated

✉ Correspondence to: De Long. Email: longted@163.com

\* Supported by the Guangzhou Huadu District Science and Technology Project (No. 20-HDWS-054).

© 2021 Huazhong University of Science and Technology

moderately differentiated gallbladder cancer, and 6 cycles of chemotherapy were administered. A positron emission tomography-computed tomography (CT) examination in March 2019 indicated recurrence, metastasis, and biliary obstruction. Biliary stent implantation was performed in May 2019. However, the patient's abdominal pain persisted, and traditional Chinese medicine was provided in addition to analgesic therapy. An enhanced CT examination of the upper abdomen prior to seed implantation suggested postoperative gallbladder cancer recurrence with neoplastic tissue around the biliary stent and in the retroperitoneum; portal venous thrombosis was also present. Iodine-125 ( $^{125}\text{I}$ ) radioactive seed implantation was selected as the main therapeutic method.

The cancer had invaded the extrahepatic bile duct, pancreatic head, duodenal ampullary portal vein, and other important organs and structures. Therefore, in accordance with the preoperative Treatment Planning System (TPS) plan (Fig. 1), we determined that 64 seeds should be implanted and that some of the needles must be routed through the bile duct and colon. The patient's clotting dysfunction was corrected before the operation, oral metronidazole was prescribed for 5 days for bowel preparation, and a cleansing enema was performed the day before surgery. The patient then underwent CT-guided  $^{125}\text{I}$  radioactive seed implantation on July 5, 2019 (Fig. 2). During the operation, two seed needles were inserted into the hilar mass through the hepatobiliary tract, and a small amount of blood flowed back through the needle core. Another three seed needles penetrated

the colonic wall and entered the tumor (Fig. 2). The patient immediately developed shivering and restlessness with a heart rate of 126 beats/min, an oxygen saturation of 88%, and a respiratory rate of 24 beats/min. Considering the possibility of bacteremia, we administered 25 mg of promethazine, 10 mg of dexamethasone, and 0.4 g of ofloxacin to stabilize the patient's vital signs. This emergency treatment gradually eased the patient's shivering, and the operation continued. Finally, 64  $^{125}\text{I}$  radioactive seeds were implanted, matching the preoperative TPS plan.

However, after returning to the ward, the patient developed a high fever and lost consciousness. Her heart rate increased to 130 beats/min, her blood pressure decreased to 76/47 mmHg, and her blood oxygen saturation decreased to 86%. Urgent blood examination revealed a low white blood cell count of  $2.2 \times 10^9/\text{L}$ ; the next day, this count increased to  $33 \times 10^9/\text{L}$ , while her procalcitonin concentration rose to 70.4 ng/mL (Fig. 3). The results of a blood culture suggested that the infectious pathogens were *Aeromonas caviae* and *Enterococcus faecalis*. Considering this finding along with her clinical manifestations and laboratory test results, we concluded that the infection had originated from the intestinal canal or biliary tract and that the bacteria had entered the bloodstream through the puncture wound, resulting in sepsis and septic shock. The patient's condition was critical.

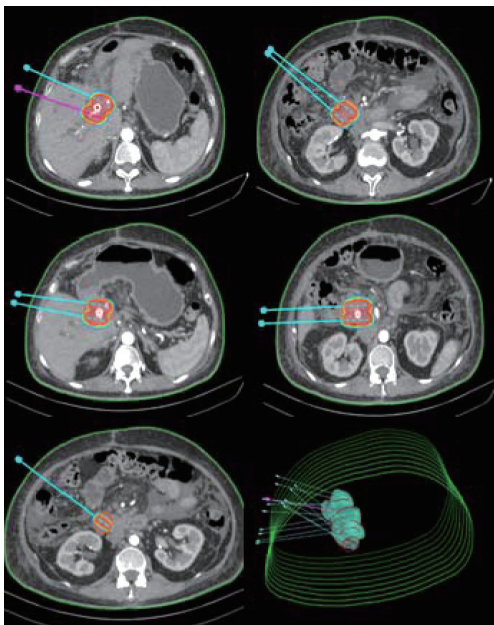


Fig. 1 Iodine-125 seed TPS plan before operation

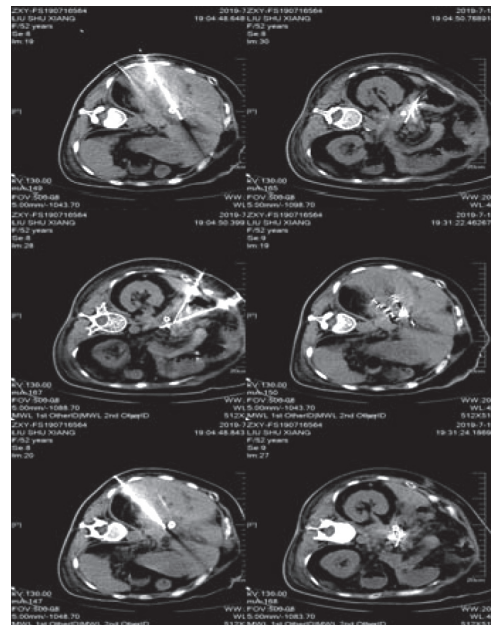


Fig. 2 Iodine-125 seed placement during operation

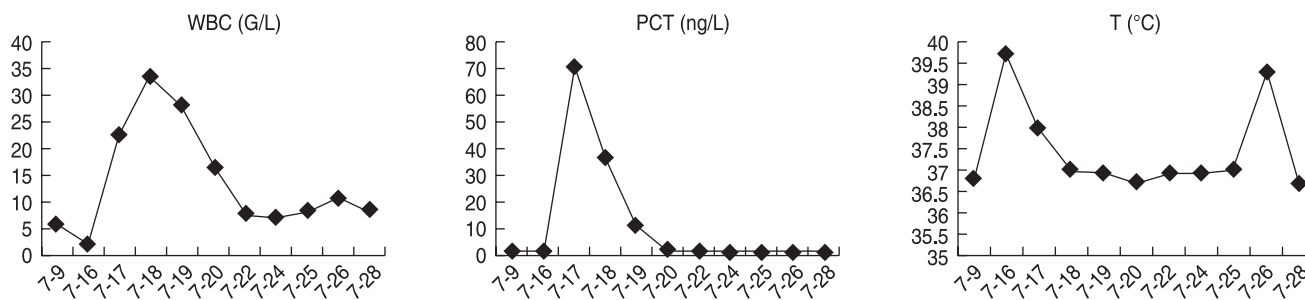


Fig. 3 Changes of infection indexes before and after treatment

### Treatment and results

The patient was definitively diagnosed and immediately given active treatment to correct the shock. Norepinephrine, vasodilators, and vasoactive drugs to raise her blood pressure were administered. According to the drug sensitivity test, vancomycin and imipenem were given as anti-infection treatments on the night of the operation, and gamma globulin was given at 5 g once daily to improve immune function. Prednisone was administered at 40 mg to 80 mg once daily to prevent damage by inflammatory factors until the patient's vital signs normalized. Additionally, water, electrolyte, and acid/base imbalances were actively corrected, and nutritional support was provided. The patient's vital signs gradually stabilized, and her consciousness returned after 13 days of treatment. Her white blood cell and neutrophil counts gradually decreased to within the normal range, and her procalcitonin concentration gradually decreased to 1.67 ng/mL.

### Discussion

Advanced gallbladder cancer is prone to recurrence after surgery and has a poor prognosis. In the present case, the patient developed local recurrence after cholecystectomy. The tumor invaded the hilar bile duct and the ampulla of Vater in the duodenum. The purpose of treatment was to reduce the cancer-related pain and shrink the tumor, and the patient had indications for seed implantation therapy. Because the tumor had an unclear structure and invaded the main portal vein and pancreatic head and surrounded the hepatobiliary duct, the surgical risk was relatively high. During the operation, reflux of blood was seen in the needle core when the needle punctured the biliary tract and intestine. The patient exhibited rapid shivering shortly thereafter, which was consistent with the entrance of bacteria into the bloodstream<sup>[12]</sup>. After returning to the ward, the patient developed a drop in blood pressure, unclear consciousness, and high fever, which were consistent with sepsis and septic shock. Her condition gradually stabilized with strong anti-infection

and systemic supportive treatments.

Although bacteremia during seed implantation has been previously reported<sup>[13–15]</sup>, severe sepsis complicated by septic shock within a very short time after the operation is rare. A significant increase in the procalcitonin concentration indicates a serious systemic inflammatory response<sup>[16]</sup>, and the main evaluation criteria for ideal infection control are stabilization of the vital signs and decreases in the infection indexes<sup>[17]</sup>. In the present case, the infection was effectively controlled while enhancing the patient's immunity, and active control of the damage secondary to the systemic inflammatory response was another key to the clinical effectiveness of the treatment.

<sup>125</sup>I seed implantation can effectively alleviate clinical symptoms of advanced tumors<sup>[18]</sup>, but surgical safety must be fully evaluated<sup>[19]</sup>. For patients in whom the puncture needle passes through the biliary tract or intestine, adequate preparation before surgery is of vital importance. If obstructive jaundice is present, biliary drainage should be performed before surgery to reduce the risk of intraoperative biliary flora entering the blood. If the treatment plan includes puncture of multiple particle needles through the intestine, the patient should undergo not only routine intestinal preparation, but also intravenous administration of antibiotics effective against gram-negative bacilli 6 h before the operation; this can effectively prevent sepsis and septic shock.

In the present case, sepsis and septic shock had occurred before the blood culture results were available, and the timely use of broad-spectrum antibiotics with effective control of systemic inflammatory factors were the keys to early rescue. Notably, in cases of severe infection, the combination of immunoglobulin therapy and vasoactive drugs can improve the rescue rate, and the treatment in this case is worthy of reference. Additionally, in the early stages of sepsis with septic shock in our patient, there was a drop in white blood cells, which was not consistent with the manifestation of severe infection; this may have been related to temporary suppression of bone marrow function caused by the infection. When combined with the patient's other clinical manifestations, this can be

used as one of the indicators to determine the presence of severe infection.

### Conflict of interest

The authors indicated no potential conflicts of interest.

### References

- Zeng L, Wang XY, Zhou LX, *et al.* Clinicopathological significance of chemotactic factor IL-8, MCP-1 and MIP-1 $\alpha$  expressions in gallbladder carcinoma. *Chinese-German J Clin Oncol*, 2013, 12: 481–486.
- Qin Q, Liu M, Wang X. Gallbladder sarcomatoid carcinoma: Seven case reports. *World J Clin Cases*, 2020, 8: 3881–3889.
- Yang XW, Chen JY, Wen ZJ, *et al.* Effect of preoperative jaundice on long-term prognosis of gallbladder carcinoma with radical resection. 2020, 18: 239.
- Liu C, Rein L, Clarke C, *et al.* Comparison of overall survival in gallbladder carcinoma at academic versus community cancer centers: An analysis of the National Cancer Data Base. *J Surg Oncol*, 2020, 122: 176–182.
- Melillo A, Linden K, Spitz F, *et al.* Disparities in treatment for gallbladder carcinoma: Does treatment site matter? *J Gastrointest Surg*, 2020, 24: 1071–1076.
- Zhang W, Shi JP, Li RT, *et al.* Effectiveness of Olaparib treatment in a patient with gallbladder cancer with an ATM-inactivating mutation. *Oncologist*, 2020, 25: 375–379.
- Jarusevicius L, Inciura A, Juozaityte E, *et al.* Comparison of implant quality between loose and intra-operatively linked iodine-125 seeds in prostate cancer brachytherapy. *J Radiat Res*, 2012, 53: 439–446.
- Straver ME, Loo CE, Alderliesten T, *et al.* Marking the axilla with radioactive iodine seeds (MARI procedure) may reduce the need for axillary dissection after neoadjuvant chemotherapy for breast cancer. *Br J Surg*, 2010, 97: 1226–1231.
- Zhang FQ, Li Q, Yang H, *et al.* Clinical value of <sup>125</sup>I seeds implantation in the treatment of primary liver cancer with portal vein tumor thrombus. *Chin J Nucl Med Mol Imaging (Chinese)*, 2020, 40: 142–146.
- Li CG, Zhou ZP, Jia YZ, *et al.* Radioactive <sup>125</sup>I seed implantation for locally advanced pancreatic cancer: A retrospective analysis of 50 cases. *World J Clin Cases*, 2020, 8: 3743–3750.
- Lee W, Daly BDT, DiPetrillo TA, *et al.* Limited resection for non-small cell lung cancer: observed local control with implantation of I-125 brachytherapy seeds. *Ann Thorac Surg*, 2003, 75: 237–243.
- Singer M, Deutschman CS, Seymour CW, *et al.* The third international consensus definitions for sepsis and septic shock (sepsis -3). *JAMA*, 2016, 315 : 801–810.
- Jiang YL, Ji Z, Guo FX, *et al.* Side effects of CT-guided implantation of <sup>125</sup>I seeds for recurrent malignant tumors of the head and neck assisted by 3D printing non co-planar template. *Radiat Oncol*, 2018, 13: 18.
- Zhang FJ, Li CX, Jiao DC, *et al.* CT guided 125iodine seed implantation for portal vein tumor thrombus in primary hepatocellular carcinoma. *Chin Med J (Engl)*, 2008, 121: 2410–2414.
- Zhang L, Chen LH, Wang J, *et al.* CT-guided radioactive <sup>125</sup>I seed implantation treatment of multiple pulmonary metastases of hepatocellular carcinoma. *Clin Radiol*, 2014, 69: 624–629.
- Liu GB, Cui XQ, Wang ZB, *et al.* Detection of serum procalcitonin and hypersensitive C-reactive protein in patients with pneumonia and sepsis. *J Biol Regul Homeost Agents*, 2018, 32: 1165–1169.
- Nobre V, Harbarth S, Graf JD, *et al.* Use of procalcitonin to shorten antibiotic treatment duration in septic patients: a randomized trial. *Am J Respir Crit Care Med*, 2008, 177: 498–505.
- Jiang P, Liu C, Wang JJ, *et al.* Computed tomography (CT)-guided interstitial permanent implantation of (<sup>125</sup>I) seeds for refractory chest wall metastasis or recurrence. *Technol Cancer Res Treat*, 2015, 14: 11–18.
- Gao F, Li CX, Gu YK, *et al.* CT-guided 125I brachytherapy for mediastinal metastatic lymph nodes recurrence from esophageal carcinoma: effectiveness and safety in 16 patients. *Eur J Radiol*, 2013, 82: e70–e75.

DOI 10.1007/s10330-020-0457-7

Cite this article as: Zhong Z, Gao F, Lv Z, *et al.* A case report of iodine-125 seed placement during operation for the treatment of advanced gallbladder carcinoma with septic shock. *Oncol Transl Med*, 2021, 7: 95–98.



# Call For Papers

## Oncology and Translational Medicine

(CN 42-1865/R, ISSN 2095-9621)

Dear Authors,

*Oncology and Translational Medicine* (OTM), a peer-reviewed open-access journal, is very interested in your study. If you have unpublished papers in hand and have the idea of making our journal a vehicle for your research interests, please feel free to submit your manuscripts to us via the Paper Submission System.

### Aims & Scope

- Lung Cancer
- Liver Cancer
- Pancreatic Cancer
- Gastrointestinal Tumors
- Breast Cancer
- Thyroid Cancer
- Bone Tumors
- Genitourinary Tumors
- Brain Tumor
- Blood Diseases
- Gynecologic Oncology
- ENT Tumors
- Skin Cancer
- Cancer Translational Medicine
- Cancer Imageology
- Cancer Chemotherapy
- Radiotherapy
- Tumors Psychology
- Other Tumor-related Contents

---

### Contact Us

Editorial office of Oncology and  
Translational Medicine  
Tongji Hospital  
Tongji Medical College  
Huazhong University of Science  
and Technology  
Jie Fang Da Dao 1095  
430030 Wuhan, China  
Tel.: 86-27-69378388  
Email: [dmedizin@tjh.tjmu.edu.cn](mailto:dmedizin@tjh.tjmu.edu.cn);  
[dmedizin@sina.com](mailto:dmedizin@sina.com)

*Oncology and Translational Medicine* (OTM) is sponsored by Tongji Hospital, Tongji Medical College, Huazhong University of Science and Technology, China (English, bimonthly).

OTM mainly publishes original and review articles on oncology and translational medicine. We are working with the commitment to bring the highest quality research to the widest possible audience and share the research work in a timely fashion.

Manuscripts considered for publication include regular scientific papers, original research, brief reports and case reports. Review articles, commentaries and letters are welcome.

### About Us

- Peer-reviewed
- Rapid publication
- Online first
- Open access
- Both print and online versions

For more information about us, please visit:

<http://otm.tjh.com.cn>



### Editors-in-Chief

Prof. Anmin Chen (Tongji Hospital, Wuhan, China)  
Prof. Shiyong Yu (Tongji Hospital, Wuhan, China)